

Inhibition of cyclooxygenases attenuates diet-
induced obesity and compensatory increased
glucose-stimulated insulin secretion in
C57BL/6J mice

KRISTIN RØEN

MASTER THESIS IN HUMAN NUTRITION



INSTITUTE OF MEDICINE, UNIVERSITY OF BERGEN (UIB)

NATIONAL INSTITUTE OF NUTRITION AND SEAFOOD RESEARCH (NIFES)

MAY 2013

Inhibition of cyclooxygenases attenuates diet-
induced obesity and compensatory increased
glucose-stimulated insulin secretion in
C57BL/6J mice

KRISTIN RØEN

MASTER THESIS IN HUMAN NUTRITION

MAY 2013



N I F E S

NASJONALT INSTITUTT
FOR ERNÆRINGS- OG
SJØMATFORSKNING

ACKNOWLEDGEMENTS

The work presented in this thesis was carried out at the National Institute of Nutrition and Seafood research (NIFES) in Bergen, during the period from autumn 2012 to spring 2013.

I would like to thank my main supervisor Dr. philos Lise Madsen for all her help and guidance throughout this study. Her great experience and enthusiasm for the field have been a great inspiration. I would also thank my co-supervisor Dr. philos Øyvind Lie for his support and help. I would like to express my greatest gratitude to Even Fjære for help with animal experiments and for answering numerous questions.

I would like to thank Aase Heltveit and Øyvind Reinhard for help and guidance handling the animals during the experiments. I would like to thank Ulrike Liisberg Aune for teaching me the real Time qPCR and histology method.

I further wish to thank my fellow master student Susanne Bjelland, as well as the PhD-students for creating a great environment and making the time writing this master thesis enjoyable.

Finally, I wish to express the warmest thanks to friends and family for their continuous support and encouragement throughout the years I have been a student. Especially thanks to Asbjørn Fauske for his patients and support throughout this period.

Bergen, May 2013

Kristin Røen

TABLE OF CONTENTS

LIST OF FIGURES	4
LIST OF TABLES	6
LIST OF ABBREVIATIONS.....	7
ABSTRACT.....	9
1.0 INTRODUCTION	10
1.1 OVERWEIGHT AND OBESITY	10
1.2 THE ADIPOSE ORGAN	11
1.3 INSULIN SECRETION AND ACTION.....	13
1.4 OBESITY AND INSULIN RESISTANCE	14
1.5 DIABETES.....	16
1.6 ADIPOSE TISSUE DYSFUNCTION AND INSULIN RESISTANCE	16
1.7 CYCLOOXYGENASES AND PROSTAGLANDINS.....	17
1.8 COX-INHIBITORS AND INDOMETHACIN	18
1.9 INTRODUCTION TO THE PRESENT INVESTIGATION.....	19
1.10 AIMS OF THE PRESENT STUDY	19
2.1 THE ANIMAL EXPERIMENTS	21
2.2 GLUCOSE TOLERANCE TEST AND GLUCOSE-STIMULATED INSULIN SECRETION	25
2.3 INSULIN TOLERANCE TEST	25
2.4 MEAL TOLERANCE TEST AND MEAL STIMULATED INSULIN SECRETION	25
2.5 TERMINATION AND COLLECTION OF TISSUE	26
2.6 INSULIN MEASUREMENT IN PLASMA USING ELISA INSULIN KIT.....	26
2.7 HISTOLOGY.....	27
2.8 REAL TIME qPCR.....	29
2.8 STATISTICAL ANALYSES	33
3.0 RESULTS.....	34
3.1 EXPERIMENT 1, PART 1	34
3.2 FEEDING EXPERIMENT 1, PART 2	44
3.3 EXPERIMENT 2	56
3.4 EXPERIMENT 3	59
4.1 INDOMETHACIN ATTENUATED HF/HS-INDUCED OBESITY, BUT DID NOT REVERSE IT	72
4.2 HF/HS+INDO-FED MICE WERE LEAN, BUT AS GLUCOSE INTOLERANT AS HF/HS-FED MICE	73
4.3 IS REDUCED GSIS RELATED TO THE REDUCED DIO IN HF/HS+INDO-FED MICE?	74
4.4 INDOMETHACIN DID NOT AFFECT MEAL STIMULATED INSULIN SECRETION IN HF/HS-FED MICE	76
4.5 METHODOLOGICAL DISCUSSION	77
4.6 THE ANIMAL MODELS RELEVANCE TO HUMANS.....	80

4.7 FUTURE PERSPECTIVES	80
5.0 CONCLUSION	82
REFERENCES	83
APPENDIX	89

LIST OF FIGURES

Figure 1.1: Adipose tissue.....	12
Figure 1.2: Obesity, inflammation and insulin resistance.....	15
Figure 1.3: Insulin resistance and insulin sensitivity.....	17
Figure 1.4: COX-inhibition.....	18
Figure 1.5: Results from a previous study performed in our group.	20
Figure 2.1: C57BL/6J mouse.....	21
Figure 2.2: Experimental design.....	23
Figure 2.3: Diets.....	24
Figure 3.1: Body weight gain and feed efficiency during 8 weeks.....	35
Figure 3.2: Body composition of fat and lean mass after 6 and 8 weeks	36
Figure 3.3: <i>i.p</i> -GTT performed after 9 weeks (body mass)	38
Figure 3.4: HOMA-IR index (body mass)	39
Figure 3.5: ITT performed after 10 weeks (body mass)	40
Figure 3.6: <i>i.p</i> -GTT performed after 9 weeks (lean mass)	42
Figure 3.7: ITT performed after 10 weeks (lean mass)	43
Figure 3.8: Body weight gain and feed efficiency during 6 weeks.....	45
Figure 3.9: MRI-scan of fat and lean mass initial, and after 4 and 6 weeks.....	46
Figure 3.10: Masses of adipose depots, pancreas and liver.....	47
Figure 3.11: Histology of adipose depot.....	48
Figure 3.12: <i>i.p</i> -GTT performed after 7 weeks (body mass).....	50
Figure 3.13: HOMA-IR index (body mass).....	51
Figure 3.14: ITT performed after 8 weeks (body mass).....	53
Figure 3.15: <i>i.p</i> -GTT performed after 7 weeks (lean mass).....	53
Figure 3.16: HOMA-IR score (lean mass).....	54
Figure 3.17: ITT performed after 8 weeks (lean mass)	54
Figure 3.18: Expression of genes involved in gluconeogenesis.....	55
Figure 3.19: <i>i.p</i> -GTT after 1 week feeding.....	57
Figure 3.20: <i>i.p</i> -GTT after 10 weeks of feeding.....	58
Figure 3.21: <i>i.p</i> -GTT after 1 week of feeding.....	60
Figure 3.22: <i>i.p</i> -GTT after 2 week of feeding.....	61

Figure 3.23: <i>i.p</i> -GTT after 3 week of feeding.....	62
Figure 3.24: <i>i.p</i> -GTT after 9 week of feeding.....	63
Figure 3.25: Initial MTT.....	65
Figure 3.26: MTT after 1 week of feeding.....	66
Figure 3.27: MTT after 2 week of feeding.....	67
Figure 3.28: MTT after 3 week of feeding.....	68
Figure 3.29: MTT after 10 week of feeding.....	69
Figure 3.29: OGTT after 8 week of feeding.....	71
Appendix:	
Figure A.1: Liver gene expression.....	92

LIST OF TABLES

Table 2.1: Components of the different diets used in the animal experiments.....	24
Table 2.2: Dehydration steps of tissue.....	27
Table 2.3: hematoxylin and eosin staining procedure.....	28
Table 2.4: The RT-reaction mixture used in a 50 µl reaction.....	31
Table 2.5: Temperature conditions during RT-reaction.....	31
Table 2.6: The thermal cycle used in a Real Time PCR machine.....	32
Table 2.7: Reaction mix with the respective primer for Real Time qPCR reaction.....	32
Appendix:	
Table A.1: Reagents in Insulin Mouse ELISA kit.....	89
Table A.2: Chemicals and reagents used in histology.....	89
Table A.3: Reagents used in RNA extraction.....	90
Table A.4: Reagents used in RT-reaction mix.....	90
Table A.5: Reagents used in Real-Time qPCR.....	90
Table A.6: List of primers used in Real-Time qPCR (obtained from Invitrogen, UK).....	91

LIST OF ABBREVIATIONS

AUC	Area under curve
BMI	Body mass index
cDNA	complementary deoxyribonucleic acid
COX	Cyclooxygenase
ELISA	Enzyme-linked immunsorbent assay
eWAT	Epididymal white adipose tissue
FIRKO	Fat-specific insulin receptor knockout
GSIS	Glucose-stimulated insulin secretion
GTT	Glucose tolerance test
HF/HS	High fat and high sucrose
HF/HS+INDO	High fat and high sucrose + indomethacin
HOMA-IR	Homeostasis Model of Assessment - Insulin Resistance
iBAT	Interscapular brown adipose tissue
INDO	Indomethacin
<i>i.p.</i> -GTT	Intraperitoneal glucose tolerance test
ITT	Insulin tolerance test
iWAT	Inguinal white adipose tissue
MRI	Magnetic resonance imaging
MSIS	Meal-stimulated insulin secretion
MTT	Meal tolerance test
OGTT	Oral glucose tolerance test
RD	Regular diet
RD+INDO	regular diet + indomethacin
RT-qPCR	Real time quantitative polymerase chain reaction
RT	Revers transcription
SEM	Standard error of the mean
T1DM	Type 1 diabetes mellitus
T2DM	Type 2 diabetes mellitus
WAT	White adipose tissue
WHO	World health organization

ABSTRACT

Obesity is considered a state of low-grade inflammation, and this inflammation is strongly related to development of systematic insulin resistance. Hyperglycemia develops during insulin resistance as insulin-stimulated glucose uptake in peripheral insulin sensitive tissues is reduced. Hepatic insulin resistance is often accompanied with increased gluconeogenesis and increased hepatic glucose output, which further increase blood glucose. To cope with the hyperglycemia, the pancreatic β -cells compensate by increasing insulin secretion. However, after a certain amount of time, the β -cells are no longer able to compensate, and insulin production stops. This may be accompanied with apoptosis in the β -cells.

Indomethacin is an NSAID and a non-selective inhibitor of cyclooxygenase 1 (COX-1) and 2 (COX-2). In this study we have demonstrated that COX-inhibition using indomethacin, attenuated high fat/high sucrose-induced obesity in C57BL/6J mice. Obesity and glucose intolerance normally co-occur, and it has been generally assumed that glucose intolerance and subsequently increased insulin secretion and insulin resistance are consequences of increased adipose tissue mass. Paradoxically, the mice were lean, but indomethacin did not prevent the reduced glucose intolerance associated with an high fat/high sucrose diet.

This study confirmed that indomethacin was able to attenuate diet-induced obesity. However, we here demonstrated that indomethacin was not able to reverse obesity. An unpublished study from our group has shown that insulin levels in both fed and fasted state in indomethacin supplemented high-fat/high-sucrose (HF/HS) fed mice were significantly lower than in HF/HS-fed mice. In this study we found that indomethacin attenuated the increased glucose-stimulated insulin secretion (GSIS) caused by the HF/HS-diet. Indomethacin was, however, unable to reduce the increased GSIS in obese mice.

Of note, we were only able to measure an effect of indomethacin when glucose was injected intraperitoneal. We could not observe a lower GSIS in HF/HS- fed mice supplemented with indomethacin when glucose was administered orally. Neither, indomethacin did not inhibit insulin secretion induced by a meal or had an acute effect on GSIS. Thus, indomethacin is able to attenuate, but not reverse HF/HS-induced GSIS.

1.0 INTRODUCTION

1.1 OVERWEIGHT AND OBESITY

World health organization (WHO) defines overweight and obesity as abnormal or excessive fat accumulation that presents a risk to health. Body mass index (BMI) is a common international measurement of overweight and obesity in adults. The BMI of a person is defined as a person's weight in kilograms divided by the square of height in meters (kg/m^2). WHO defines a BMI greater than or equal to 25 as overweight and a BMI greater than or equal to 30 as obesity (WHO 2012).

Prevalence of overweight and obesity

The prevalence of overweight and obesity is increasing at an alarming rate in countries throughout the world (Kelly, Yang et al. 2008). Since 1980, the worldwide obesity has nearly doubled. According to data from 2008, more than 1.4 milliard adults above 20 years and older were overweight, 500 millions of them were obese. The prevalence of obesity is considered higher among women in all world regions, with 300 million obese women and 200 million obese men (Kelly, Yang et al. 2008). The highest obesity prevalence is in westernized countries (WHO 2012). There are many reasons for the development of overweight and obesity, but the main underlying reason is an imbalance in energy-intake and consumption. One cause of this imbalance may due to a western diet, high in fat and sugar, together with an inactive lifestyle (Zimmet and Alberti 2006).

Health consequences of overweight and obesity

Obesity is a global health concern, as it is a important risk factor for development of type 2 diabetes, cardiovascular disease and certain types of cancer (Zimmet and Alberti 2006). The risk of disease development increases with increased BMI. Overweight and obesity are the fifth leading risk for death worldwide, and there are also linked more death causes to overweight and obesity than underweight (WHO 2012).

1.2 THE ADIPOSE ORGAN

The adipose organ can broadly be divided into white adipose tissue (WAT) and brown adipose tissue (BAT). The two adipose tissues have opposite functions in the energy metabolism. Whereas fat cells in WAT store energy, fat cells in BAT oxidized fat and release the energy in form of heat (Nakagami 2013).

White adipose tissue

WAT is the main energy storing tissue and can respond rapidly and dynamically to alterations in nutrient status and it has an almost unlimited capacity to expand (Wronska and Kmiec 2012). However, adipocytes can reach diffusional limit of oxygen during an increased and rapidly growth and this may results in hypoxia (figure 1.1). As illustrated in figure 1.1, development of obesity results from an increase in adipocytes number and/or size, and this is accompanied by generation of new blood vessels (Sun, Kusminski et al. 2011). Diet-induced weight loss leads to reduced lipid content in the adipocytes and thereby a reduction in adipocyte volume, but the number of adipocytes is not reduced (Madsen, Liaset et al. 2008).

The increase in hyperplasia and/or hypertrophy in adipocytes during development of obesity is strongly associated with a low-grade inflammation in WAT (figure 1.1) (Frühbeck 2008). The obese state is associated with recruitment of macrophages, and these cells are regarded as particularly important in the inflammatory response in WAT. Several other types of immune cells are also present in WAT during an obese state, including lymphocytes, natural killer cells, and mast cells (Sell and Eckel 2010). There is an increased expression and secretion of a number of pro-inflammatory adipokines in the obesity state. These adipokines modulate insulin resistance in WAT, and includes tumor necrotic factor alpha, leptin, adiponectin, retinol binding protein-4, chemerin and monocyte chemoattractant protein 1. The increased production of adipokines occurs mainly in WAT, but influences also other insulin sensitive tissues as the liver and skeletal muscle (Trayhurn 2013).

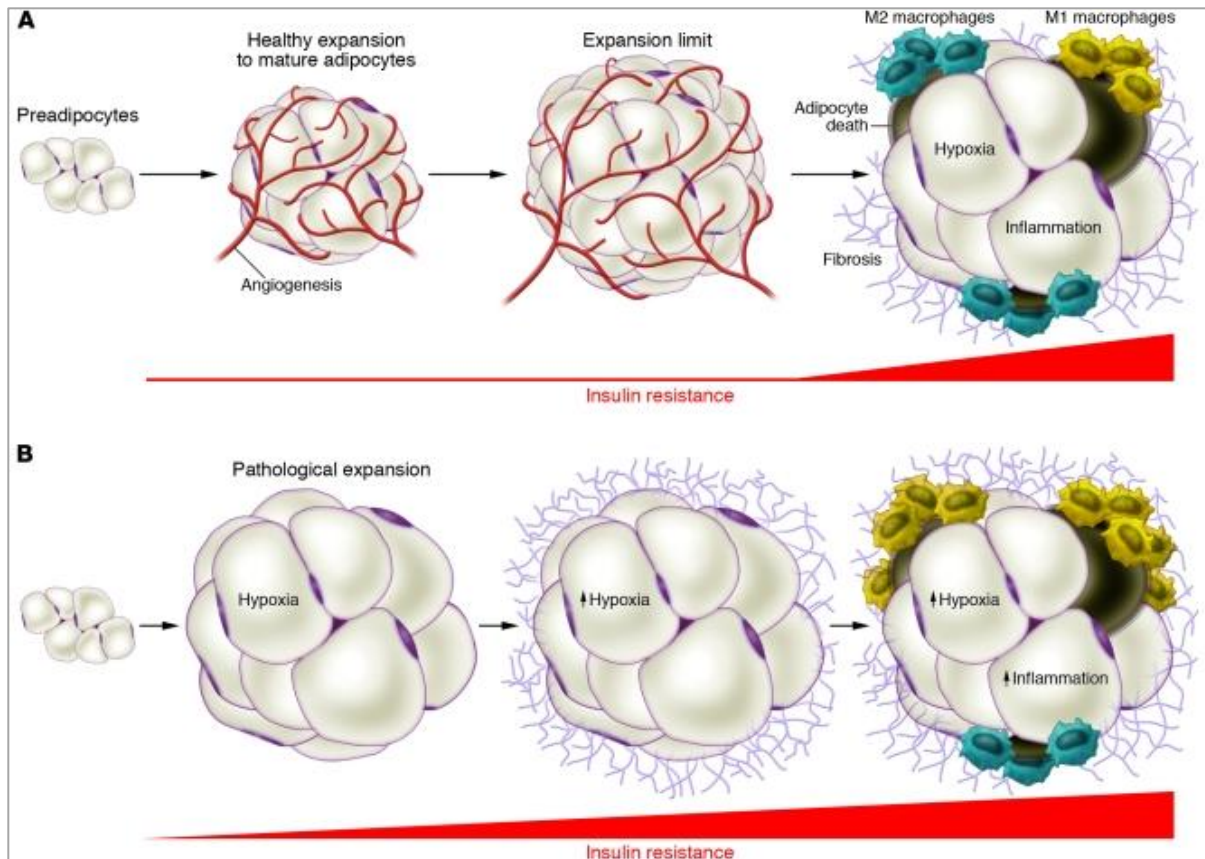


Figure 1.1: The connection between adipose tissue expansion, inflammation and insulin resistance. **A:** Healthy adipose tissue expansion consists of an enlargement of adipose tissue through recruitment of adipogenic precursor cells, along with an adequate angiogenic response. **B:** In contrast, pathological adipose tissue expansion consists of massive enlargement of existing adipocyte and limited angiogenesis, resulting in hypoxia. M1-stage macrophage infiltration leads to a inflammatory response that is strongly associated with insulin resistance (Sun, Kusminski et al. 2011).

Brown adipose tissue

BAT is able to convert energy to heat by the tissue-specific uncoupling protein 1 (UCP1). Activation of BAT through diet-induced thermogenesis has become interesting for obesity researchers, as it might represent a tool for treatment of obesity and thereby other metabolic diseases. Thus, the interest in BAT has increased tremendously during the last years (Cypess, White et al. 2013). For decades, it was generally assumed that BAT was virtually non-existent in adult humans. This view was dramatically changed in 2009 with the demonstration of BAT in adults (Cypess, Lehman et al. 2009; van Marken Lichtenbelt, Vanhomerig et al. 2009; Virtanen, Lidell et al. 2009; Zingaretti, Crosta et al. 2009).

1.3 INSULIN SECRETION AND ACTION

Insulin is an anabolic hormone which participate in nutrient transport into cells, regulation of gene expression, modification of enzyme activate and regulation of energy homeostasis (de Luca and Olefsky 2008). Insulin is secreted from the pancreatic β -cells in response to increased blood glucose and it is an essential hormone for regulation of glucose homeostasis (Klover and Mooney 2004). Glucose is the most crucial stimulator of insulin secretion. However, the insulin secretion from the β -cells cells are additionally under control an array of other stimulatory and inhibitory factors. This includes neurotransmitters, hormones and nutrients (Henquin, Ravier et al. 2003).

Regardless of blood glucose levels, the β -cells constantly synthesizes insulin and stores it in vacuoles in the pancreas. When blood glucose levels increase, insulin is released from the vacuoles in the amount to ensure the blood glucose within normal range (Uchizono, Alarcon et al. 2007). Insulin secretion may occur in a biphasic manner during a abnormal amount of glucose intake, such as during a glucose tolerance test (Caumo and Luzi 2004). A rapid and large increase in blood glucose concentration leads to a quick and transient acceleration in a first phase insulin secretion, followed by a second phase, where the secretion is stabilized or progressively increased (Henquin 2009). Under physiological conditions, such as after a balanced meal, glucose concentration increase gradually and the insulin response in the blood does not show clear signs of a biphasic shape (Caumo and Luzi 2004).

Insulin regulates glucose homeostasis by stimulating glucose uptake in skeletal muscle and furthermore stimulates conversion of glucose to glycogen (Epstein, Shepherd et al. 1999). It is generally believed that approximately 75% of the blood glucose is taken up by skeletal muscle (Lin and Sun 2010). In the liver, insulin promotes glycogen synthesis and stimulates lipogenesis while inhibiting gluconeogenesis. Insulin suppresses lipolysis and stimulates lipogenesis in the adipose tissue (Samuel and Shulman 2012). In conclusion, insulin stimulates storage of glucose and fat and inhibits gluconeogenesis and lipolysis, classifying insulin as an anabolic hormone.

The importance of insulin signaling in obesity development is underscored by the finding that fat-specific insulin receptor knockout (FIRKO) mice lacking insulin receptors in adipose tissue are protected against obesity and obesity related glucose intolerance (Bluher, Michael et al. 2002). Moreover, obesity development is strongly attenuated in $ins1^{+/-};Ins2^{-/-}$ mice, that have 50 % lower insulin production than wild type mice (Mehran, Templeman et al. 2012).

1.4 OBESITY AND INSULIN RESISTANCE

Low-grade inflammation associated with obesity is an important mechanism in decreased insulin sensibility in adipose tissue, liver and skeletal muscle (Donath and Shoelson 2011). Obesity causes excessive growth of adipose depots with adipocyte hypertrophy and hyperplasia. This fat overload leads to an activation of inflammatory pathways and subsequent paracrine/autocrine-mediated cellular insulin resistance (figure 1.2) (de Luca and Olefsky 2008).

Studies have showed a connection between intramyocellular lipid accumulation and reduced insulin mediated glucose uptake in skeletal muscle (Jacob, Machann et al. 1999; Sinha, Dufour et al. 2002). During insulin resistance in skeletal muscle, accumulation of intramyocellular lipid and inflammation impairs the insulin mediated glucose uptake in the skeletal muscle. Glucose transport and glycogen synthesis is impaired; resulting in a reduced efficiency of glucose uptake and increased blood glucose delivered to the liver (Petersen and Shulman 2002). During hepatic insulin resistance the increased lipid accumulation and inflammation impairs the ability of insulin to inhibit gluconeogenesis and this leads to an increased glucose output. In contrast, lipogenesis remains unaffected and together with the increased delivery of dietary glucose, this leads to increased lipogenesis and may cause non-alcoholic fatty liver disease (Samuel, Liu et al. 2004). However, impaired insulin action in the adipose tissue might actually be a good thing, as mice lacking insulin receptors in adipose tissue not only are protected against diet-induced obesity, but also have increased longevity and life-span (Bluher, Michael et al. 2002). Insulin resistance in adipose tissue will inhibit lipolysis, which will promote re-esterification of lipids in other tissues, such as liver and further exacerbates the insulin resistance (Samuel and Shulman 2012).

To compensate for the high blood glucose due to increased hepatic glucose production and impaired glucose uptake by peripheral insulin-sensitive tissue, the pancreatic β -cells respond by increasing the insulin production (Chang-Chen, Mullur et al. 2008). However, it appears that the β -cells are able to compensate for a limited amount of time, as insulin production eventually stops and the β -cells may undergo apoptosis (Maraschin Jde 2012). Obese persons often have increased levels of free fatty acids (FFA) together with the hyperglycemia. FFA has shown to increase insulin secretion and when high FFA levels are chronically high this has shown to impair glucose-stimulated insulin secretion (GSIS) (Goh, Mason et al. 2007). Fatty acids are also reported to induce apoptosis of β -cells *in vitro*, by a mechanism called lipotoxicity (Kharroubi, Ladrière et al. 2004).

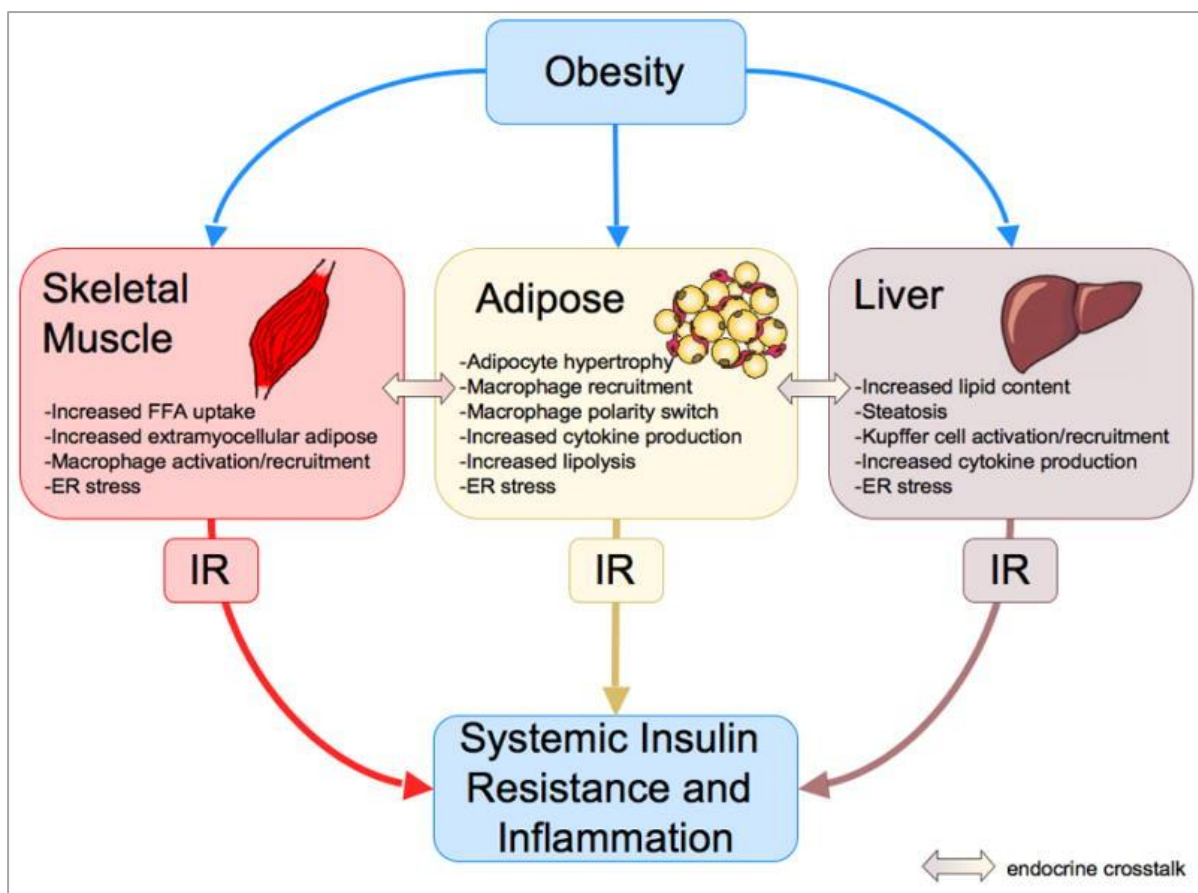


Figure 1.2: The role of obesity in development of inflammation and insulin resistance. Obesity-induced changes in skeletal muscle, adipose tissue, and liver results in inflammation and insulin resistance (IR) (de Luca and Olefsky 2008).

1.5 DIABETES

Diabetes, characterized by hyperglycemia, is divided into; type 1 diabetes mellitus (T1DM) and type 2 diabetes mellitus (T2DM). T1DM is characterized by cellular mediated autoimmune destruction of the pancreatic β -cells, that leads to a completely lack of insulin production (Kaul, Tarr et al. 2012). T1DM counts for only 5-10 % of those with diabetes. T2DM is associated with obesity and accounts for 90-95 % of those with diabetes and is increasing at an alarming rate. T2DM is developed from an deficiency or defect in insulin secretion due to the peripheral insulin resistance (Maraschin Jde 2012). When diabetes is not treated, chronic hyperglycemia may cause irreversible damage to the eyes, kidneys, nerves and blood vessels (Bailes 2002).

1.6 ADIPOSE TISSUE DYSFUNCTION AND INSULIN RESISTANCE

To maintain a stable blood glucose level during impaired insulin sensitivity, the pancreatic β -cells compensate by increasing insulin secretion. Hyperglycemia occurs when the β -cells are unable to compensate for the impaired insulin sensitivity and thereby leading to development of T2DM (Kahn, Hull et al. 2006; Giacca, Xiao et al. 2011). Insulin resistance is strongly associated with obesity, but not all obese individuals develop hyperglycemia, insulin resistance or T2DM. It appears that the development of insulin resistance is dependent on the degree of adipose tissue dysfunction (Kloting, Fasshauer et al. 2010). This dysfunction is characterized by increased visceral fat accumulation, increased adipocyte hypertrophy, and higher macrophage infiltration into visceral fat (Bluher 2009). The notion that insulin resistance is not always associated with obesity in general is illustrated by the finding by (Kloting, Fasshauer et al. 2010). These authors showed that insulin resistance was associated with adipose tissue inflammation in obese human with similar BMI (Figure 1.3).

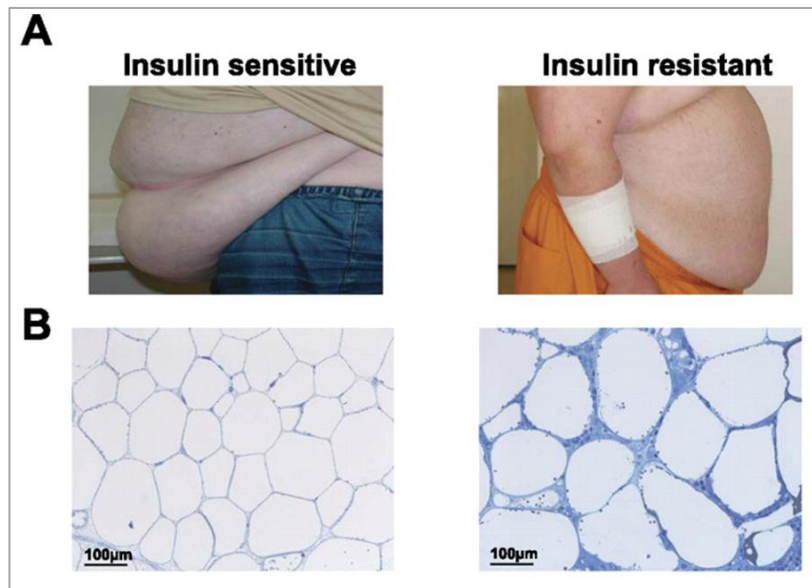


Figure 1.3: Insulin sensitivity and insulin resistance. **A:** Representative photographs for the insulin sensitive and insulin resistance morbidly obese phenotype from a study performed by (Kloting, Fasshauer et al. 2010). **B:** H&E staining of omental adipose tissue sections from representative study individuals, illustrating increased adipocyte size and macrophage infiltration in an insulin resistance state compared with the insulin sensitive state. Initial magnification X20 (Kloting, Fasshauer et al. 2010).

1.7 CYCLOOXYGENASES AND PROSTAGLANDINS

Cyclooxygenases (COX) catalyzes the first two steps in the biosynthesis of prostaglandins (PGs), from arachidonic acid (AA). The PGs are lipid mediators, involved in physiological function as protection of stomach mucosa, aggregation of platelets and regulation of kidney function (Harizi, Corcuff et al. 2008). They have also pathological functions such as involvement in inflammation, fever and pain (Smith, DeWitt et al. 2000). There are two isozymes of COX; COX-1 and COX-2. Whereas COX-1 is constitutively expressed in most tissues and produces PGs important for maintaining physiological functions, COX-2 is generally expressed in tissue at very low levels and is up-regulated by inflammatory mediators and forms PGs which are important in inflammation (Vane, Bakhle et al. 1998).

COX possesses two catalytic sites; the first is a COX-active site, converting AA to the endoperoxide PGG₂. The second, a peroxidase active site, then converts the PGG₂ to PGH₂ and PGH₂ is further processed by specific synthases to form PGs, prostacyclin and thromboxane A₂. PGs and PGE₂ prostacyclin are the main inflammatory mediators (Simmons, Botting et al. 2004).

1.8 COX-INHIBITORS AND INDOMETHACIN

COX-inhibitors or non-steroidal anti-inflammatory drugs (NSAIDs) are medicaments used for pain killing, anti-pyretic, and anti-inflammatory properties. They have an inhibitory effect on COX and thereby blocking production of PGs. NSAIDs are the most commonly used drugs in USA, representing as many as 70 million prescription and 30 billion sales yearly (Mitchell, Akarasereenont et al. 1993).

Indomethacin is a highly potent NSAID and was frequently used by patients with rheumatic disorders, but not as much with minor pain. It has a bioavailability up to 100 % with an oral administration and the half-life is 2.5 to 11.5 hours. Indomethacin has a high risk of side effects such as dizziness, headache and more (Norsk legemiddelhandbok 2010). Indomethacin is a non-selective inhibitor of COX-1 and COX-2, leading to a inhibition of PG syntheses from AA (figure 1.4) (Botting 2006). Most NSAIDs inhibits both COX-1 and COX-2, but they differ in their selectivity towards the isozymes. Indomethacin has been shown to be 60 times more potent in inhibition of COX-1 compared to COX-2. Indomethacin inhibits PG synthesis by binding to the active seat of the enzyme and influences a conformational change of the protein, making the enzyme inactive (Mitchell, Akarasereenont et al. 1993).

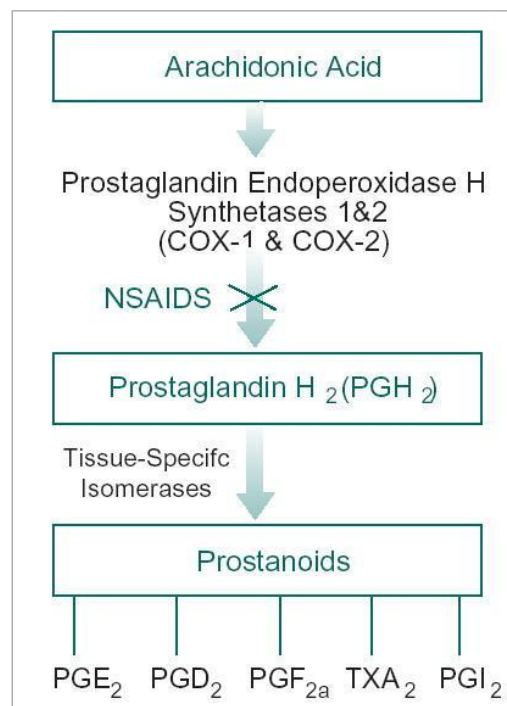


Figure 1.4: NSAIDs inhibit the synthesis of prostaglandins from Arachidonic acid (Gonzalez-Angulo, Fuloria et al. 2002)

1.9 INTRODUCTION TO THE PRESENT INVESTIGATION

Earlier studies from this group have shown that cold- and diet-induced UCP1 expression in inguinal white adipose tissue (iWAT) requires COX-activity (Madsen, Pedersen et al. 2010). Inclusion of indomethacin in a very high fat (VHF)-diet stimulates obesity development in Sv129 mice. This mouse strain is protected against diet-induced obesity, at least in part, by their ability to increase UCP1 expression in iWAT (Guerra, Koza et al. 1998; Vitali, Murano et al. 2012). The diet-induced UCP1 expression within iWAT in C57BL/6J mice is relative low, and an unpublished study in our group showed that inhibition of COX using indomethacin, prevented diet-induced obesity in C57BL/6J mice, see figure 1.5 adapted from Fjære et al. 2013 (manuscript in prep).

Obesity and glucose intolerance normally occur together, and it has been generally assumed that glucose intolerance, increased insulin secretion and insulin resistance are consequences of increased adipose tissue mass (Kahn and Flier 2000). Paradoxically, although the HF/HS+INDO-fed mice were lean and had no reduction in insulin sensitivity, indomethacin did not prevent the glucose intolerance associated with an HF/HS-diet (figure 1.5). Moreover, insulin levels in both fed and fasted state were significantly lower in HF/HS+INDO-fed mice compared to HF/HS-fed mice (figure 1.5). This suggests that the increased insulin secretion induced by the HF/HS-diet was reduced by indomethacin.

1.10 AIMS OF THE PRESENT STUDY

This study aimed to investigate the mechanism(s) by which indomethacin attenuates DIO in mice fed a HF/HS-diet and investigate if indomethacin is able to reverse obesity in mice fed a HF/HS-diet. We furthermore aimed to investigate why glucose tolerance is impaired in lean and insulin sensitive HF/HS+INDO. Therefore, we aimed to examine if the effect of indomethacin on glucose-stimulated insulin secretion was an acute effect or if indomethacin specifically inhibits the compensatory insulin secretion induced by a HF/HS-diet. Finally, we aimed to explore the possibility that indomethacin could attenuate insulin secretion in response to a meal where indomethacin was included.

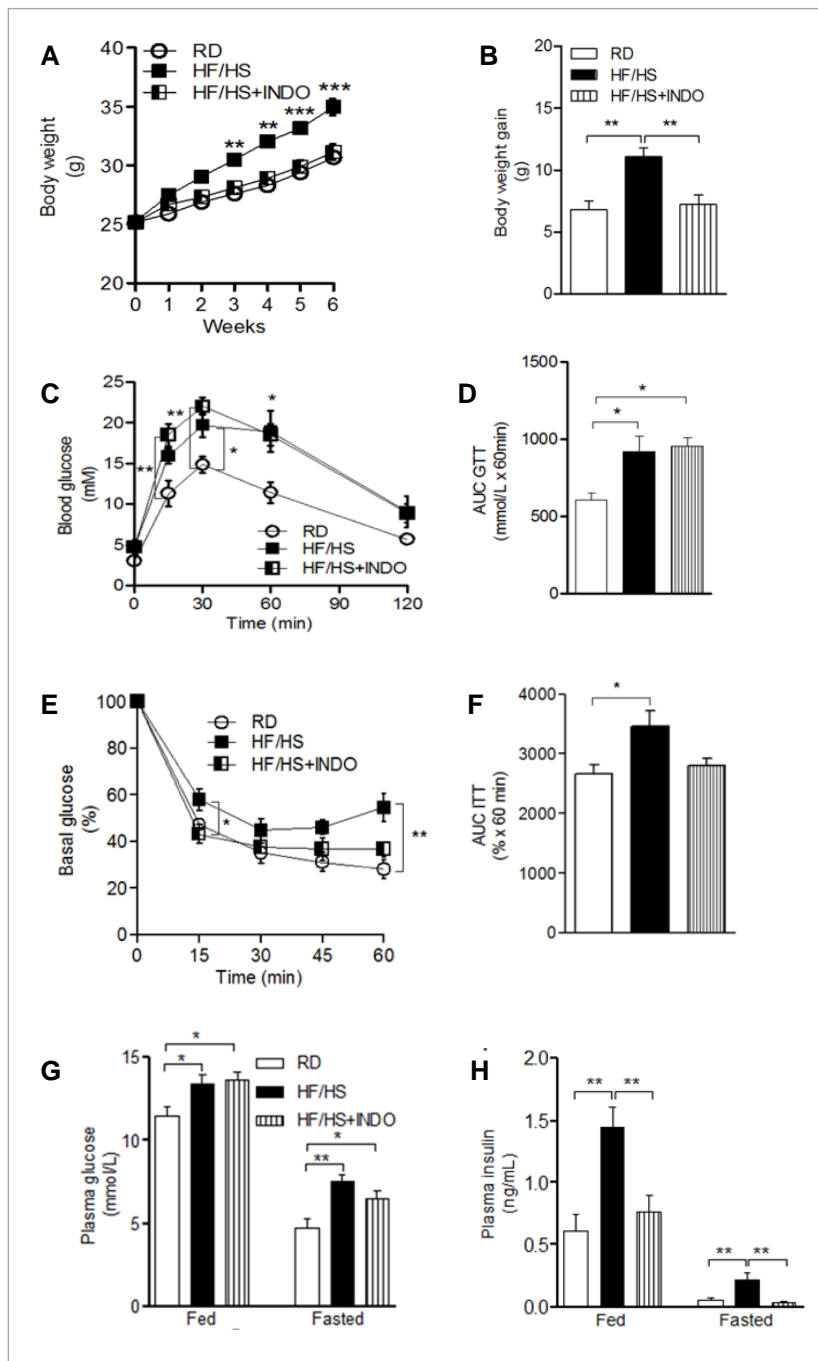


Figure 1.5: Results from a previous study performed in our group. Male C57BL/6J mice were fed regular diet (RD), high fat/high sucrose (HF/HS) diet or high fat/high sucrose diet added indomethacin (HF/HS+INDO). **A:** Body weight development during 6 weeks of feeding. **B:** Mean total body weight gain after 6 weeks of feeding. **C:** Intra-peritoneal glucose tolerance test (i.p-GTT) (2g/kg) performed on mice fasted for 6 hours. **D:** AUC i.p-GTT **E:** Insulin tolerance test (ITT) after 6 weeks on their respective diets. **F:** AUC ITT. **G:** Plasma glucose fed and fasted state. **H:** Plasma insulin fed and fasted state. All results are presented as mean \pm SEM. Statistical differences are denoted with stars; * $P \leq 0.05$, ** $P \leq 0.01$. Figures adapted from: Even Fjære, Ulrike L. Aune, Alisom H. Keenan, Tao Ma, Haldis Lillefosse, Yannan Xi, John W. Newman, Fawaz G Haj, Bjørn Liaset, karsten Kristiansen and Lise Madsen, "Indomethacin treatment prevents diet-induced obesity and insulin resistance, but not glucose intolerance in C57BL/6J mice", manuscript in preparation.

2.0 MATERIALS AND METHODS

2.1 THE ANIMAL EXPERIMENTS

The animal model

We used the C57BL/6JBomTac mouse strain as a model in all experiments. This mouse strain is commonly used in metabolic studies, because these mice rapidly develop obesity, glucose intolerance and insulin resistance when fed a high fat and high sucrose (HF/HS) (Surwit, Feinglos et al. 1995) and a high fat (HF) diet (Montgomery, Hallahan et al. 2013). During normal development, when fed a regular diet with 6 % fat, the C57BL/6J mice have an average body mass of 29, 97 gram at 16 weeks of age. In average, the blood glucose levels are 159-mg/dl and the liver masses 1.444 gram (The jackson Laboratory 2007).



Figure 2.1: C57BL/6J mouse. A frequently used animal model in studies of obesity and related metabolic diseases (The jackson Laboratory 2013).

Animal care

Male C57BL/6J mice eight-week of age, were obtained from Taconic, Denmark. The mice were housed in individual cages, and kept in a 12 hours light/dark cycle at 28-30 C° and approximately 50-55 % humidity. After one week of acclimatization, mice were assigned to different experimental diets. During the experiments the mice had free access to the respective diets and tap water. The mice were fed three times a week and received fresh water two times per week. The caloric intake for each mouse was calculated from the feed given excluding the collected feed remnants. The mice were weighted once a week and MRI-scanned (Bruker Minispec LF50mq7.5) before the experiment startup and during the experiments. The Norwegian State board of biological experiments approved all protocols used in the experiments.

Experimental setup

This master thesis consists of three animal experiments.

Experiment 1:

This first experiment was separated in two parts.

Part 1: Sixty male C57/BL6 mice were weighted and MRI-scanned before they were divided into three different groups (n=20) and fed a regular diet (RD), a high fat/high sucrose (HF/HS) diet, or an HF/HS diet supplemented with 16ppm indomethacin (HF/HS+INDO). The mice were grouped based on their body mass and fat mass, to make the groups as similar as possible and fed their respective diets for 10 weeks. After 6 weeks a second MRI-scan was performed. After 9 and 10 weeks, an intraperitoneal glucose tolerance test (*i.p*-GTT) and insulin tolerance test (ITT) were performed, respectively. Glucose and insulin were dosed based on total body- and lean mass, on half of each experimental groups. After 10 weeks of feeding the mice fed HF/HS+INDO were terminated, whereas the RD- and HF/HS-fed mice were used in the part 2 of the experiment (figure 2.2.A).

Part 2: The mice fed the RD- and HF/HS-diets from part 1 were divided into two subgroups. Based on body mass and fat mass, the RD-fed mice were divided into one subgroup continuously fed RD (n=8) and one subgroup fed RD+INDO (n=8). The mice fed HF/HS-diet from part 1 were also divided in two groups; one continuously fed the HF/HS-diet (n=9) and one with a HF/HS+INDO (n=9) (figure 2.2.A). Fractions of the C57BL/6J mice are high- and low gainers, respectively (Koza, Nikonova et al. 2006). As an important aim in this part was to investigate if indomethacin was able to reverse obesity in HF/HS-fed mice and/or reduce adipose tissue mass in RD-fed mice, it was important that the body fat content were comparable within each subgroup at onset of the experiment. Therefore, 5 mice from the RD and 4 mice from the HF/HS group were excluded after MRI-scan before onset of part 2.

Experiment 2:

Twenty male C57BL/6J mice were used in a 10-week long experiment. After one week on a RD, the mice were fed an HF/HS-diet. After both 1 week of RD-feeding and after 9 weeks of HF/HS-feeding, the mice were divided into two cohorts and an *i.p.*-GTT was performed. One cohort was injected with indomethacin (2,5 mg kg/body mass) dissolved in saline, (Enos, Davis et al. 2012) or the saline solution precisely 1 hour before the *i.p.*-GTTs were performed.

Experiment 3:

Sixty male C57BL/6J mice were weighed and MRI-scanned before they were divided into three different diet groups (n=20). To ensure comparable initial body mass and fat mass within each experimental group, the mice were weighed and MRI-scanned before assigned to their respective diets. The mice were fed an RD, an HF/HS diet, or an HF/HS+INDO-diet. An *i.p.*-GTT was performed after 1, 2, 3, and 9 weeks, and an oral glucose tolerance test (OGTT) after 8 weeks of feeding. A meal tolerance test (MTT) was performed at the onset of the experiment (initial MTT) and after 1, 2, 3, and 10 weeks of feeding (figure 2.2.B).

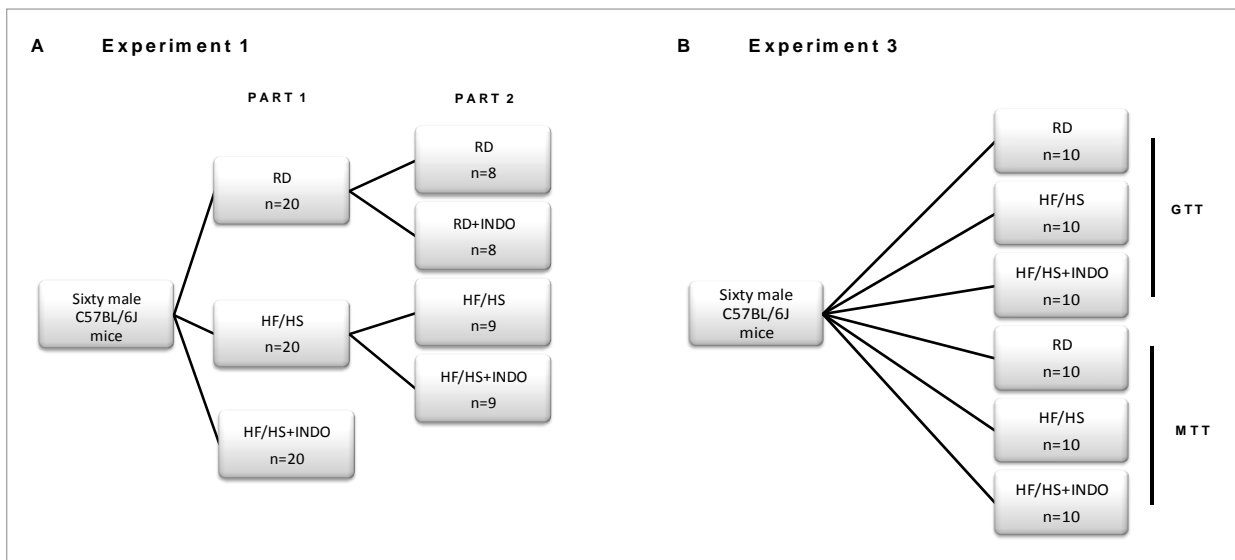


Figure 2.2: Experimental design. **A:** Experiment 1. **B:** Experiment 3.

Experimental diets

In the animal experiments, four different diets were used: RD, RD+INDO, HF/HS and HF/HS+INDO. Details regarding the composition of the diets are shown in table 2.1. The diets were obtained from Ssniff, Spezialdiaten, Germany and were specially designed for rodents. The producer mixed the non-selective COX-inhibitor indomethacin into the diets. The concentration of indomethacin was added at a concentration of; 16-mg/kg diet. The diets were stored at -20 °C during the experiments.

Table 2.1: Components of the different diets used in the feeding experiments.

Ingredients	RD (g/100g)	RD+INDO (g/100g)	HF/HS (g/100g)	HF/HS+INDO (g/100g)
Energy	18,0 MJ ME/Kg	18,0 MJ ME/Kg	20,1 MJ ME/Kg	20,1 MJ ME/Kg
Protein	20,8	20,8	17,7	17,7
Fat	4,2	4,2	25,1	25,1
Starch	46,8	46,8	-	-
Fiber	5,0	5,0	5,0	5,0
Sugar	10,8	10,8	44,6	44,6
Crude ash	5,6	5,6	3,4	3,4
Indomethacin	-	0,0016	-	0,0016

Figure 2.3 gives a schematic presentation of the metabolizable energy distribution in the RD- and HF/HS-diets. The RD contained 18,0 MJ/kg of energy and the HF/HS diets contained 20,1 MJ/kg of energy.

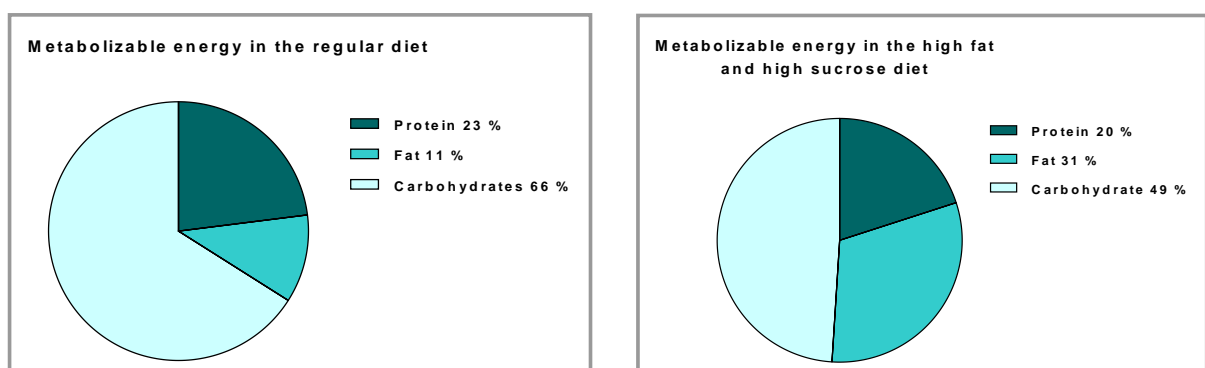


Figure 2.3: Distribution of metabolizable energy in the regular diet and high fat/high sucrose diet.

2.2 GLUCOSE TOLERANCE TEST AND GLUCOSE-STIMULATED INSULIN SECRETION

Glucose tolerance test (GTT) is a commonly used method in diabetes research to evaluate glucose homeostasis in mice (Andrikopoulos, Blair et al. 2008). The mice were placed in new cages in the morning and fasted for 6 hours to achieve baseline blood glucose levels. The mice had tap water available during the fasting period, but not during the test. The amount of glucose injected intraperitoneal (*i.p*) or orally gavage was based on their body mass, (2 mg/g body mass) or on their lean mass (3 mg/g lean mass). The blood samples were collected by tail puncture and measured using a glucometer (Contour next USB glucometer, Bayer healthcare, USA). Blood glucose levels were measured before the injection with glucose (0 minutes). After the injection, the blood glucose was measured after 15, 30, 60 and 120 minutes. To evaluate glucose-stimulated insulin secretion (GSIS), 20 μ l of blood were collected before the injection with glucose and 15 minutes after the injection. The blood was centrifuged 10 minutes with 1300 x g, and 7-10 μ l of plasma was pipetted in new tubes and stored at -80 °C until analyzing plasma insulin with ELISA insulin kit.

2.3 INSULIN TOLERANCE TEST

The insulin tolerance tests (ITT) were performed according to a protocol described by (Bruning, Winnay et al. 1997). To achieve comparable blood glucose levels between the mice, all mice were allowed to eat for one hour followed by one hour of fasting before the ITT was performed. The blood glucose was measured, using a glucometer as described above before the intraperitoneal injection with insulin and after 15, 45 and 60 minutes. The amount of insulin injected was based on their body mass (0.75 U/g body mass), or lean mass (1 U/g lean mass).

2.4 MEAL TOLERANCE TEST AND MEAL STIMULATED INSULIN SECRETION

The meal tolerance test (MTT) was performed after the description from (Coate and Huggins 2010). The mice were fasted over night and the blood glucose levels were measured after the 16 hours of fasting. The mice had tap water available during the fasting and during the meal. The mice were feed 0.7 gram of their respective diets and they were allowed to eat for 20 minutes. Blood glucose levels were measured when feed remaining (if any) was removed (designated time 0), and 15, 30, 60 and 120 minutes after the meal using a glucometer as

described above. To measure meal stimulated insulin secretion (MSIS), 20 μ l of blood were collected before the meal and 15 minutes after the meal. The blood were centrifuged as described above and 7-10 μ l of plasma were transferred to new tubes and stored in -80 °C until analyzing the plasma insulin levels with ELISA insulin kit.

2.5 TERMINATION AND COLLECTION OF TISSUE

The mice were anaesthetized with isofluran (Isoba-Vet, Schering Plough Denmark) using the anesthesia apparatus Univentor 400 Anesthesia Unit (Univentor Limited, Sweden) and terminated with cardiac puncture. 0.8 μ l of blood was collected from the heart with a syringe and placed in a tube that contained the anticoagulant EDTA. The samples were then centrifuged at 1300 x g in 10 minutes to separate plasma from red blood cells. Inguinal- (iWAT), epididymal- (eWAT), interscapulat (iBAT) -adipose tissue and liver tissue were dissected out, weighted, placed in plastic bags and freeze clamped before they were quickly transferred to dry ice and later stored at -80 °C until further analyses. Parts of eWAT, iWAT and liver were fixed in 4 % formaldehyde and later prepared for histological examination.

2.6 INSULIN MEASUREMENT IN PLASMA USING ELISA INSULIN KIT

Insulin (mouse) ELISA-kit (DRG Instruments, GmbH, Germany) was used to measure insulin levels in plasma. For reagents see appendix table A.1. Two monoclonal anti-insulin antibodies are directed against separate determinants on the insulin molecule. One of the anti-insulin antibodies is bound to the well and the other is conjugated with peroxidase. Both of the anti-insulin antibodies react with the insulin in the samples. Unbound conjugated antibodies are removed by washing. The bound conjugated antibodies are detected with a spectrophotometer after reaction with 3,3',5,5'-tetramethylbenzidine. It's proportional to the amount of insulin present in the sample (User's manual Insulin Mouse ELISA).

All reagents and plasma samples were brought to room temperature before use. Standards were analyzed in duplicates. 5 μ g of plasma was diluted with 5 μ g of calibrator 0 and 10 μ g of the calibrators and the plasma was added to a 96-well plate. 100 μ g of enzyme conjugate were added to each well and the plate was covered with plastic and placed on a shaker (Labsystems iEMS Reader MF) for 2 hours. After incubation the samples were washed 6

times with an automatic washer (Skan washer 300 version B). 200 µg of TMB substrate solution were added to each well and the plate was incubated for 15 minutes in room temperature in the dark. 50 µg of stop solution were added to each well and put on a shaker for 5 seconds. The absorbance was measured at 450 nm using a plate reader (Labsystems iEMS reader MF) (User's manual Insulin Mouse ELISA).

2.7 HISTOLOGY

Sections from eWAT, iWAT, iBAT and liver were subjected to H&E after fixation, dehydration and paraffin embedding. For reagents see appendix table A.2.

Fixation

Small sections of tissue were fixated in 4 % paraformaldehyde and 0.1 M phosphate buffer (PB) directly after dissection. After 15 hours of fixation, the samples were washed once in 0.1 M PB, and then left for 1 hour in the buffer before dehydration.

Dehydration and infiltration

Water and the fixative solutions from the tissue were removed with repeatedly replace the fixative with increasing concentration of alcohol. Dehydration steps are listed in table 2.2.

Table 2.2: Dehydration steps of tissue

Reagent	Time (min)
75 % Alcohol	45
95 % Alcohol	45 x 2
100 % Alcohol	45 x 3
Xylen	45 x 2
Paraffin	overnight
Paraffin	15 x 2

When the tissues were completely dehydrated in 100 % alcohol, the alcohol was replaced with Xylen, a medium both soluble in alcohol and paraffin. The tissues were infiltrated in liquid paraffin (Histowax, histolab products AB, Sweden), heated to 60 C° and stored overnight.

Paraffin embedding and sectioning

The tissues were embedded in paraffin using EC 350 paraffin embedding center (Microtom international, GmbH, Germany). A microtome (Leica RM2165, Germany) was used to cut 3-4 μm thin slices from the embedded tissue. The sections were carefully placed in a bath with ddH₂O added some drops of methanol. The methanol is added to help the tissue to stretch. The sections were transferred to microscope slides and left to dry overnight.

Hematoxylin and eosin staining

Before the tissue sections were stained by hematoxylin and eosin (H&M) they were rehydrated. Hematoxylin stains the nucleus of the cell and eosin stains the cytoplasm. Table 2.3 presents the procedure of rehydration, staining and dehydration of the tissue sections. After staining, the slides were dehydrated and mounted with a xylene-based glue and cover glass, and left to dry over night.

Table 2.3: hematoxylin and eosin staining procedure

Reagent	Time
Xylene	2 x 10 min
100 % EtOH	2 x 10 min
95 % EtOH	2 x 5 min
75 % EtOH	5 min
50 % EtOH	5 min
ddH ₂ O	5 min
Hematoxylin	2 min
H ₂ O	wash
Eosin	30 sec
H ₂ O	wash
ddH ₂ O	1 min
50 % EtOH	2 min
75 % EtOH	2 min
95 % EtOH	2 x 2 min
100 % EtOH	2 x 5 min
Xylene	2 x 5 min

Microscopy

The stained sections of iWAT, eWAT, iBAT and liver were visually examined and photographed using lab Olympus BX 51 binocular microscope.

2.8 REAL TIME qPCR

Real Time qPCR is a fluorescence-based method used for analyzing gene expression. The final results represent the mRNA expression at the time of the sample collection. The relatively simple design and the ability to handle large number of samples are some of the advantages with this method (Valasek and Repa 2005). Liver tissue from experiment 1 part 2 was analysed with Real Time q-PCR.

RNA purification

The first step in the RNA purification was to homogenize the liver tissue in Triazol, a solution containing phenol and guanidinium salts. Chloroform was added to separate RNA from DNA and proteins, isopropanol was added to extract RNA from the water phase (NIFES 2005). RNA is vulnerable and easily degraded if not carefully handled and it is important to isolate RNA of good quality to produce accurate and reliable results for the Real Time qPCR analyses (Valasek and Repa 2005). Reagents and chemicals used in RNA purification are listed in appendix table A.3.

Homogenization: Small pieces of frozen liver tissue were put in single tubes with 1 ml of Triazol and 2-4 beads. The tubes were then homogenized with a machine (Precellys 24 lysis & homogenization instrument, Bertin Technologies) who shacked the tubes at 6000 rpm for 3x10 seconds (NIFES 2005).

RNA purification: Homogenized samples were centrifuged 10 minutes at 12000 g at 4 °C. The homogenate was then added to clean tubes and 200 µl of chloroform was added and the tubes were shacked for 15 seconds. The mixed solution was incubated for 3 minutes in room temperature. The samples were then centrifuged 15 minutes at 12 000 x g at 4 °C. After the centrifugation, the solution contained two phases; the upper blank phase contained the RNA and was transferred to a new tube and 500µl isopropanol was added. The mixture was incubated for 10 minutes at room temperature and subsequently for 10-60 minutes at 4 °C. The samples were centrifuged 20 minutes at 12000 x g. After centrifugation the supernatant was removed with a pipette and the RNA-pellet was washed by adding 1 ml of cold 75% ethanol in the tube. The tubes were vortexed until the RNA-pellet loosened from

the bottom of the tube and subsequently centrifuged 5 minutes at 13000 x g. After 3 washes the supernatant was removed by decanting with a pipette. The RNA pellet was dried and resolved in 50-200 μ l ddH₂O. The RNA concentration was measured using the Nanodrop ND 1000 (NIFES 2005).

RNA concentration and purity on the Nanodrop ND-1000

The RNA concentrations were measured using a Nanodrop 1000 spectrophotometer (Saveen Werner, Sweden). RNA concentrations were measured at wavelength 260 nm and acceptable values for concentration were in within a range of 50-3000 ng/ μ l. The instrument calculated ratio of wavelength 260/230 nm, this ratio is a good indicator of sample purity. A ratio between 1,7-2,0 is considered as approved purity. A low ratio can be a sign of high salt content in the sample or other impurities (NIFES 2005).

The RNA quality is measured on a bioanalyzer. The measurements on the Nanodrop spectrometer examine only concentration and purity of the samples, but not the sample quality.

cDNA synthesis using Reverse Transcription reaction

The RNA is reversed transcribed to cDNA with the Reverse Transcription (RT)- reaction using the enzyme reverse transcriptase. Reagents and chemicals used in RT-reaction are listed in appendix table A.4. cDNA is synthesized from RNA from the samples, by using Multiscribe reverse transcriptase with Oligo d(T)₁₆ primer . To ensure that the RNA concentration was acceptable, all samples were measured with Nanodrop ND-1000. RNA or ddH₂O was added to achieve the desired concentration of 50 ng/ μ l (+/- 5%) (NIFES 2005).

A pool of RNA with 5 μ l from each sample was prepared and subsequently a series of dilutions was made from this pool, this represented the samples for a standard curve at the 96-RT plate. The RT-reaction mix was prepared with the ingredients listed in table 2.4 (NIFES 2005).

Table 2.4: The RT-reaction mixture used in 50 μ l reaction (NIFES 2005).

Reagents	50 μ l	Concentration
RNase free ddH ₂ o	8,9	
TaqMan RT buffer 10X	5,0	1X
MgCl ₂ (25mM)	11,0	5,5 mM
GeneAmp ® deoxyNTP Blend (10 nM)	10,0	500 μ M per dNTP
Oligo d(T) ₁₆ primer (50mM)	2,5	2,5 μ M
RNase inhibitor (20U/ μ l)	1,0	0,4 U/ μ l
MultiScribe™ Reverse Transcriptase	1,67	1,67 U/ μ l

40 μ l of the RT-reaction mix was distributed in each well. A clean plastic cover was placed on top and the plate was centrifuged for 1 minute at 50 x g. The plate was then placed in the Gene Amp. PCR system 9700 PCR machine (Applied biosystems, USA). The terminal cycling parameters for RT-reaction are shown in table 2.5. The RT-plates were stored at -20 °C until use.

Table 2.5: Temperature conditions during RT-reaction.

Step	Temperature (°C)	Time (minutes)
Incubation	25	10
Reverse transcriptase reaction	48	60
Reverse transcriptase inactivation	95	5
End	4	∞

Determination of gene expression by RealTime qPCR

The Real Time qPCR was used to measure the gene expression of the liver tissue. The target DNA sequence was the cDNA synthesized in the RT-reaction. The thermal cycle program used at the Lightcycler 480 is listed in table 2.6. The pre-incubation activates the FastStart DNA polymerase. The second step is amplification of target DNA and the amplification continues in 40 cycles. Each new cycle starts with primer annealing to target sequence followed by elongation. The fluorescent SYBR Green is a DNA binding dye, amplified cDNA and increase fluorescence intensity. The fluorescence is high at high rates of double stranded DNA (dsDNA) and low intensity when the presence of dsDNA is low. A fluorescence sensitive instrument is monitoring the fluorescence at the end of every PCR cycle and thereby monitoring amplification of DNA during the whole process. The fluorescence is

detected at wavelength 510 nm using a charge-coupled device camera. The original amount of target sequence correlates with the cycle time (Ct), when the fluorescence reaches a threshold level. The Ct value is thereby used for a quantitative determination of gene expression.

There are three steps in a PCR reaction. The first step is denaturation at 98 °C. The high temperature denatures the DNA strands and melts the DNA into single strands. The second step is to lower the temperature to 60 °C, now the primer binds to their specific sites. Finally the temperature rises to 72 °C and the complementary strand extension from each annealed primer.

Table 2.6: The thermal cycle program used in a RealTime PCR machine.

Step	Temperature (°C)	Time	Number of cycles
Pre- incubation	95	5 minutes	1
Amplification	95	10 seconds	40
	60	20 seconds	
	72	30 seconds	
Melting point analyzing	95	5 seconds	1
	65	1 minute	
	97		
Cooling	40	10 seconds	1

A reaction mix was prepared with the following ingredients for a full plate (Table 2.7) (NIFES 2005). 110 µl of reaction-mix was pipette into 8 wells on a strip and a plastic cover put on top. The RT-plate was vortexes at 1100 rpm for 3 minutes and then centrifuged at 1000 x g in 1 minute. The RT-plate and the 8 wells strip with the mix was placed in a pipette robot (Biome 3000 Laboratory Automation Workstation, Beckman Coulter, USA). The Real Time plate was centrifuged at 1500 x g in 2 minutes and placed in the Light Cycler 480 Real-Time PCR system (Roche, Norway) (NIFES 2005).

Table 2.7: Reaction mix with the respective primer for Real Time qPCR reaction (NIFES 2005).

Reagents	Amount
ddH ₂ O	331 µl
Primer 1 (forward)	5,7 µl
Primer 2 (reverse)	5,7 µl
Cyber Green	570 µl

2.8 STATISTICAL ANALYSES

Statistical analyses of data were performed with GraphPad Prism v 6.0. The homogeneity of the variances in the data was tested using Bartlett's test of equal variances. Where there was no significant difference in variance or normality, one-way ANOVA were used to compare differences between the RD, HF/HS and HF/HS+INDO fed mice, followed by Tukey's Multiple Comparison Test. In part 2 in experiment 1, an unpaired T-test was performed between the RD- and RD+INDO-fed mice, and between the HF/HS- and HF/HS+INDO-fed mice. Dixon's Q-test was used for detection of single outliers.

Results were considered significant different with a P-value < 0.05. All results are presented as mean \pm SEM. Statistical differences are denoted with stars; * P \leq 0.05, ** P \leq 0.01, *** P \leq 0.001, **** P \leq 0.0001.

3.0 RESULTS

3.1 EXPERIMENT 1, PART 1

INDOMETHACIN REDUCED BODY WEIGHT GAIN AND FEED EFFICIENCY

To confirm the ability of indomethacin to attenuate high fat high sucrose (HF/HS)-induced obesity in C57BL/6J mice, a 10-week feeding experiment was performed. Three different diets were used; HF/HS-diet, HF/HS+INDO-diet and RD (chow) as a reference. The body weight development during the feeding experiment is shown in figure 3.1.A.

As expected, HF/HS-fed mice gained significantly more weight than the RD-fed mice. Confirming an earlier unpublished study in our group, the body weight gain was significantly reduced by inclusion of indomethacin in the HF/HS-diet (figure 3.1.B). This difference in weight gain could not be explained by differences in the energy intake, as this was similar between the HF/HS- and HF/HS+INDO-fed mice (Figure 3.1.C). Thus, the feed efficiency was lower in HF/HS+INDO-fed mice, than in HF/HS-fed mice (figure 3.1.D).

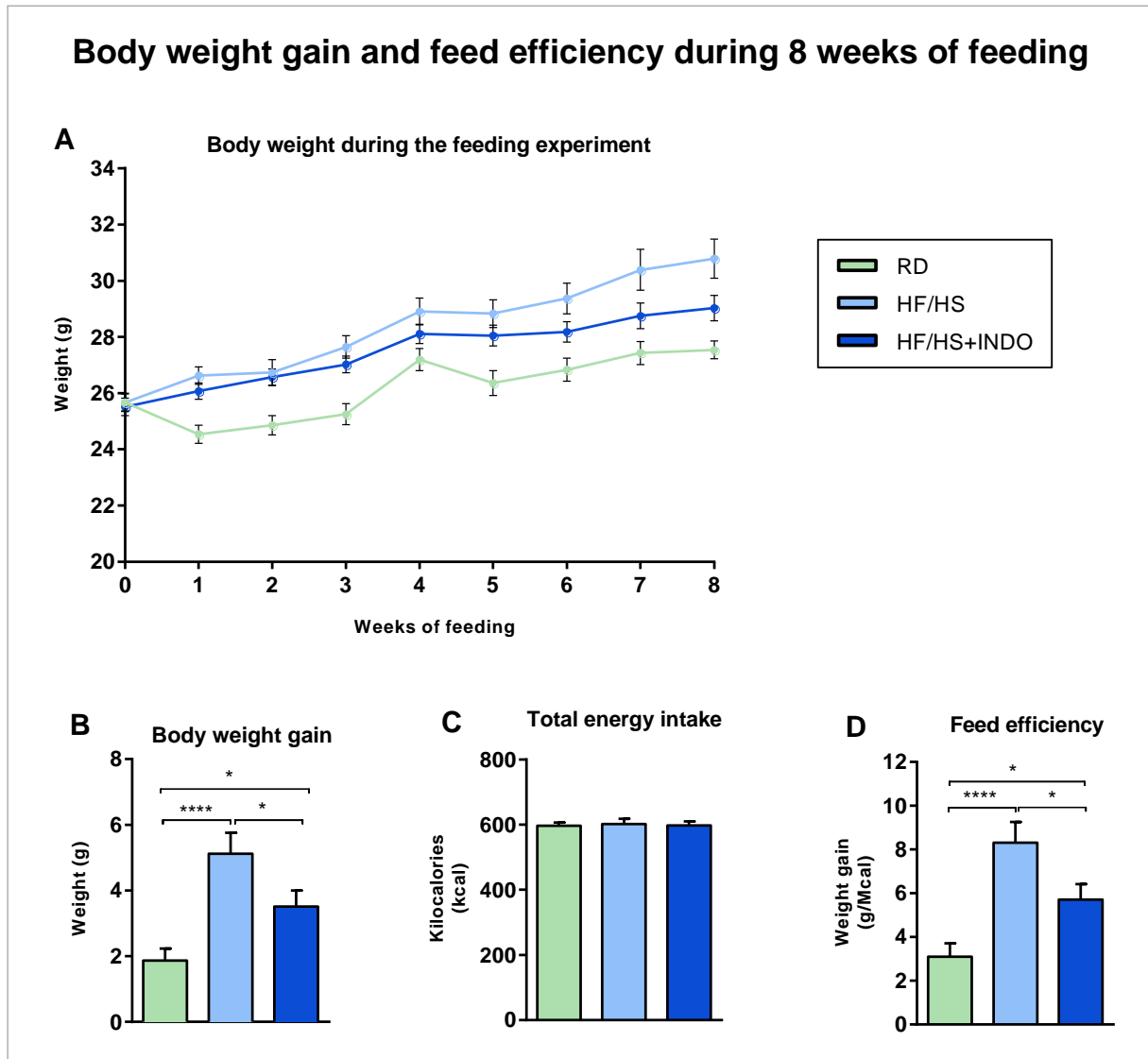


Figure 3.1: Male C57BL/6J mice ($n=18-20$) were fed a high fat/high sucrose-diet with and without indomethacin and a regular-diet for 10 weeks. All results in this figure present data before the testing was performed. **A:** Body weight development during the first 8 weeks of the feeding experiment. **B:** Body weight gain after 8 weeks of feeding. **C:** Total energy intake (kcal) during the 8 weeks of feeding. **D:** Feeding efficiency was calculated based on energy intake and weight gain. All results are presented as mean \pm SEM. Statistical differences are denoted with stars; * $P \leq 0.05$, ** $P \leq 0.01$, *** $P \leq 0.001$, **** $P \leq 0.0001$.

INDOMETHACIN ATTENUATED HF/HS-INDUCED OBESITY DEVELOPMENT

HF/HS+INDO-fed mice gained significantly less body weight than HF/HS-fed mice. To confirm that indomethacin attenuated HF/HS-induced obesity, a MRI-scan was performed after 6 and 8 weeks of feeding. After 6 weeks, HF/HS+INDO-fed mice had significantly less fat mass than HF/HS-fed mice (figure 3.2.A). The difference in fat mass was even more pronounced after 8 weeks on their respective diets (figure 3.2.B). After 6 weeks of feeding, lean mass was not significantly different between RD, HF/HS and HF/HS+INDO-fed mice (figure 3.2.C). However, after 8 weeks, both HF/HS- and HF/HS+INDO-fed mice had lower lean mass than the RD-fed mice (figure 3.2.D). This indicates that indomethacin attenuates the HF/HS-induced growth of fat mass.

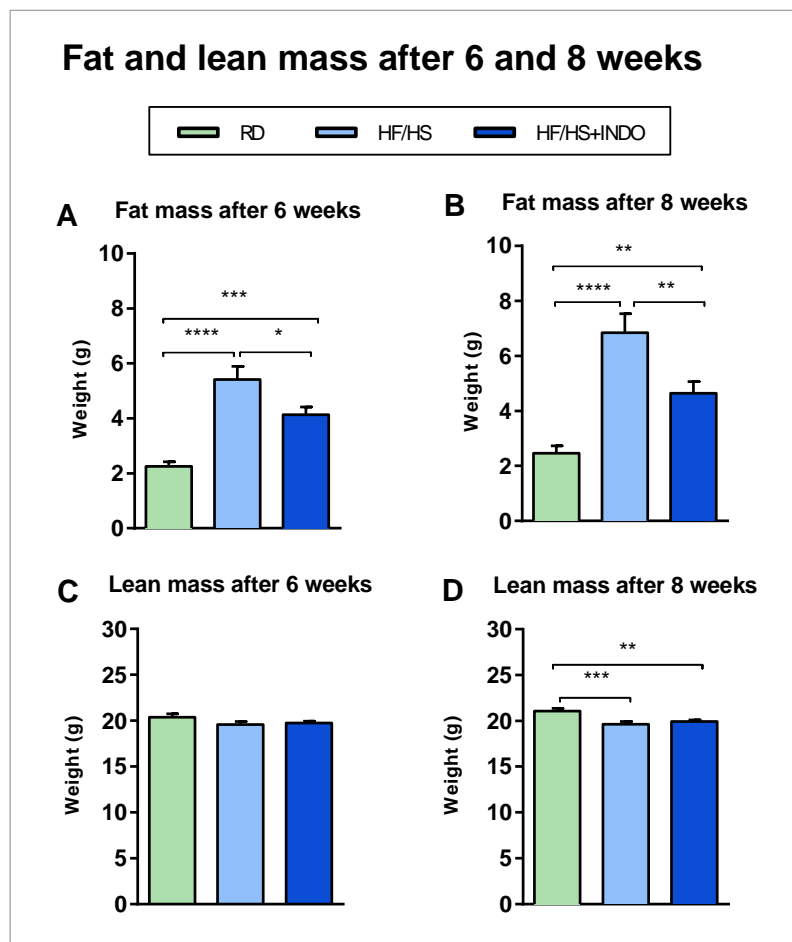


Figure 3.2: Body composition of fat mass and lean mass of the male C57BL/6 mice (n=18-20) after 6 and 8 weeks on their respective diets. **A:** Fat mass (g) after 6 weeks of feeding **B:** Fat mass (g) after 8 weeks of feeding **C:** Lean mass (g) after 6 weeks of feeding **D:** Lean mass (g) after 8 weeks of feeding. All results are presented as mean \pm SEM. Statistical differences are denoted with stars; * $P \leq 0.05$, ** $P \leq 0.01$, *** $P \leq 0.001$, **** $P \leq 0.0001$.

INDOMETHACIN DID NOT PREVENT HF/HS-INDUCED GLUCOSE INTOLERANCE

As mentioned, obesity and impaired glucose tolerance normally occur together, and it has been assumed that the impaired glucose tolerance and the following increased insulin secretion and insulin resistance are consequences of increased adipose tissue mass. Thus, the earlier unpublished findings that HF/HS+INDO-fed mice have improved insulin sensitivity, co-occurring with impaired glucose tolerance are surprising. To confirm this somewhat paradoxical phenotype, an *i.p.*-GTT was performed in the fasted state after 9 weeks of feeding. Insulin levels were measured in the fasted state and 15 minutes after glucose injection to determine glucose-stimulated insulin secretion (GSIS).

Blood glucose levels before and after *i.p.*-injection of glucose (2 mg/g body mass) are shown in figure 3.3.A. Calculation of area under curve (AUC) showed that mice fed a HF/HS-diet with and without indomethacin, had significantly impaired glucose tolerance compared with RD-fed mice. In agreement with an earlier unpublished study performed in our group, the AUC from the *i.p.*-GTT indicated no significant difference between HF/HS-fed mice and HF/HS+INDO-fed mice (figure 3.3.B).

Fasting blood glucose levels are presented in figure 3.3.C. Compared with RD-fed mice, fasting blood glucose levels were significantly increased in HF/HS-fed mice, but not in HF/HS+INDO-fed mice. 15 minutes after the glucose injection, there were no significant difference in blood glucose levels between HF/HS- and HF/HS+INDO-fed mice, but HF/HS-fed mice had significant higher blood glucose levels than RD-fed mice (figure 3.3.D).

As expected, the HF/HS-diet led to a significant increase in plasma insulin levels in the fasted state. Importantly, this was not seen when indomethacin was added in the feed (figure 3.3.F). Furthermore, compared with RD-fed mice, the insulin levels 15 minutes after the *i.p.*-injection were significantly higher in mice fed the HF/HS-diet. Insulin levels 15 minutes after *i.p.*-injection was not significantly higher in mice fed HF/HS+INDO than in RD-fed mice (figure 3.3.G). Thus, the change in plasma insulin levels from fasted state to 15 minutes after the *i.p.*-injection were significant increase in the HF/HS-fed mice, but not when indomethacin was added in the feed.

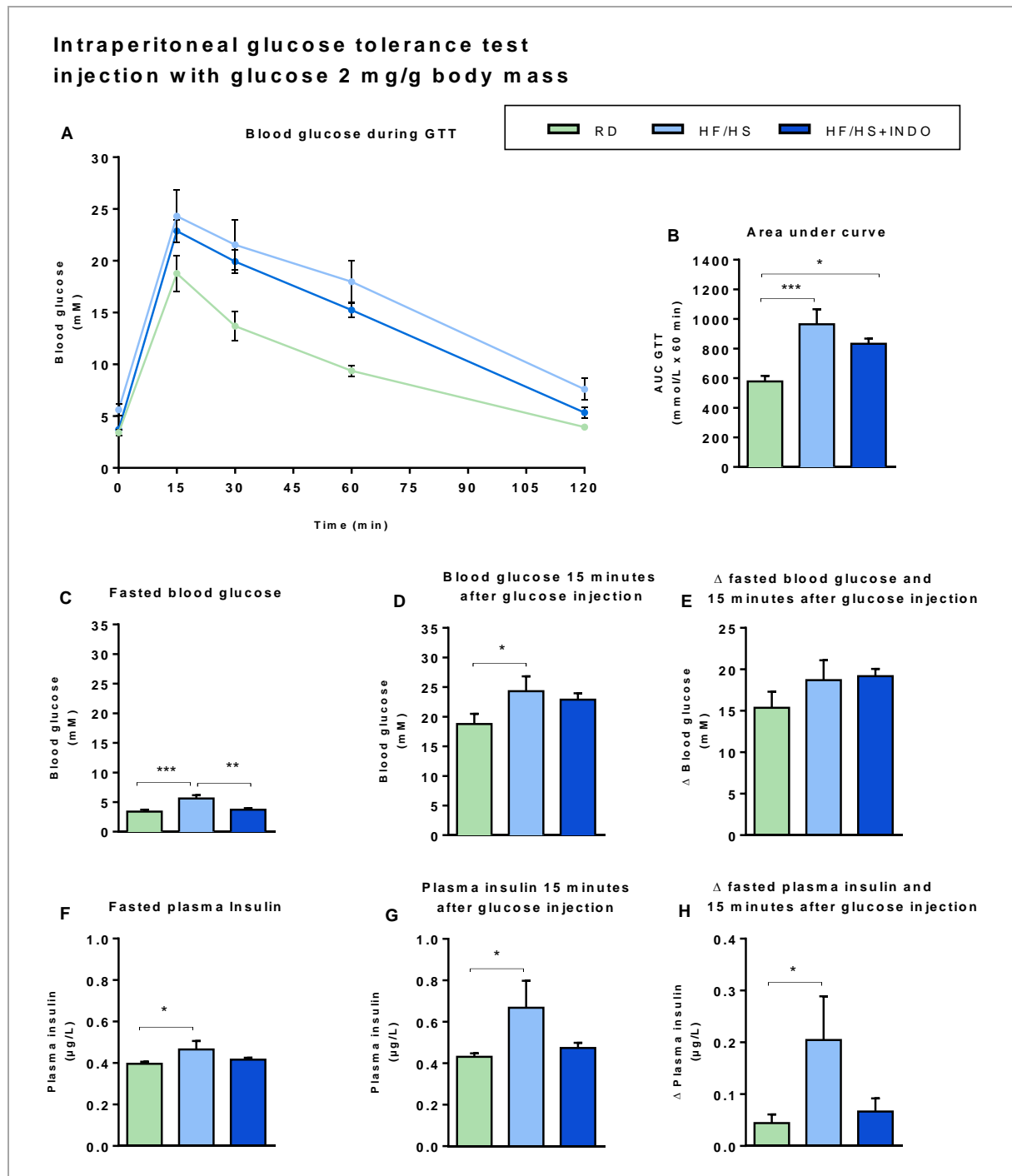


Figure 3.3: An *i.p.*-GTT was performed after 9 weeks on mice fed RD, HF/HS and HF/HS+INDO ($n=10$). The mice had fasted for 6 hours when the test started. The mice were given an intraperitoneal (*i.p.*)-injection with glucose (2mg/g body mass) **A:** Blood glucose during the *i.p.*-GTT, the blood glucose levels were measured before- and 15, 30, 60 and 120 minutes after *i.p.*-injection. **B:** AUC. **C:** Blood glucose after 6 hours of fasting. **D:** Blood glucose levels 15 minutes after the *i.p.*-injection **E:** Change in blood glucose from fasted to 15 min after the *i.p.*-injection. **F:** Plasma insulin after 6 hours of fasting. **G:** Plasma insulin 15 minutes after the *i.p.*-injection. **H:** Glucose stimulated insulin secretion, the change in plasma insulin from fasted to 15 minutes after the *i.p.*-injection. All results are presented as mean \pm SEM. Statistical differences are denoted with stars; * $P \leq 0.05$, ** $P \leq 0.01$, *** $P \leq 0.001$.

INDOMETHACIN ATTENUATED HF/HS-INDUCED INSULIN RESISTANCE EVALUATED BY HOMA-IR INDEX

To evaluate the insulin sensitivity, a homeostasis model assessment-insulin resistance (HOMA-IR) index of all mice was calculated. A high HOMA-IR score indicates insulin resistance or T2DM. HOMA-IR index is normally calculated from fasted plasma levels of glucose and insulin in the same mouse (Bonora, Formentini et al. 2002). Here, we used fasted blood glucose and serum plasma insulin levels to calculate HOMA-IR in the formula: $(\text{Fasting blood glucose (mmol/L)} \times \text{fasting plasma insulin (mU/L)})/22,5$

The calculated HOMA-IR score is presented in figure 3.4. The HOMA-IR score was significantly higher in HF/HS-fed mice than both RD- and HF/HS+INDO-fed mice. This indicates that indomethacin attenuates HF/HS-induced insulin resistance.

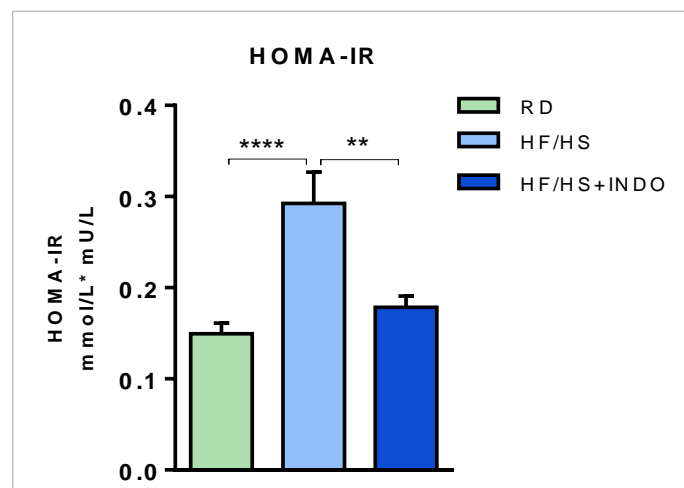


Figure 3.4: HOMA-IR score determined from blood glucose and plasma insulin levels in mice fed RD, HF/HS and HF/HS+INDO. All results are presented as mean \pm SEM. Statistical differences are denoted with stars; * $P \leq 0.05$, ** $P \leq 0.01$, *** $P \leq 0.001$, **** $P \leq 0.0001$.

INDOMETHACIN DID NOT IMPROVE INSULIN SENSITIVITY WHEN MEASURED BY INSULIN TOLERANCE TEST

The HOMA-IR index indicates that indomethacin attenuates HF/HS-induced insulin resistance. To confirm this, an ITT was performed (figure 3.5). Surprisingly, AUC showed that there were no significant differences between RD, HF/HS or HF/HS+INDO-fed mice in the ITT.

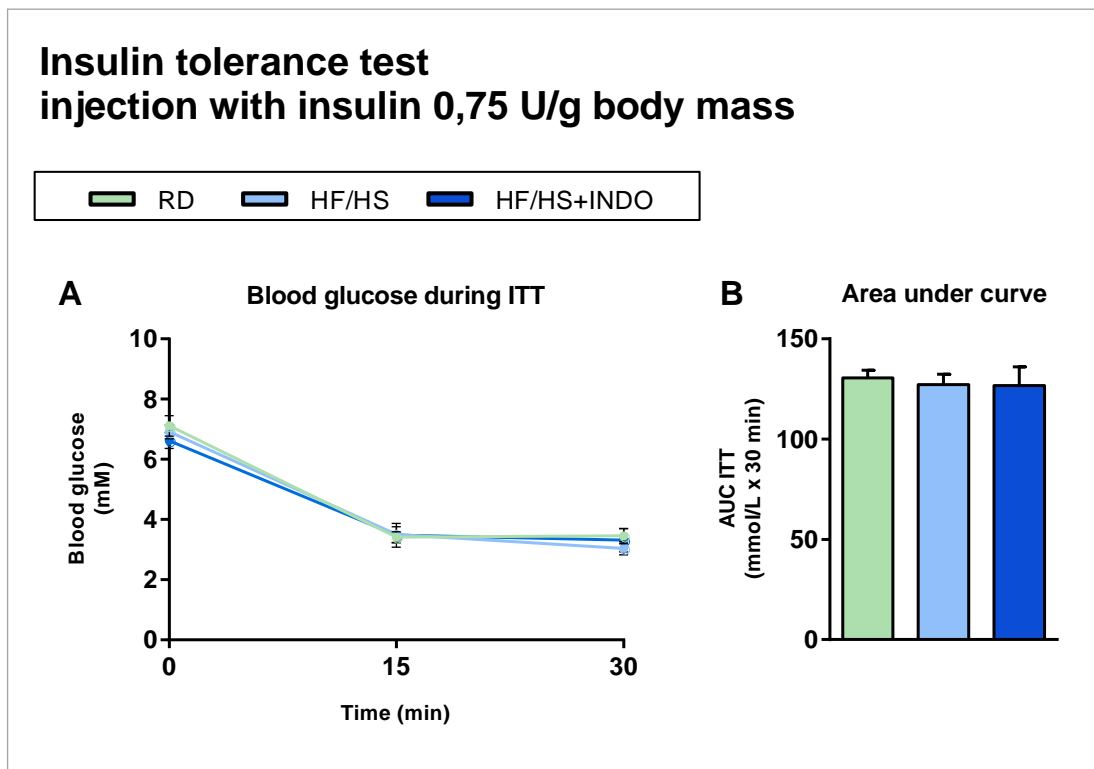


Figure 3.5: An ITT was performed after 10 weeks on mice fed RD, HF/HS and HF/HS+INDO (n=10) **A:** measurement of blood glucose levels before and 15 and 30 minutes after i.p injection with insulin **B:** AUC. All results are present as mean \pm SEM.

EVALUATION OF *i.p*-GTT AND ITT ON INJECTION DOSE BASED ON BODY MASS VS. LEAN MASS

It is generally accepted that approximately 75% of the glucose is taken up in skeletal muscle (Lin and Sun 2010). Therefore, when glucose is injected based on total body mass, glucose tolerance measured by an *i.p*-GTT might thus simply reflect an increased adipose tissue mass. Conversely, if the dose of insulin injected during the ITT is based on total body mass, obese mice are injected with a higher dose of insulin than lean mice, and might thus appear more insulin sensitive. Therefore, to re-evaluate the glucose intolerance and insulin sensitivity, the *i.p*-GTT and ITT were re-performed. Here the glucose and insulin load injected were calculated based on lean body mass.

***i.p*-GTT - injection dose based on total body mass vs. lean mass**

The *i.p*-GTT performed on injection dose based on lean mass confirmed the reduced glucose tolerance in both HF/HS- and HF/HS+INDO-fed mice (figure 3.6). Moreover, as seen when the glucose load was based on body weight, AUC was not significantly different between HF/HS- and HF/HS+INDO-fed mice.

The *i.p*-GTT verified that fasting blood glucose levels were significantly increased in HF/HS-fed mice compared to RD-fed mice. Furthermore, there was no difference between HF/HS- and HF/HS+INDO-fed mice in fasted blood glucose levels or blood glucose levels 15 minutes after the *i.p*-injection (figure 3.6.D). This was not observed when glucose load was based on body mass.

Fasted plasma insulin and plasma insulin levels 15 minutes after the *i.p*-injection were not significant different between the RD- and HF/HS-fed mice when injection dose was based on lean mass (figure 3.6.F and 3.6.G). Moreover, plasma insulin had the same tendency in difference between the HF/HS- and HF/HS+INDO-fed mice as seen in the *i.p*-GTT based on injection dose on body mass.

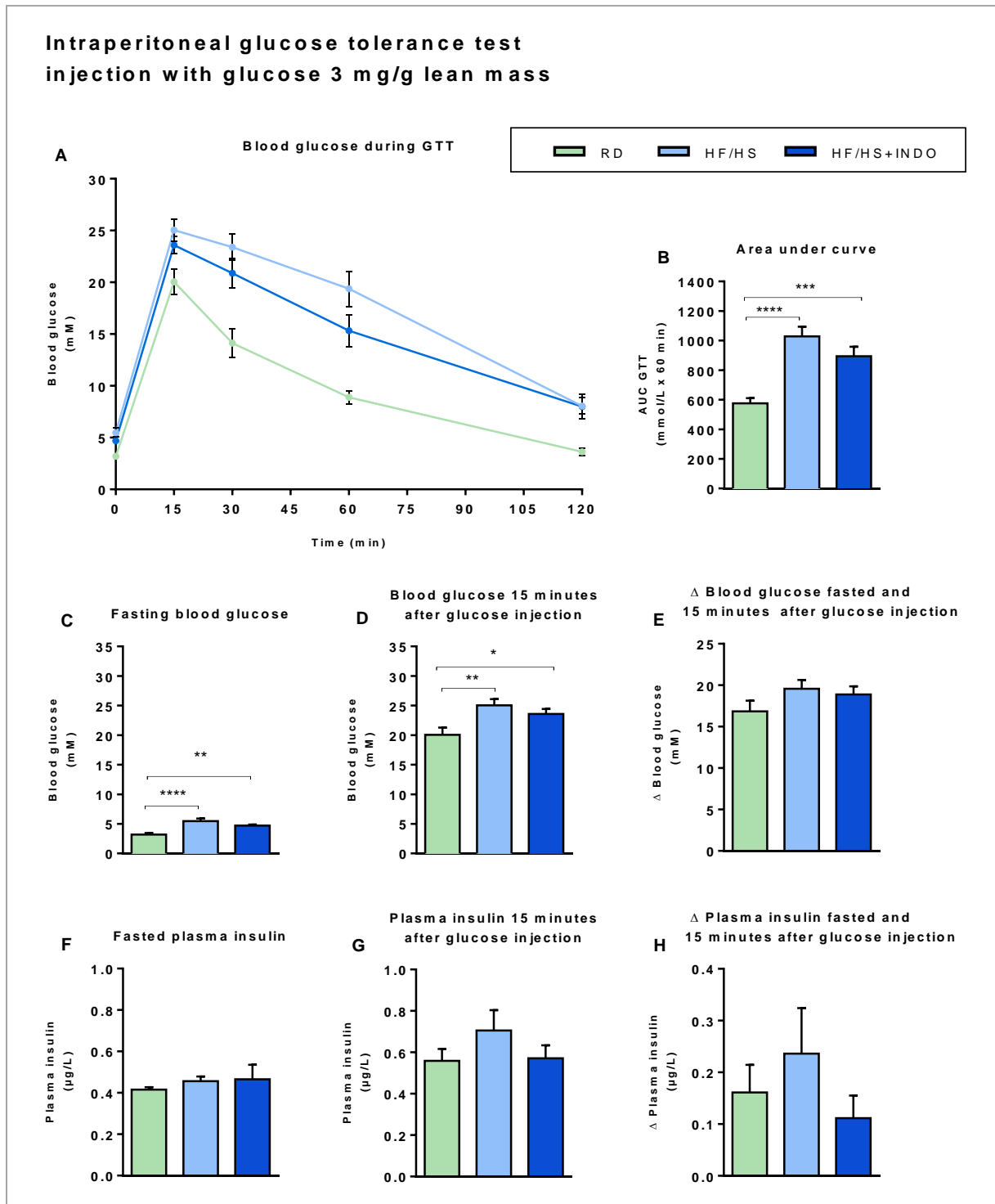


Figure 3.6: An *i.p.*-GTT was performed after 9 weeks on mice fed RD, HF/HS and HF/HS+INDO ($n=10$). The mice had fasted for 6 hours when the test started. The mice were given an intraperitoneal (*i.p.*)-injection with glucose (2mg/g lean mass). **A:** Blood glucose during the *i.p.*-GTT, the blood glucose levels were measured before- and 15, 30, 60 and 120 minutes after *i.p.*-injection. **B:** AUC. **C:** Blood glucose after 6 hours of fasting. **D:** Blood glucose levels 15 minutes after the *i.p.*-injection **E:** Change in blood glucose from fasted to 15 min after the *i.p.*-injection. **F:** Plasma insulin after 6 hours of fasting. **G:** Plasma insulin 15 minutes after the *i.p.*-injection. **H:** Glucose stimulated insulin secretion, the change in plasma insulin from fasted to 15 minutes after the *i.p.*-injection. All results are presented as mean \pm SEM. Statistical differences are denoted with stars; * $P \leq 0.05$, ** $P \leq 0.01$, *** $P \leq 0.001$, **** $P \leq 0.0001$.

ITT - injection dose based on lean mass

The ITT based on injection dose given on lean mass verified no significant differences in AUC between the RD, HF/HS and HF/HS+INDO-fed mice (figure 3.7).

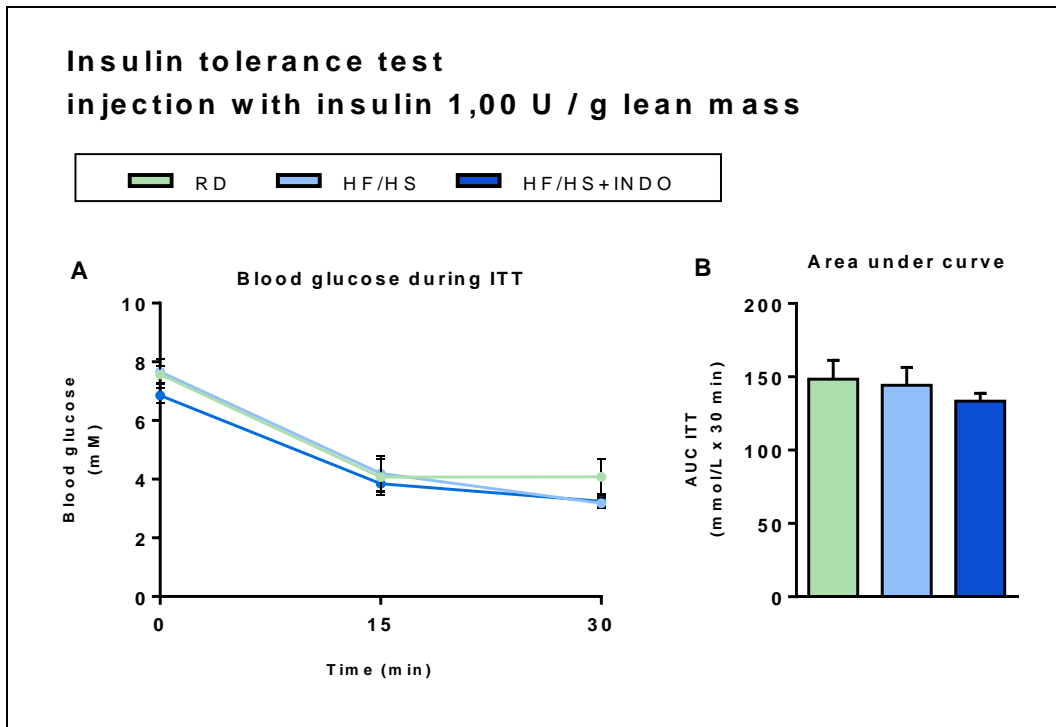


Figure 3.7: An ITT was performed on mice fed RD, HF/HS and HF/HS+INDO after 10 week of feeding (n=8-10) **A:** Blood glucose levels before and 15 and 30 minutes after *i.p* injection with insulin **B:** AUC. All results are present as mean \pm SEM.

3.2 FEEDING EXPERIMENT 1, PART 2

Part 1 of in feeding experiment 1 confirmed that indomethacin is able to attenuate HF/HS-induced obesity, but not glucose intolerance in C57BL/6J mice. Since the reduced obesity development was accompanied with reduced feed efficiency, we investigated if indomethacin is able to reverse HF/HS-induced obesity. Moreover, we asked if indomethacin would influence the glucose tolerance in mice fed a RD (chow) diet.

To investigate this, we took advantage of the obese HF/HS-fed mice from the first part in feeding experiment 1 with a mean body mass of 32.6 gram and 7.8 gram fat mass. Based on body mass and fat mass this group of mice was divided into two subgroups of mice that were fed the HF/HS-diet. One subgroup was continually fed the HF/HS-diet and the other subgroup was fed HF/HS+INDO. To investigate if indomethacin would influence glucose tolerance in mice fed a RD (chow) diet, we took advantage of the RD-fed mice from the first part in feeding experiment 1, by dividing this group of mice into one RD and one RD+INDO subgroup.

INDOMETHACIN DID NOT REDUCE BODY WEIGHT OR FEED EFFICIENCY IN OBESE HF/HS-FED MICE

The body weight development during the feeding experiment is shown in figure 3.8.A. Indomethacin did not reduce the obesity in the HF/HS-fed mice (figure 3.8.B). The energy intake was similar in the HF/HS- and HF/HS+INDO-fed mice (Figure 3.8.C) and consequently there were no differences in feed efficiency between HF/HS- and HF/HS+INDO-fed mice (figure 3.8.D).

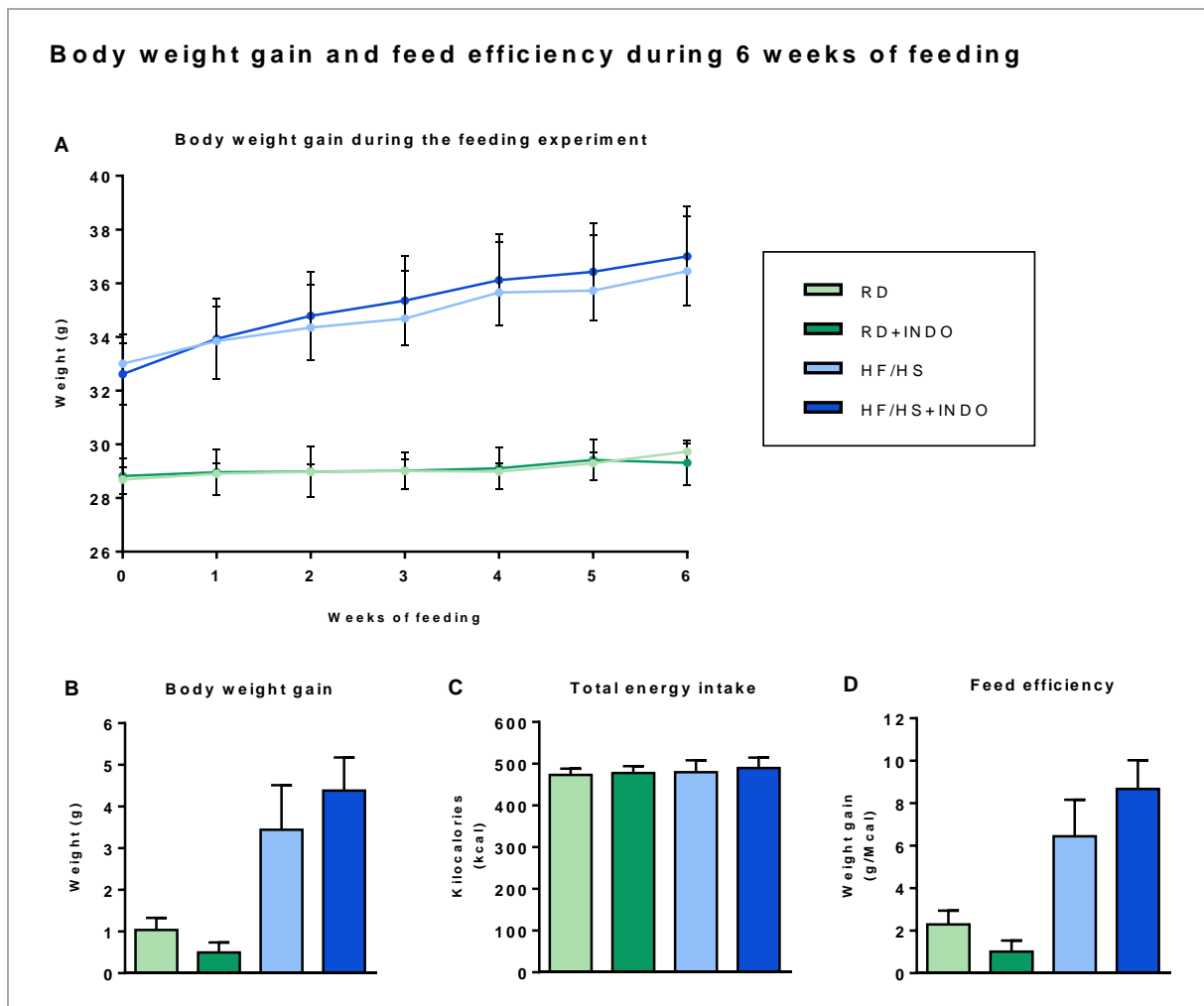


Figure 3.8: Male C57BL/6 mice ($n=7-9$) were fed a RD-, RD+INDO-, HF/HS- and HF/HS+INDO-diet for 8 weeks. All results in this figure present data before the testing was performed. **A:** Body weight development during the first 6 weeks of the feeding experiment: **B:** Body weight gain after 6 weeks of feeding. **C:** Total energy intake (kcal) during the 6 weeks of feeding, estimated from the food given excluding the collected food remnants. **D:** Feeding efficiency was calculated based on energy intake and weight gain. All results are present as mean \pm SEM.

INDOMETHACIN DID NOT REDUCE FAT MASS IN OBESE MICE

HF/HS+INDO fed mice gained the same amount of body mass as the HF/HS-fed mice. To confirm that indomethacin was unable to reverse HF/HS-induced obesity, a MRI-scan was performed after 4 and 6 weeks of feeding. Indomethacin did not reduce fat mass in HF/HS - or RD-fed mice during the 6 weeks of feeding, and was thereby unable to reverse obesity (figure 3.9.B and 3.9.C). There was no difference in lean mass (figure 3.9.E and 3.9.F).

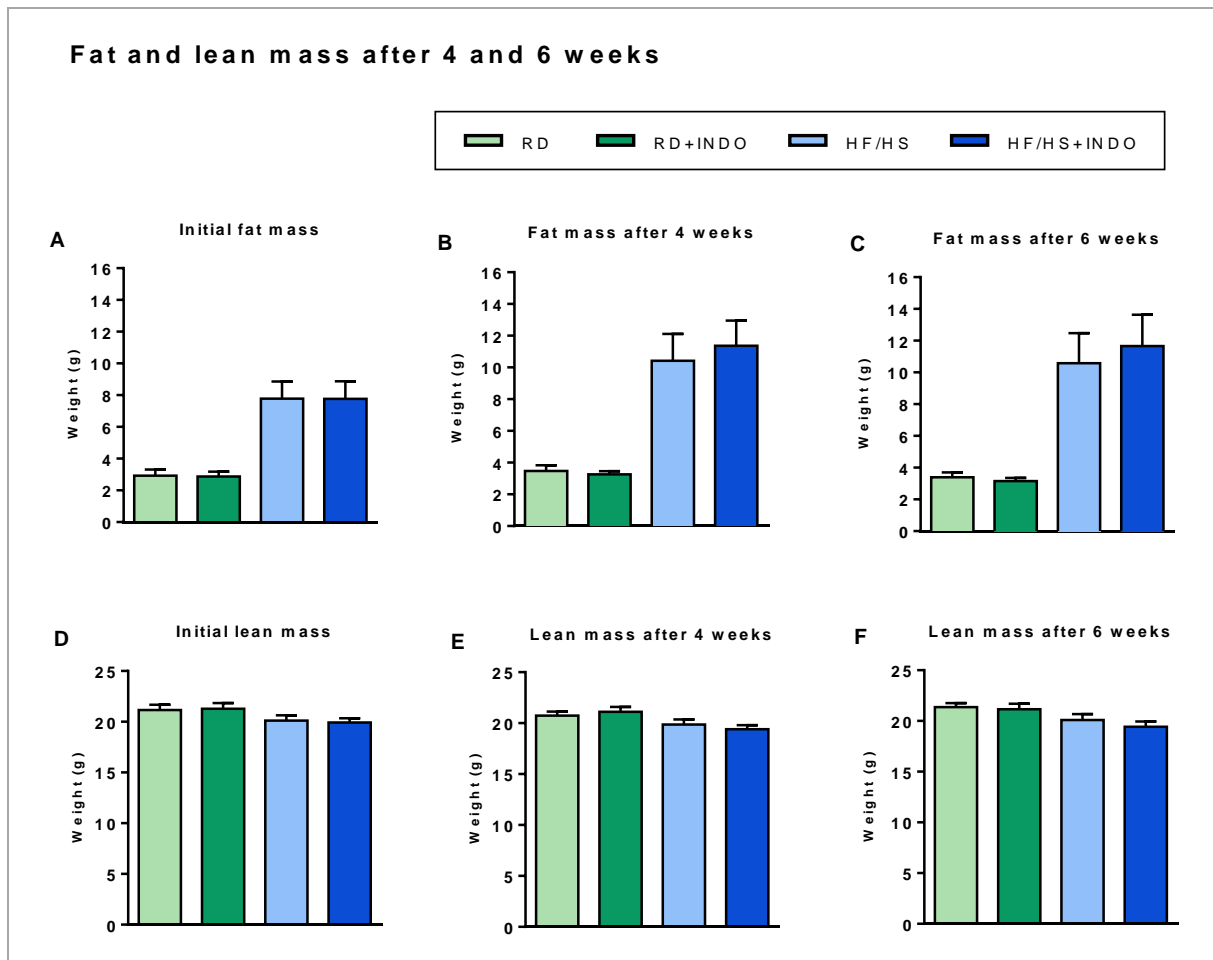


Figure 3.9: MRI-scan of fat- and lean mass of the male C57BL/6 mice ($n=7-9$) was performed at start (initial) and after 4 and 6 weeks on their respective diets. **A:** fat mass (g) when the experiment started. **B:** fat mass weight (g) after 4 weeks of feeding. **C:** fat mass weight (g) after 6 weeks of feeding. **D:** Lean mass weight (g) when the experiment started. **E:** Lean mass weight (g) after 4 weeks of feeding. **F:** Lean mass weight (g) after 6 weeks of feeding. Results are present as mean \pm SEM.

INDOMETHACIN DID NOT REDUCE THE MASS OF ADIPOSE DEPOTS, PANCREAS OR LIVER MASS IN OBESE MICE

The MRI-scan showed no significant reduction in fat mass after 4- or 6 weeks of feeding in HF/HS+INDO fed mice compared to HF/HS-fed mice- or RD+INDO-fed mice compared to RD-fed mice. To verify that the masses of the adipose tissue depots were unchanged, eWAT, iWAT and iBAT were dissected out and weighted. The mice were terminated after 8 weeks of feeding.

Indomethacin had no effect in reducing weight in the adipose tissue depots; eWAT (figure 3.10.A), iWAT (figure 3.10.B) or iBAT (figure 3.10.C) between HF/HS- and HF/HS+INDO-fed mice. Nor did indomethacin reduce pancreas or liver mass (figure 3.10.D and 3.10.E). RD-fed mice had significantly more eWAT- and iBAT mass than RD+INDO-fed mice (figure 3.10.A and 3.10.C). However, indomethacin did not statistically induce any difference in masses of iWAT, pancreas and liver (figure 3.10.B, 3.10.D and 3.10.E).

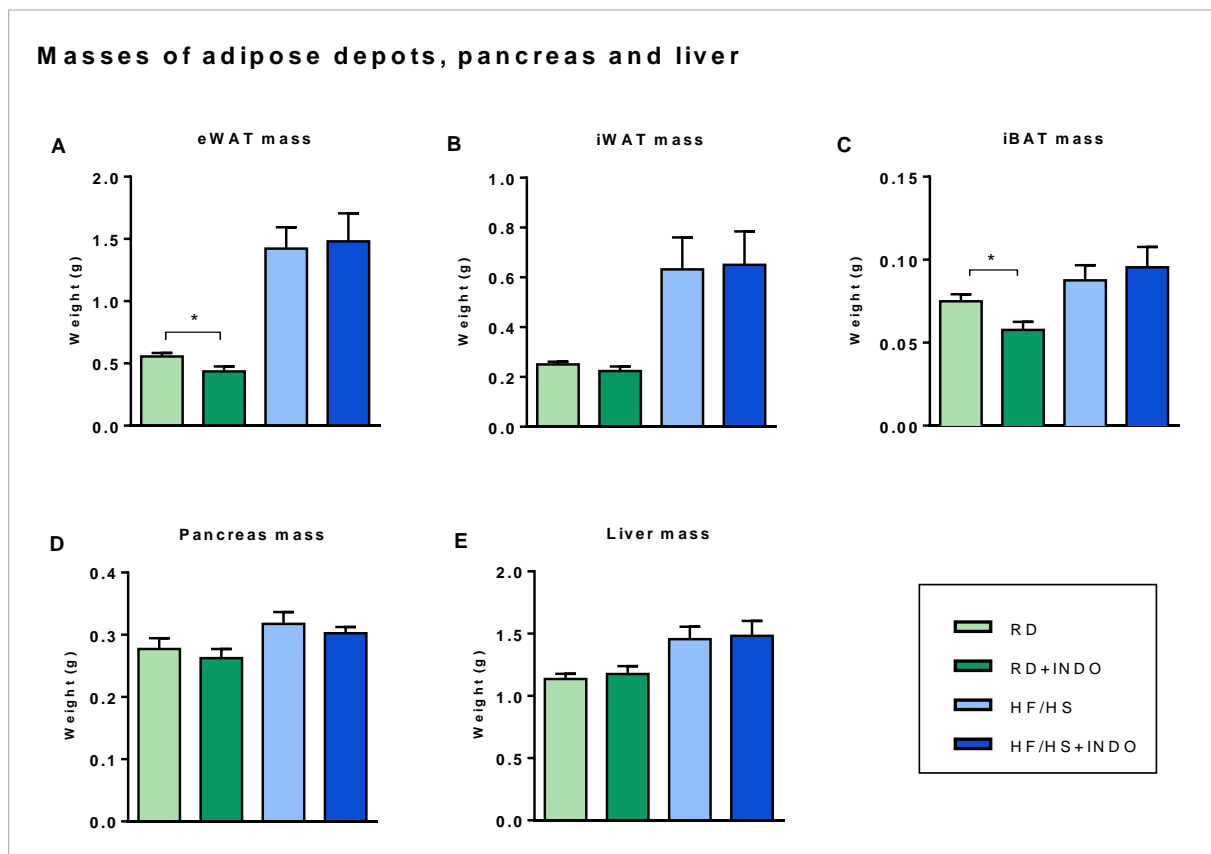


Figure 3.10: Masses of adipose depots, pancreas and liver after dissection of mice fed RD, RD+INDO, HF/HS, HF/HS+INDO (n=7-9). **A:** Mass (g) of eWAT **B:** Mass (g) of iWAT **C:** Mass (g) of iBAT **D:** Mass (g) of pancreas **E:** Mass (g) of liver. All results are presented as mean \pm SEM. Statistical differences are denoted with stars; * $P \leq 0.05$.

HISTOLOGY INDICATED NO DIET-INDUCED HYPERTROPHY OF WAT

An earlier unpublished study in our group has shown smaller adipose size in both iWAT and eWAT in HF/HS+INDO-fed mice compared to HF/HS-fed mice, indicating that indomethacin attenuates diet-induced hypertrophy. To evaluate if indomethacin could reverse the hypertrophy in obese mice, eWAT and iWAT tissue sections were colored with H&E and examined in microscope. The representative photographs from the histology analyses showed no effect of indomethacin on adipocyte size in eWAT (figure 3.11.A) or iWAT (figure 3.11.B).

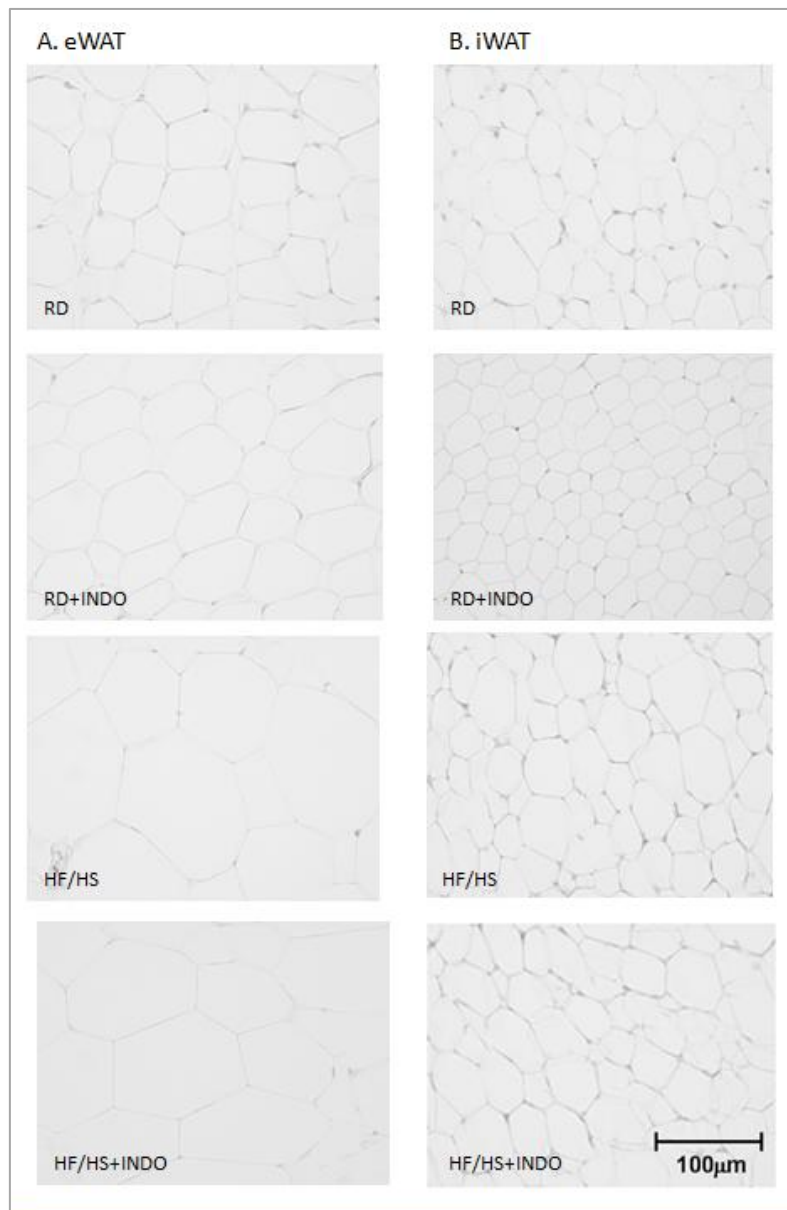


Figure 3.11: Representative microscope pictures of adipose depot from mice with an average weight in each diet group. Stained with H&E, from dissection of mice fed RD, RD+INDO, HF/HS and HF/HS+INDO. The magnification was set at 400X. **A:** eWAT. **B:** iWAT.

INDOMETHACIN DID NOT REDUCE THE HF/HS-INDUCED GLUCOSE INTOLERANCE IN OBESE MICE

Part 1 of feeding experiment 1, verified that indomethacin was unable to attenuate diet-induced glucose intolerance, although HF/HS-induced obesity was partly prevented. We therefore asked if indomethacin had any effect on the glucose tolerance in RD-fed mice, or mice already obese. Thus, an *i.p*-GTT was performed after 7 weeks of feeding.

The AUC showed that indomethacin had no effect on glucose tolerance in obese HF/HS-fed mice (figure 3.12.B). There was also no difference in AUC between RD and RD+INDO-fed mice. No difference seen between HF/HS- and HF/HS+INDO-fed mice in fasted blood glucose levels (figure 3.12.C) or blood glucose levels 15 minutes after the glucose administration (figure 3.12.D). The change in blood glucose levels from fasted to 15 minutes after the *i.p*-injection were reduced in HF/HS+INDO-fed mice, compared with HF/HS-fed mice ($P=0,0397$) (figure 3.12.E). Moreover, fasted blood glucose levels were lower in RD-fed mice than RD+INDO-fed mice ($P=0,0398$) (figure3.12.C).

Indomethacin had no effect on reducing GSIS during the *i.p*-GTT. Plasma insulin levels in fasted state (figure 3.12.F) and 15 minutes after the *i.p*-injection (figure 3.12.G) indicated no difference between the HF/HS- and HF/HS+INDO-fed mice. Additionally there was no difference between RD- and RD+INDO-fed mice.

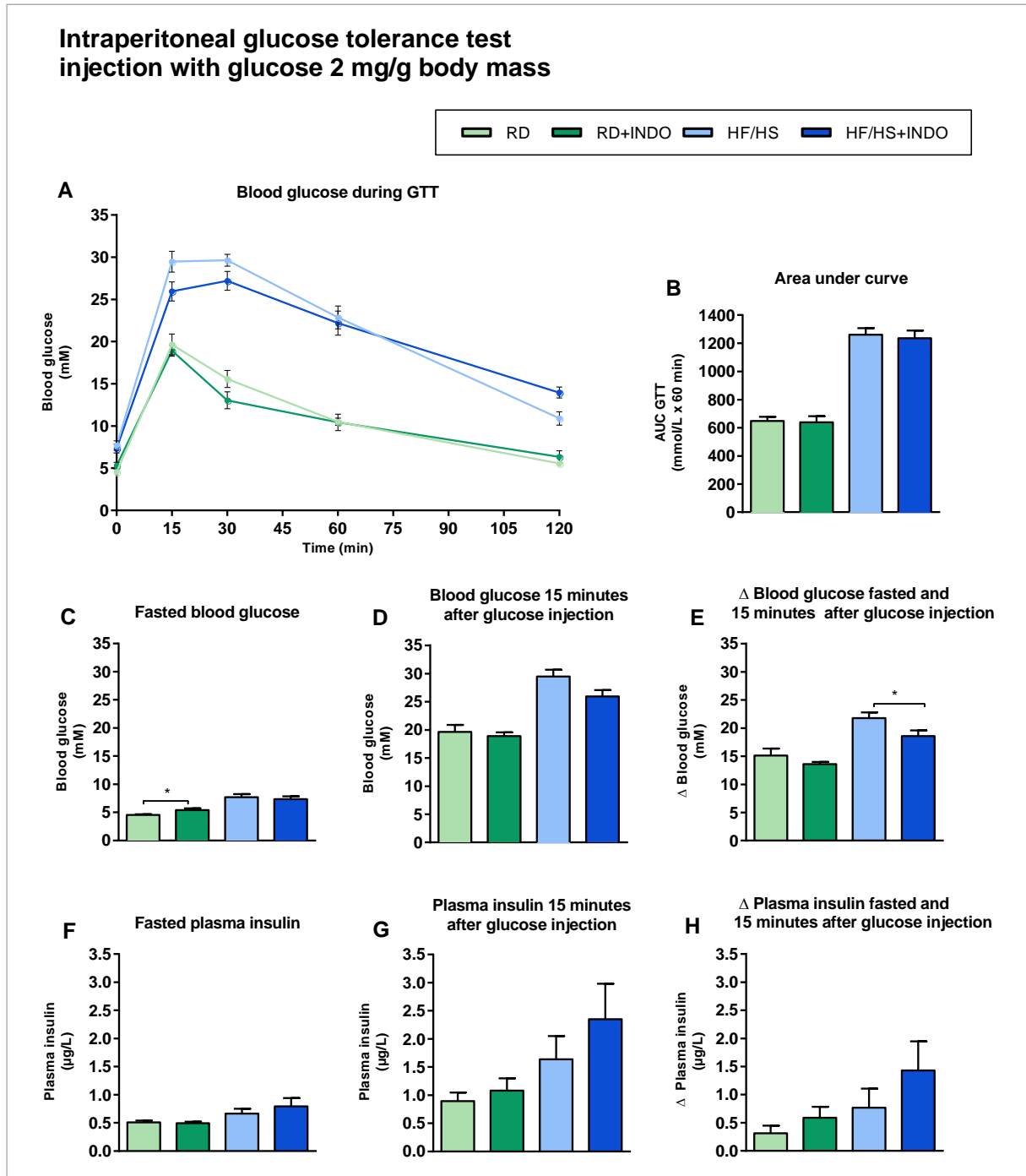


Figure 3.12: An *i.p.*-GTT was performed after 7 weeks on mice fed RD, RD+INDO, HF/HS and HF/HS+INDO ($n=7-9$). The mice had fasted for 6 hours when the test started. The mice were given a *i.p.*-injection with glucose (2mg/g body mass). **A:** Blood glucose during the *i.p.*-GTT, the blood glucose levels were measured before- and 15, 30, 60 and 120 minutes after *i.p.*-injection. **B:** AUC. **C:** Blood glucose after 6 hours of fasting. **D:** Blood glucose levels 15 minutes after the *i.p.*-injection. **E:** Change in blood glucose from fasted to 15 min after the *i.p.*-injection. **F:** Plasma insulin after 6 hours of fasting. **G:** Plasma insulin 15 minutes after the *i.p.*-injection. **H:** Glucose stimulated insulin secretion, the change in plasma insulin from fasted to 15 minutes after the *i.p.*-injection. All results are presented as mean \pm SEM. Statistical differences are denoted with stars; * $P \leq 0.05$.

INDOMETHACIN DID NOT REVERSE HF/HS-INDUCED INSULIN RESISTANCE EVALUATED BY HOMA-IR INDEX

The calculated HOMA-IR index is presented in figure 3.13 the values were measured from blood glucose and plasma insulin. The HOMA-IR indicates that indomethacin did not reverse HF/HS-induced insulin resistance.

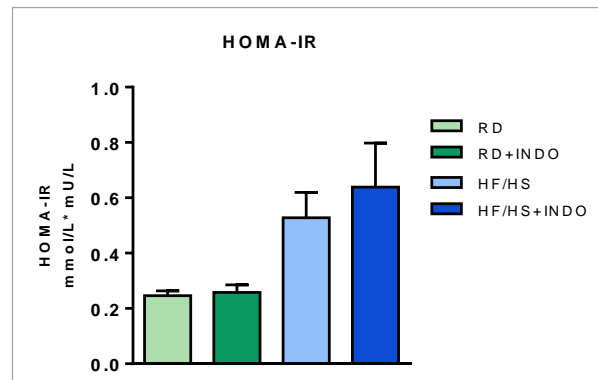


Figure 3.13: HOMA-IR score determined from fasting blood glucose and fasting plasma insulin levels of mice fed RD, RD+INDO, HF/HS and HF/HS+INDO. Results are present as mean \pm SEM.

INSULIN SENSITIVITY IS NOT INFLUENCED BY INDOMETHACIN IN RD-FED OR IN OBESE HF/HS-FED MICE

To verify that insulin sensitivity was unchanged in these mice an ITT was performed (figure 3.14). The AUC showed no significant differences between HF/HS- and HF/HS+INDO-fed mice in the ITT. Nor was any difference between RD- and RD+INDO-fed mice observed. Together, the HOMA-IR and *i.p*-GTT indicate that indomethacin did not have an effect on attenuating HF/HS-induced insulin resistance.

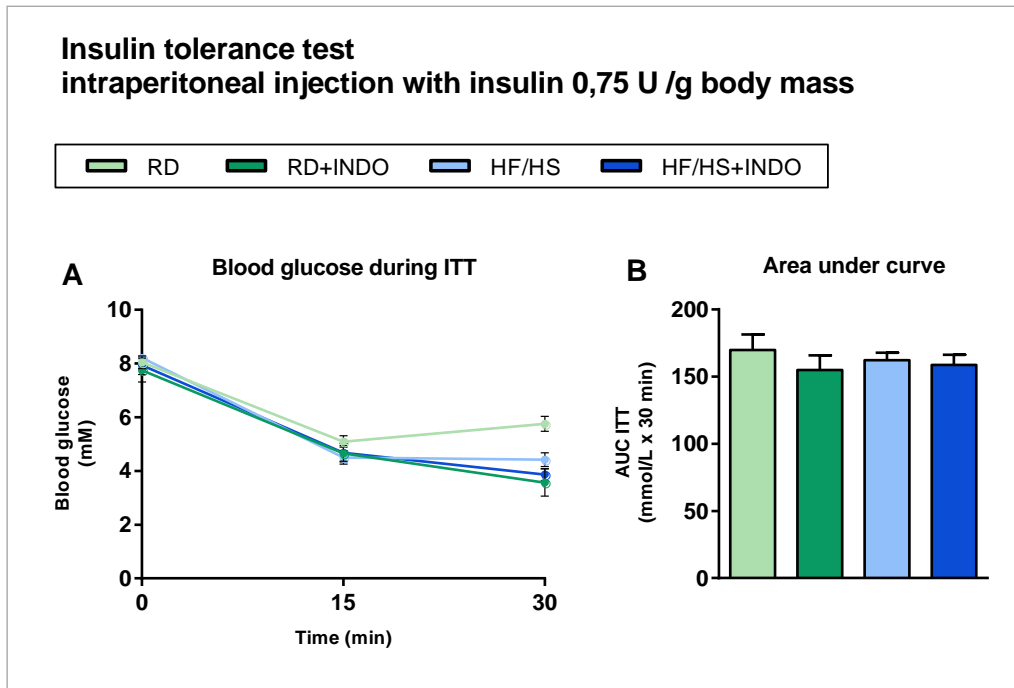


Figure 3.14: An ITT was performed on mice fed RD, RD+INDO, HF/HS and HF/HS+INDO after 8 week of feeding (n=7-9). **A:** measurement of blood glucose levels before and 15 and 30 minutes after *i.p* injection with insulin **B:** AUC. Results are present as mean \pm SEM.

EVALUATION OF *i.p*-GTT AND ITT ON INJECTION DOSE BASED ON BODY MASS VS. LEAN MASS

An *i.p*-GTT was performed on the same subset of mice (figure 3.15). Here, the glucose and insulin load injected were calculated based on lean body mass. The AUC verified that indomethacin had no effect on glucose tolerance in obese HF/HS-fed mice. The AUC also confirms that there is no difference between RD- and RD+INDO-fed mice. This *i.p*-GTT further verifies that indomethacin had no effect on blood glucose levels or insulin levels in HF/HS-fed mice. The significant difference in changes in blood glucose from fasted to 15 minutes after the *i.p*-injection between the HF/HS- and HF/HS+INDO-fed mice was not significantly different when the glucose load was injected based on lean mass. Furthermore, the slight but significant difference in fasting blood glucose levels between RD- and RD+INDO-fed mice were not observed when the glucose load was injected based on lean mass.

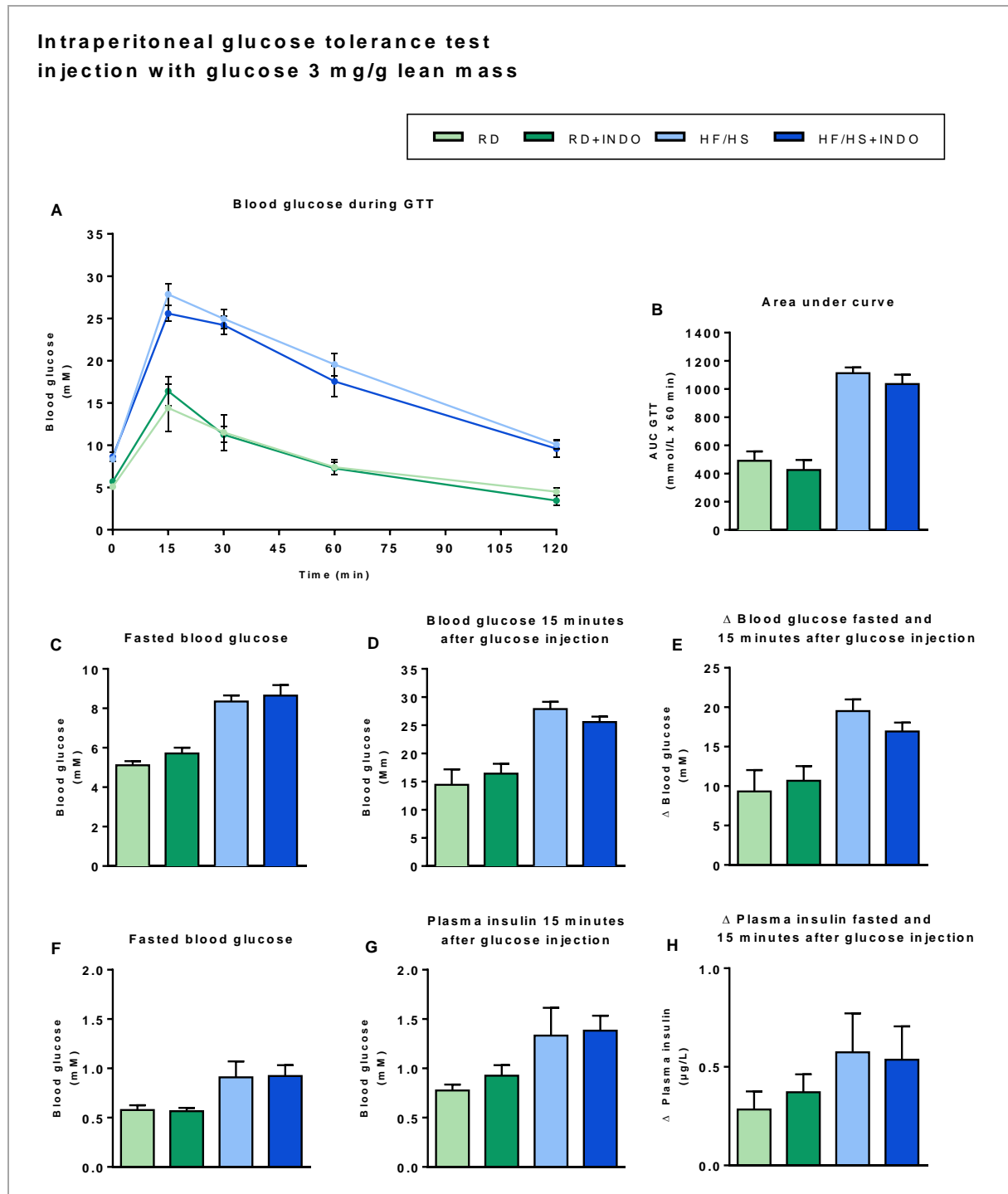


Figure 3.15: An *i.p.*-GTT was performed after 7 weeks on mice fed RD, RD+INDO, HF/HS and HF/HS+INDO ($n=7-9$). The mice had fasted for 6 hours when the test started. The mice were given an *i.p.*-injection with glucose (2mg/g lean mass) **A:** Blood glucose during the *i.p.*-GTT, the blood glucose levels were measured before- and 15, 30, 60 and 120 minutes after *i.p.*-injection. **B:** AUC. **C:** Blood glucose after 6 hours of fasting. **D:** Blood glucose levels 15 minutes after the *i.p.*-injection **E:** Change in blood glucose from fasted to 15 min after the *i.p.*-injection. **F:** Plasma insulin after 6 hours of fasting. **G:** Plasma insulin 15 minutes after the *i.p.*-injection. **H:** Glucose stimulated insulin secretion, the change in plasma insulin from fasted to 15 minutes after the *i.p.*-injection. All results are present as mean \pm SEM.

The calculated HOMA-IR index is presented in figure 3.16, the values were measured from blood glucose and plasma insulin. The HOMA-IR verifies that indomethacin did not attenuate HF/HS-induced insulin resistance.

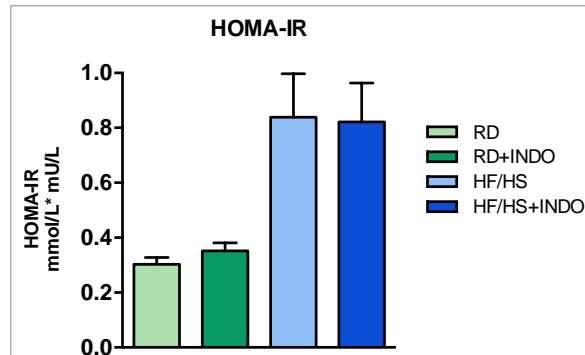


Figure 3.16: HOMA-IR score determined from fasting blood glucose and fasting plasma insulin levels of mice fed RD RD+INDO, HF/HS and HF/HS+INDO. Results are present as mean \pm SEM.

ITT - injection dose based on body mass vs. lean mass

An additional ITT was performed on the same subset of mice (figure 3.17). Here, insulin load injected was calculated based on lean body mass. AUC verifies that there was no significant difference between HF/HS- and HF/HS+INDO-fed mice in the ITT. Nor was the AUC different between the RD- and RD+INDO-fed mice. The HOMA-IR index and the ITT confirm that indomethacin did not reverse HF/HS-induced insulin resistance.

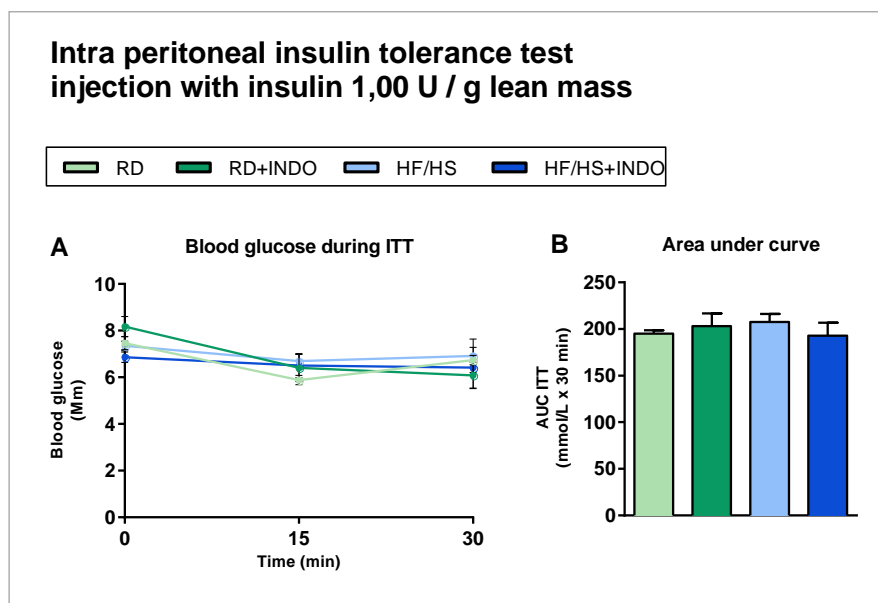


Figure 3.17: An ITT was performed on mice the mice after 8 weeks of feeding. $n=7-9$. **A:** measurement of blood glucose levels before and 15-and 30 minutes after *i.p.*-injection with insulin **B:** AUC. Results are present as mean \pm SEM.

INDOMETHACIN HAD NO EFFECT OF EXPRESSION OF GENES INVOLVED IN GLUCONEOGENESIS

Increased gluconeogenesis is often accompanied by increased hepatic glucose output. Unpublished results from this group have shown that inclusion of indomethacin in an HF/HS-diet lead to increased expression of *Pck1*. This was accompanied with increased hepatic glucose output, measured by a pyruvate tolerance test. To investigate if indomethacin increased expression of *Pck1* in obese mice, and/or in RD-fed mice, RNA was purified from the liver of these mice and expression levels determined with real-time qPCR. Expression levels of *Pck1* and Glucose 6-phosphate (*G6P*) were, however, similar in all groups of mice (figure 3.18).

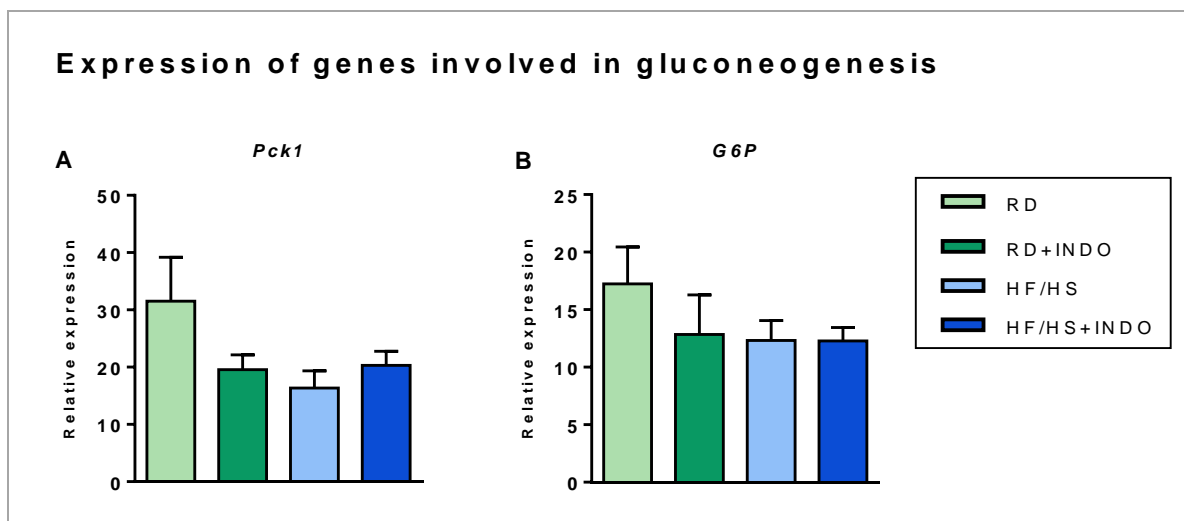


Figure 3.18: Relative mRNA expression of genes involved in gluconeogenesis in RD, RD+INDO, HF/HS and HF/HS+INDO -fed mice. **A:** *PCK1*. **B:** *GP6*. Results are present as mean \pm SEM.

In conclusion, indomethacin attenuated HF/HS-induced obesity, but not glucose intolerance in HF/HS-fed mice. However, indomethacin was not able to reverse obesity or influence glucose tolerance in already obese HF/HS-fed mice. Increased GSIS was attenuated in mice fed HF/HS+INDO compared to HF/HS-fed mice; however, the GSIS were not reduced in already obese HF/HS+INDO-fed mice. The HOMA-IR indicated that indomethacin could, at least in part prevent HF/HS-induced insulin resistance, but not reverse it. Together, this suggests that indomethacin attenuates the HF/HS-induced GSIS and the HF/HS+INDO-fed mice are by this reason as glucose intolerant as the HF/HS-fed mice.

3.3 EXPERIMENT 2

INDOMETHACIN DID NOT ACUTE REDUCE GSIS

To investigate if indomethacin had an acute effect on GSIS in HF/HS-fed mice, an *i.p*-GTT was performed. The first *i.p*-GTT (figure 3.19) was performed on RD-fed mice after 1 week of feeding. Half of the mice were given indomethacin (2.5 mg/ kg body mass) and the rest a control solution (saline) gavage, one hour before the *i.p*-GTT was performed.

RD-fed mice given indomethacin had increased blood glucose levels during the *i.p*-GTT compared to RD-fed mice administrated the control solution (saline) (figure 3.19.D), However, insulin levels were not decreased compared to mice given the saline solution. Indomethacin had no acute effect in inhibiting GSIS in RD-fed mice.

After the *i.p*-GTT, all mice started on an HF/HS-diet. An additional *i.p*-GTT was performed after 10 weeks of HF/HS-feeding. There was no difference between HF/HS-fed mice given indomethacin or saline before the *i.p*-GTT (figure 3.20). Thus, indomethacin had no acute effect in inhibiting GSIS in either RD- or HF/HS-fed mice.

Indomethacin injected orally gavage (2.5 mg/kg body mass) 1 hour before an *i.p.*-GTT on RD-fed mice

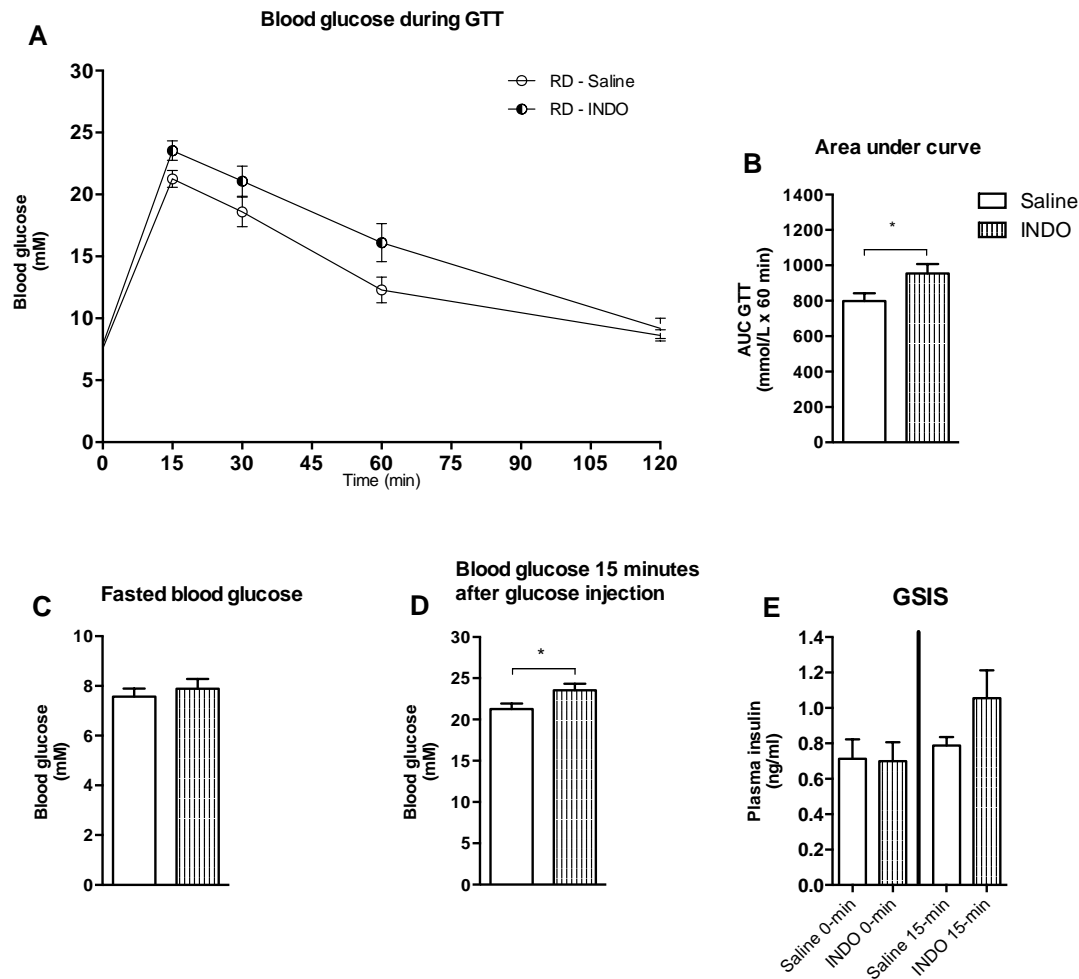


Figure 3.19: An *i.p.*-GTT was performed on RD-fed mice ($n=10$) after 1 week of feeding. Half of the mice received indomethacin (2.5mg/kg body mass) injected gavage and the rest a control solution (saline), 1 hour before an *i.p.*-Injection with glucose (2 mg/g body mass). The mice had fasted in 6 when the test started. **A:** Blood glucose during the *i.p.*-GTT. **B:** AUC. **C:** Blood glucose after 6 hours of fasting. **D:** Blood glucose levels 15 minutes after the glucose injection. **E:** Plasma insulin after 6 hours of fasting and plasma insulin 15 minutes after the glucose injection. All results are presented as mean \pm SEM. Statistical differences are denoted with stars; * $P \leq 0.05$.

Indomethacin injected orally gavage (2.5 mg/kg body mass) 1 hour before an *i.p.*-GTT on HF/HS-fed mice

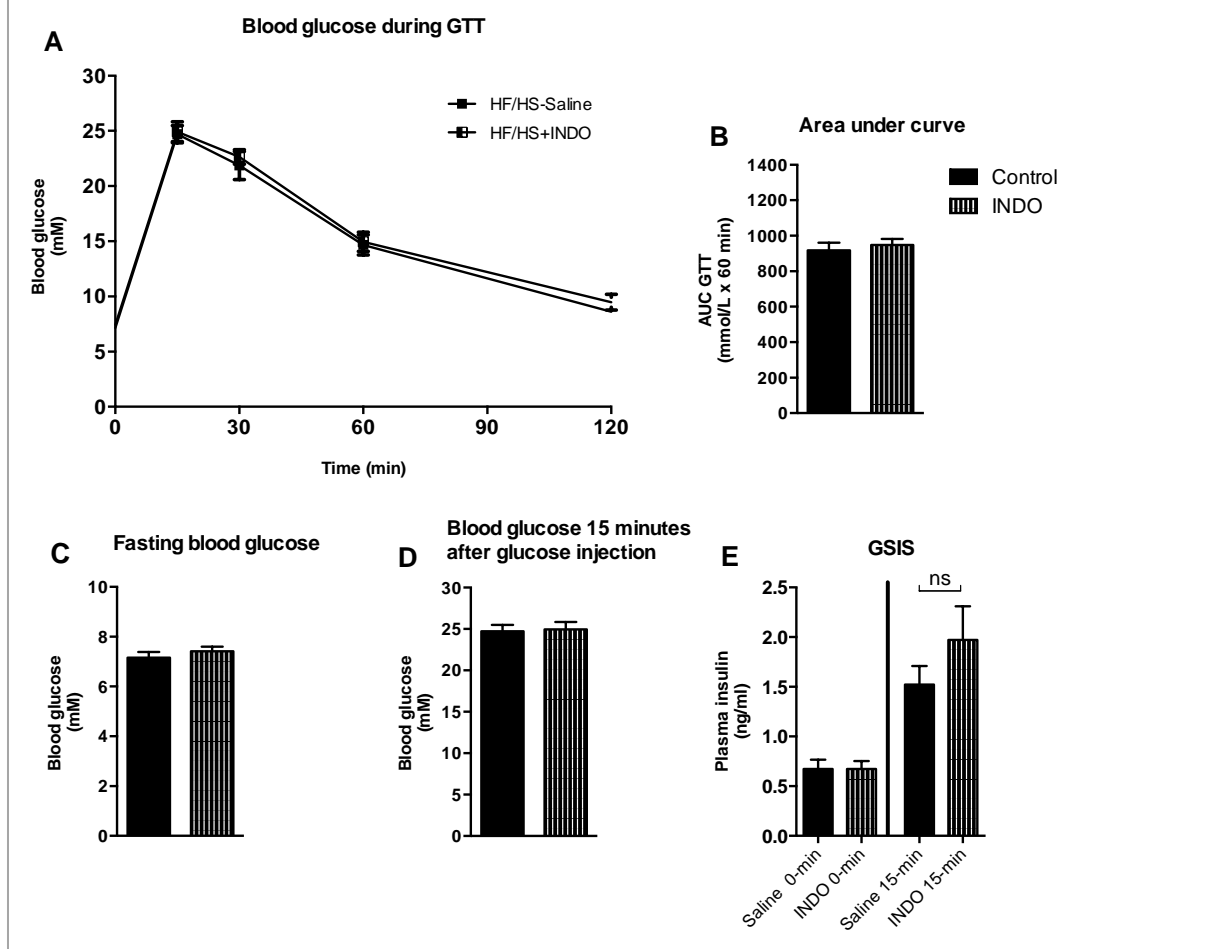


Figure 3.19: An *i.p.*-GTT was performed on HF/HS-fed mice ($n=10$) after 10 weeks of feeding. Half of the mice received indomethacin (2.5mg/kg body mass) injected gavage and the rest a control solution (saline), 1 hour before an *i.p.*-injection with glucose (2 mg/g body mass). The mice had fasted in 6 when the test started **A:** Blood glucose during the *i.p.*-GTT. **B:** AUC. **C:** Blood glucose after 6 hours of fasting. **D:** Blood glucose levels 15 minutes after the glucose injection. **E:** Plasma insulin after 6 hours of fasting and plasma insulin 15 minutes after the glucose injection. All results are presented as mean \pm SEM. Statistical differences are denoted with stars; * $P \leq 0.05$.

3.4 EXPERIMENT 3

INDOMETHACIN ATTENUATED HF/HS-INDUCED GSIS AFTER 3 WEEKS OF FEEDING

Indomethacin had no acute inhibiting effect on GSIS in either RD or HF/HS-fed mice. The finding that indomethacin did not have an acute effect in inhibiting GSIS, imply that the impaired GSIS is an effect of indomethacin on the HF/HS-induced GSIS. To investigate if the inhibited GSIS in HF/HS+INDO fed mice is an early event, a new feeding experiment was performed. Thirty C57BL/6 mice (n=10) were fed RD, HF/HS and HF/HS+INDO and an *i.p*-GTT was performed once a week in a total of three weeks, and after 9 weeks of feeding.

Calculation of AUC demonstrated that compared with RD-fed mice, the glucose tolerance was not significantly reduced by the HF/HS-diet before week 3 (Figure 3.23.B). Surprisingly, AUC showed that HF/HS+INDO-fed mice more glucose intolerance than HF/HS-fed mice after 1 and 2 weeks of feeding (Figure 3.21.B and 3.22.B). After 3 and 9 weeks of feeding, AUC was comparable in HS/HS-and HF/HS+INDO-fed mice (figure 3.23.B and 3.24.B).

Similarly, compared with RD-fed mice, blood glucose 15 minutes after injection was higher in HF/HS+INDO-fed mice but HF/HS-fed mice after 1 and 2 weeks (figure 3.21.D and 3.22.D). After 3 and 9 weeks, blood glucose levels in HF/HS+INDO-fed mice and HF/HS-fed was comparable (figure 3.23.D and 3.24.D). Together, this indicates that HF/HS+INDO-fed mice developed glucose intolerant before HF/HS-fed mice.

Compared with RD-fed mice, GSIS tended to increase in both HF/HS- and HF/HS+INDO-fed mice after 2 weeks of feeding (figure 3.22.G). However, after 3 and 9 weeks, GSIS was significantly increased in HF/HS-, this was not seen in HF/HS+INDO-fed mice (figure 3.23.G and 3.24.G).

Intraperitoneal glucose tolerance test after 1 week of feeding injection with glucose 2 mg/g body mass

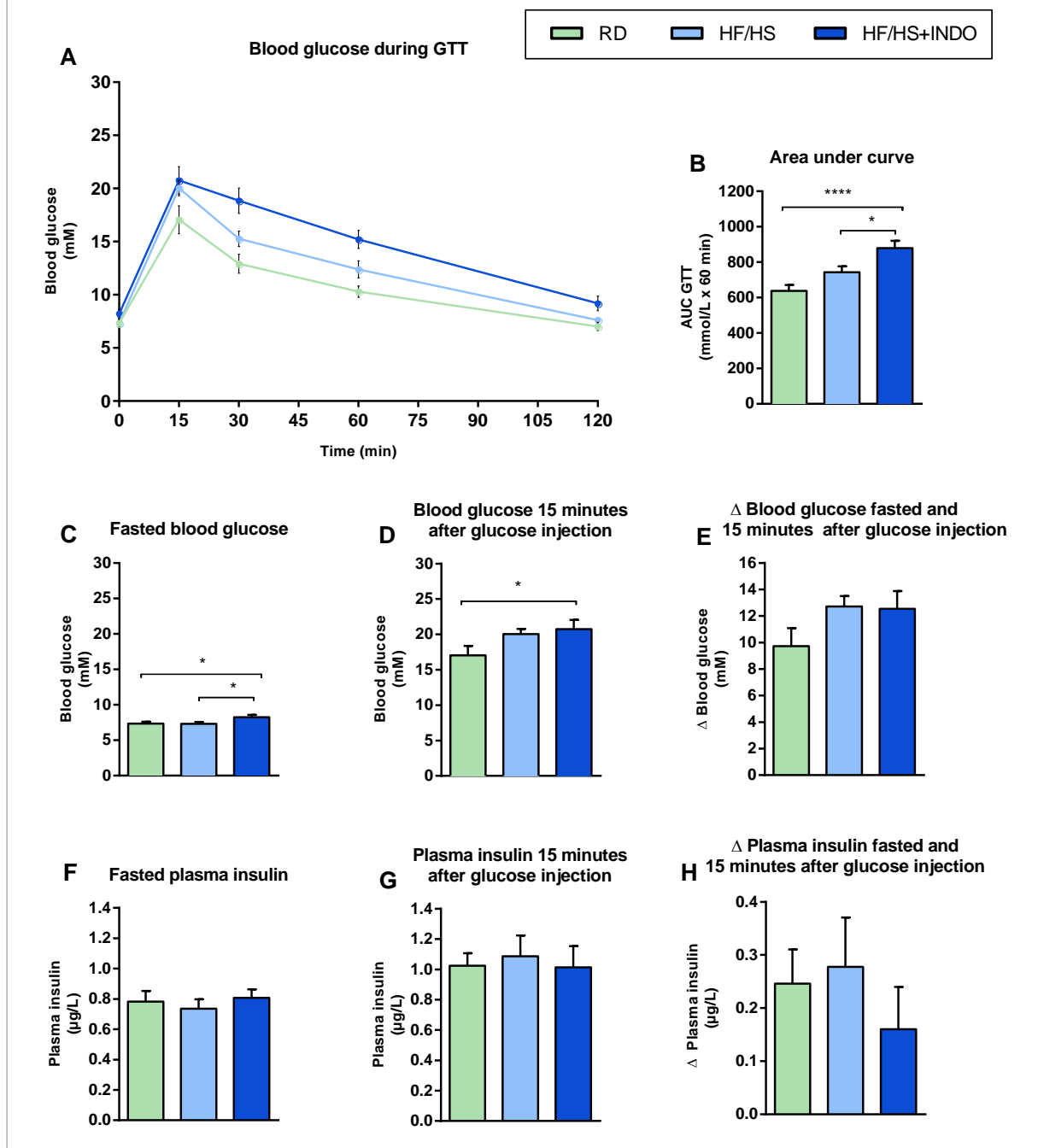


Figure 3.21: An i.p-GTT was performed after 1 week on male C57BL/6 mice fed RD, HF/HS and HF/HS+INDO (n=10). The mice had fasted in 6 when the test started. The mice were given an i.p-injection with glucose (2 mg/g body mass). **A:** Blood glucose during the GTT, the blood glucose levels were measured before the glucose injection and 15, 30, 60 and 120 minutes after. **B:** AUC **C:** Blood glucose after 6 hours of fasting. **D:** Blood glucose levels 15 minutes after the glucose injection **E:** Change in blood glucose from fasted to 15 minutes after the i.p-injection. **F:** Plasma insulin after 6 hours of fasting. **G:** Plasma insulin 15 minutes after the i.p-injection. **H:** Glucose stimulated insulin secretion, the change in plasma insulin from fasted to 15 minutes after the i.p-injection. All results are presented as mean \pm SEM. Statistical differences are denoted with stars; * $P \leq 0.05$, ** $P \leq 0.01$, *** $P \leq 0.001$, **** $P \leq 0.0001$.

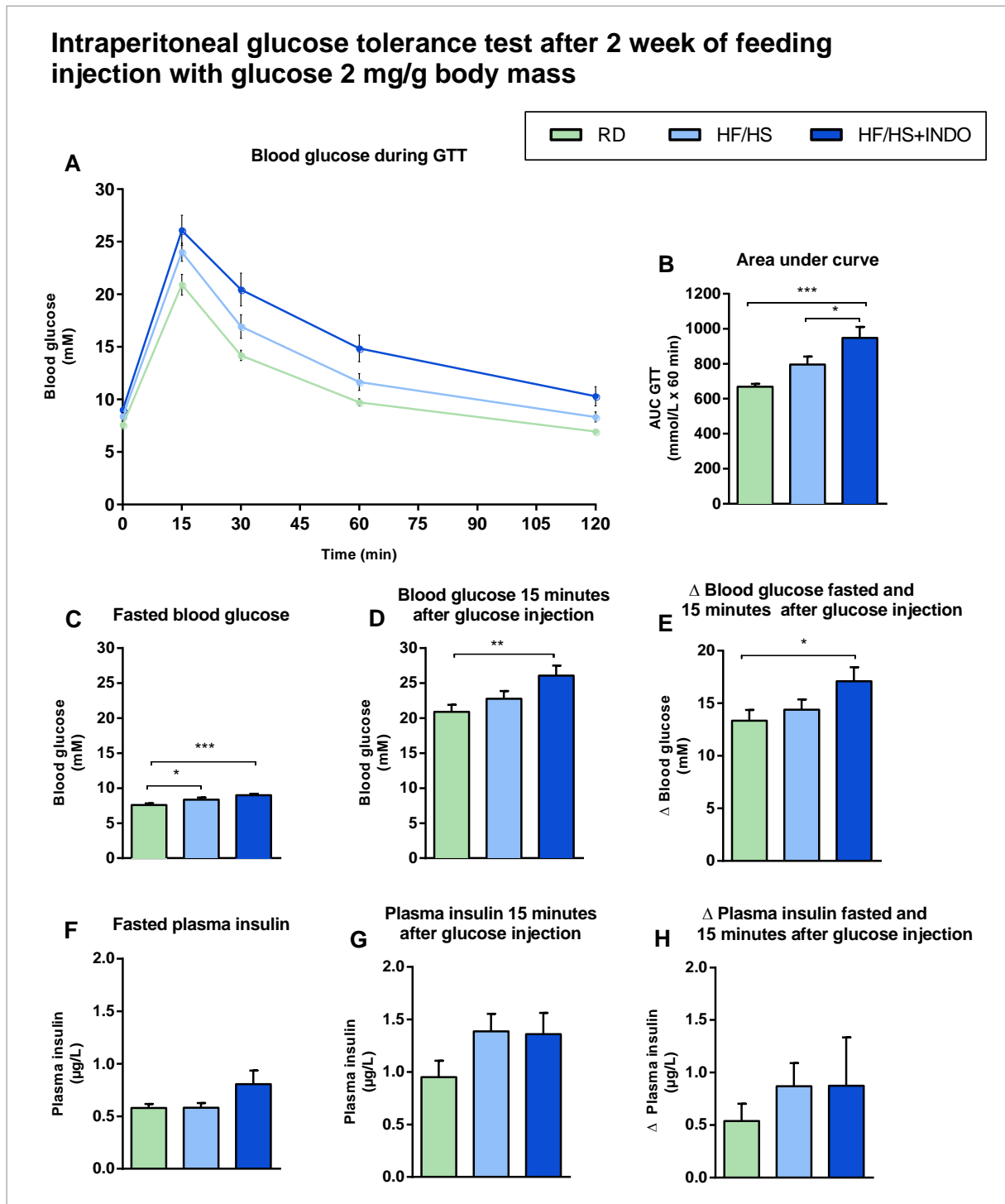


Figure 3.22: An i.p-GTT was performed after 2 weeks on male C57BL/6 mice fed RD, HF/HS and HF/HS+INDO ($n=10$). The mice had fasted in 6 when the test started. The mice were given an i.p-injection with glucose (2 mg/g body mass). **A:** Blood glucose during the GTT, the blood glucose levels were measured before the glucose injection and 15, 30, 60 and 120 minutes after. **B:** AUC **C:** Blood glucose after 6 hours of fasting. **D:** Blood glucose levels 15 minutes after the glucose injection **E:** Change in blood glucose from fasted to 15 minutes after the i.p-injection. **F:** Plasma insulin after 6 hours of fasting. **G:** Plasma insulin 15 minutes after the i.p-injection. **H:** Glucose stimulated insulin secretion, the change in plasma insulin from fasted to 15 minutes after the i.p-injection. All results are presented as mean \pm SEM. Statistical differences are denoted with stars; * $P \leq 0.05$, ** $P \leq 0.01$, *** $P \leq 0.001$.

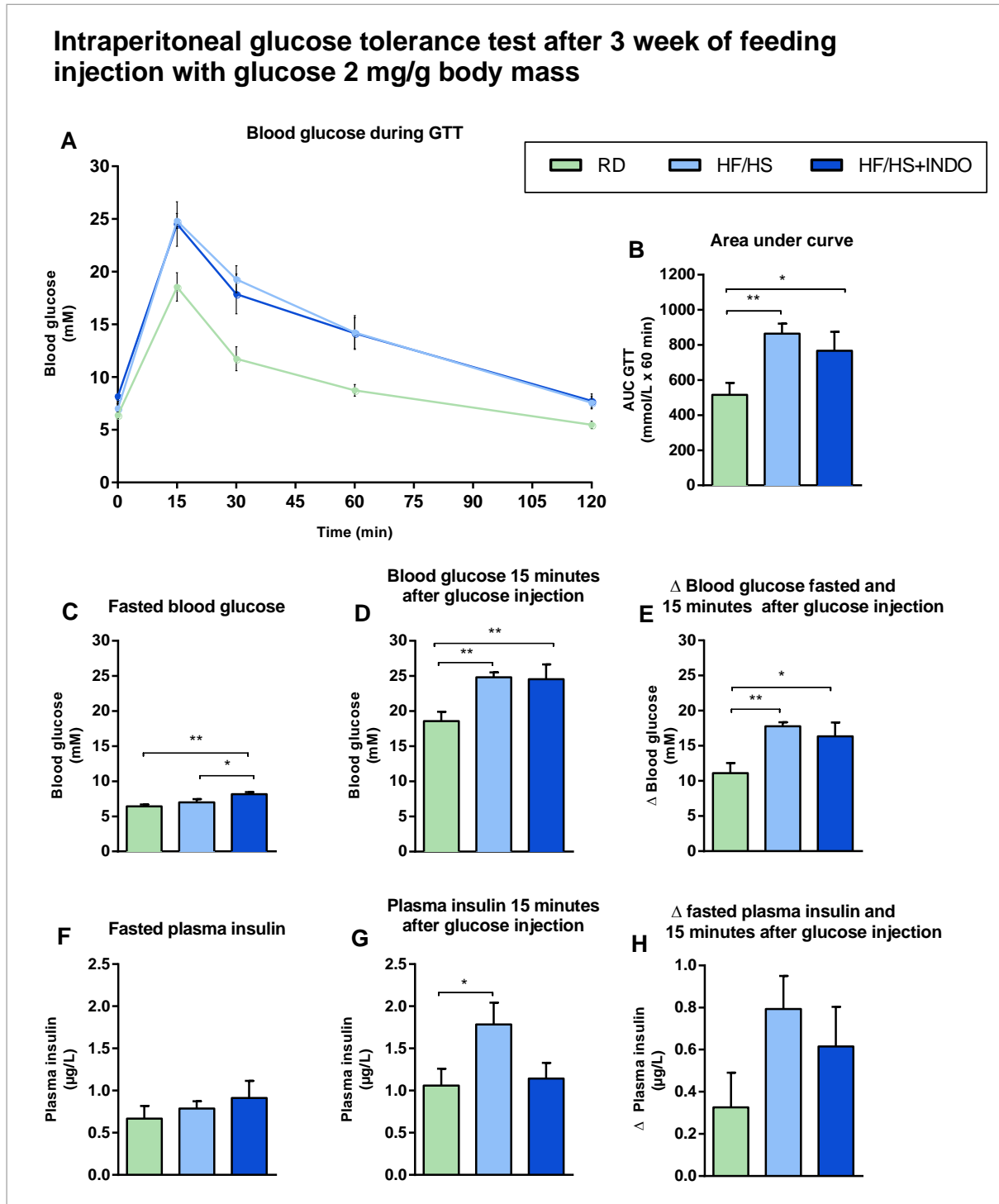


Figure 3.23: An *i.p.*-GTT was performed after 3 weeks of feeding on male C57BL/6 mice fed RD, HF/HS and HF/HS+INDO ($n=10$). The mice had fasted for 6 hours before testing. The mice were given injected with 2mg glucose /g BW () **A:** Blood glucose levels were measured before and 15, 30, 60 and 120 minutes after the glucose injection. **B:** Area under curve **C:** Blood glucose after 6 hours of fasting. **D:** Blood glucose levels 15 minutes after the glucose injection **E:** Change in blood glucose from fasted to 15 min after the glucose injection. **F:** Plasma insulin after 6 hours of fasting. **G:** Plasma insulin 15 minutes after the glucose injection. **H:** Glucose stimulated insulin secretion, the change in plasma insulin from fasted to 15 minutes after the glucose injection. All results are presented as mean \pm SEM. Statistical differences are denoted with stars; * $P \leq 0.05$, ** $P \leq 0.01$.

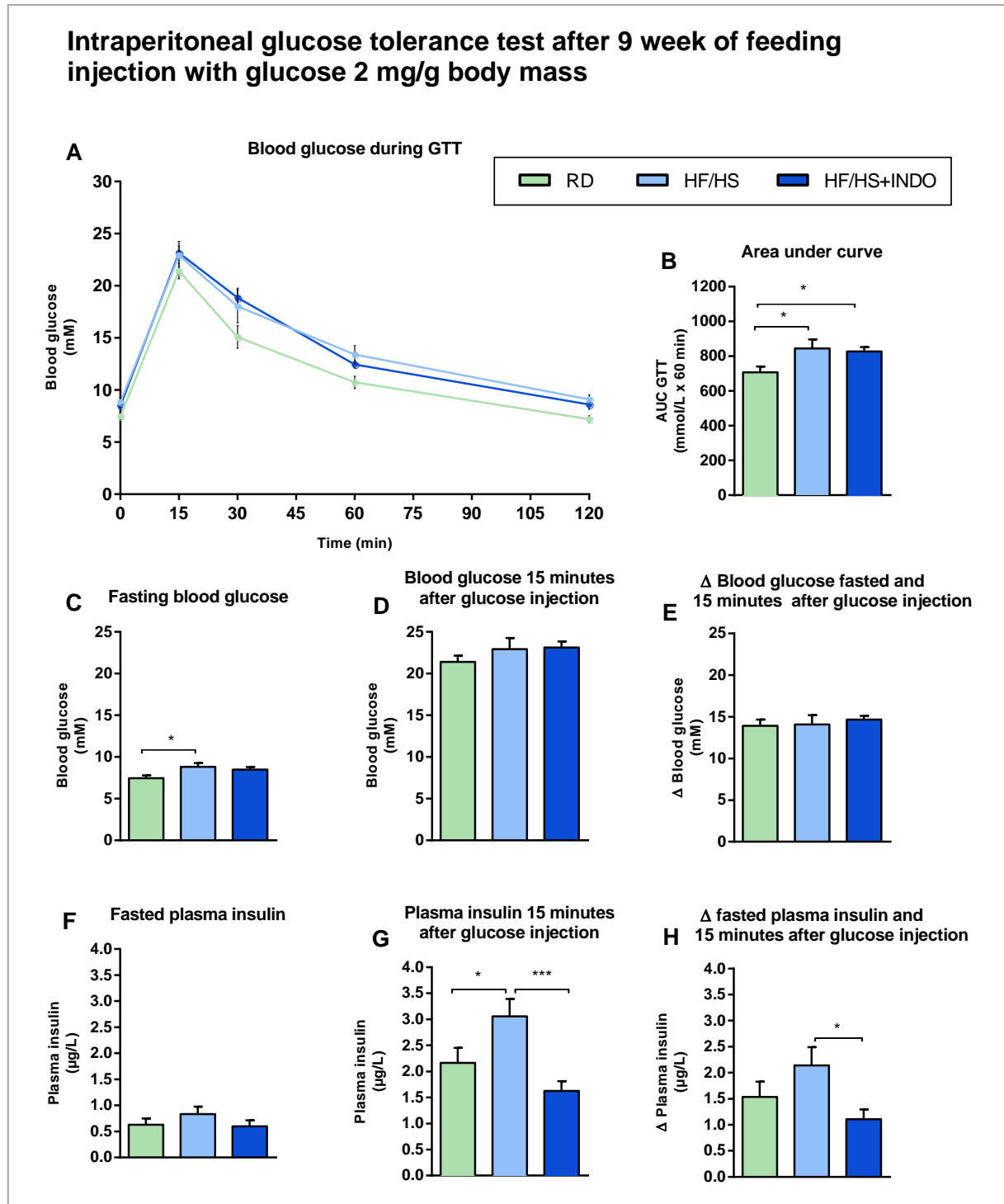


Figure 3.24: An *i.p.*-GTT was performed after 9 weeks of feeding on male C57BL/6 mice fed RD, HF/HS and HF/HS+INDO ($n=10$). The mice had fasted for 6 hours before testing. The mice were *i.p.*-injected with 2 mg glucose /g body mass. **A:** Blood glucose levels were measured before and 15, 30, 60 and 120 minutes after the glucose injection. **B:** Area under curve **C:** Blood glucose after 6 hours of fasting. **D:** Blood glucose levels 15 minutes after the glucose injection **E:** Change in blood glucose from fasted to 15 min after the glucose injection. **F:** Plasma insulin after 6 hours of fasting. **G:** Plasma insulin 15 minutes after the glucose injection. **H:** Glucose stimulated insulin secretion, the change in plasma insulin from fasted to 15 minutes after the glucose injection. All results are presented as mean \pm SEM. Statistical differences are denoted with stars; * $P \leq 0.05$, ** $P \leq 0.01$, *** $P \leq 0.001$.

INDOMETHACIN DID NOT ATTENUATE MEAL-STIMULATED INSULIN SECRETION

Measurements of plasma insulin levels 15 minutes after *i.p.*-injection with glucose, demonstrated that GSIS was attenuated when indomethacin was added to the HF/HS-diet after 3 weeks of feeding. When glucose is injected *i.p.*, blood glucose concentration is rapidly elevated. Such abrupt and marked increase in blood glucose concentration does not occur after intake of food and can be considered as non-physiological. Under physiological conditions, such as after a meal, glucose concentration increase gradually and insulin is secreted more slowly. Thus, we wanted to investigate if indomethacin influenced insulin secretion in response with the respective diets. Therefore, thirty C57BL/6 mice (n=10) were fed RD-, HF/HS- and HF/HS+INDO-diet for 10 weeks. A MTT was performed once a week for 3 weeks and after 10 weeks. An initial MTT was performed using the experimental diets at onset of the experiment.

The RD contained a high amount of carbohydrates (66 E% carbohydrates), and this led to higher postprandial glucose concentrations than the HF/HS-diets (49 E% carbohydrates), despite smaller meal size (figure 3.25.C and 3.26.C). Blood glucose levels measured 15 minutes after the meal AUC demonstrated a similar response in HF/HS- and HF/HS+INDO-fed mice during the initial MTT (figure 3.25.B and 3.25.E). Postprandial glucose responses remained similar throughout the experiment, but the difference between RD-fed mice and the HF/HS+/-INDO-fed mice appeared to decrease. After 10 week there were still no difference between the HF/HS- and HF/HS+INDO-fed mice and both were significantly different from RD-fed mice in blood glucose after the meal (figure 3.29.E). Insulin levels were measured at fasting state and meal stimulated insulin secretion (MSIS) was measured after 15 minutes. In keeping with the higher postprandial glucose levels induced by RD compared with the HF/HS-diets, MSIS was initially significantly higher when mice were fed the RD. A similar tendency was seen after 1, 2 and 3 and 10 weeks of feeding, but the difference between RD and HF/HS+/- INDO was not statistically significant after 1 and 2 weeks of feeding. After 3 weeks of feeding this statistically difference occurred. At no time, a difference in MSIS between HF/HS- and HS/HS+INDO fed mice was observed, leading us to the conclusion that indomethacin had no effect in attenuating MSIS in HF/HS -fed mice.

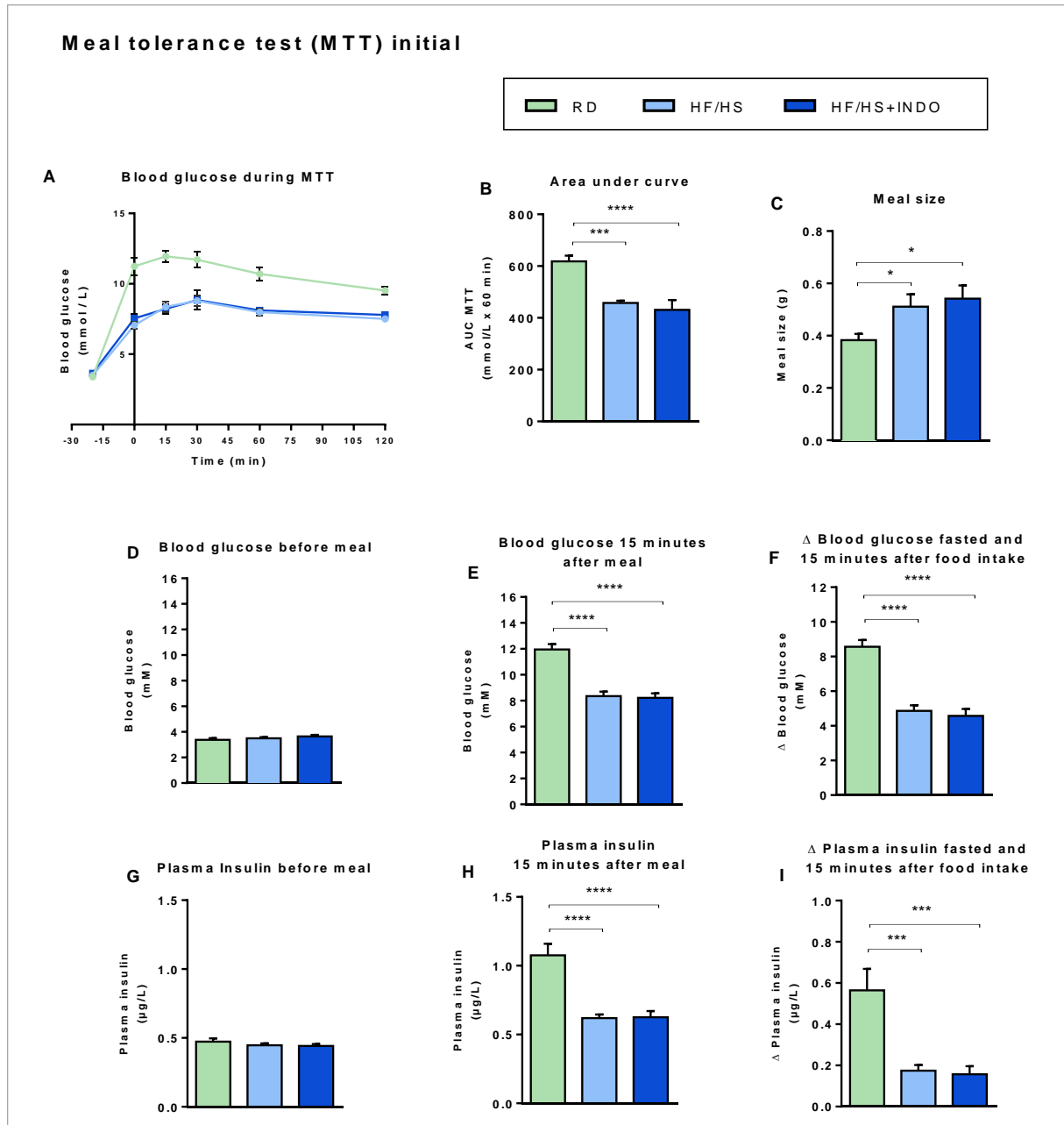


Figure 3.25: An MTT was performed on male C57BL/6J mice ($n=10$) before onset of the experiment. All mice were fed a RD in 1 week before the initial MTT. The mice had fasted in 16 hours when the test started. The mice were given 1 gram feed of; RD, HF/HS or HF/HS+INDO in a 20 minute period **A:** Blood glucose levels during the MTT, the blood glucose levels were measured before the meal (-20 min) and when the feed was taken away (0 min), 15, 30, 60 and 120 minutes after. **B:** Area under curve **C:** Meal size was calculated by the feed eaten subtracted from the feed given. **D:** Blood glucose after 16 hours of fasting. **E:** Blood glucose levels 15 minutes after the meal. **F:** Change in blood glucose levels from fasted to 15 minutes after the meal. **G:** Plasma insulin from 16 hours of fasting. **H:** Plasma insulin levels 15 minutes after meal. **I:** Meal stimulated insulin secretion, the change in plasma insulin from fasted to 15 minutes after the meal. All results are presented as mean \pm SEM. Statistical differences are denoted with stars; * $P \leq 0.05$, ** $P \leq 0.01$, *** $P \leq 0.001$, **** $P \leq 0.0001$.

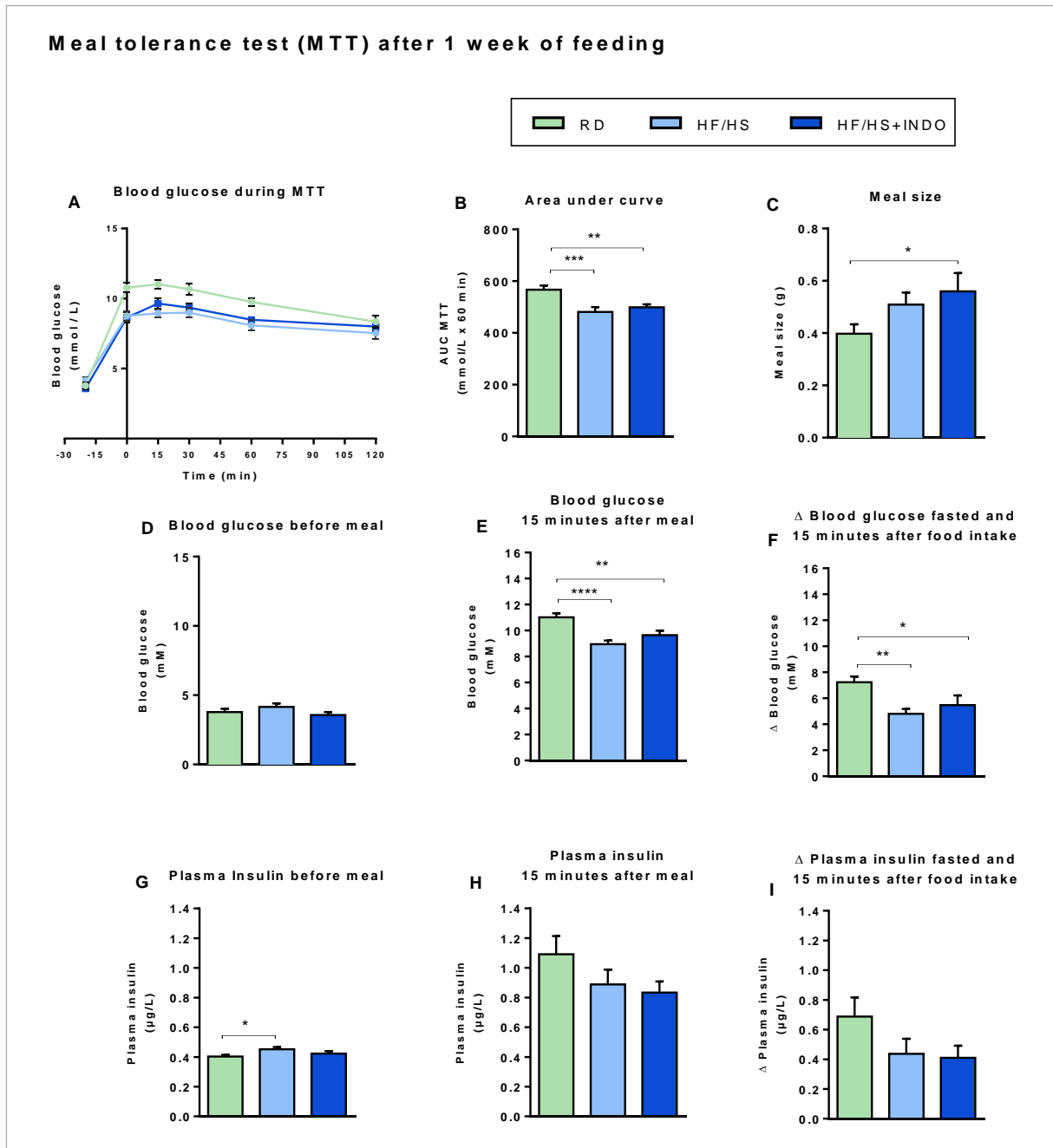


Figure 3.26: An MTT was performed on male C57BL/6J mice ($n=10$) after 1 week of feeding. The mice had fasted in 16 hours when the test started. The mice were given 1 gram feed of; RD, HF/HS or HF/HS+INDO in a 20 minute period **A:** Blood glucose levels during the MTT, the blood glucose levels were measured before the meal (-20 min) and when the feed was taken away (0 min), 15, 30, 60 and 120 minutes after. **B:** AUC. **C:** Meal size was calculated by the feed eaten subtracted from the feed given. **D:** Blood glucose after 16 hours of fasting. **E:** Blood glucose levels 15 minutes after the meal. **F:** Change in blood glucose levels from fasted to 15 minutes after the meal. **G:** Plasma insulin from 16 hours of fasting. **H:** Plasma insulin levels 15 minutes after the meal. **I:** Meal stimulated insulin secretion, the change in plasma insulin from fasted to 15 minutes after the meal. All results are presented as mean \pm SEM. Statistical differences are denoted with stars; * $P \leq 0.05$, ** $P \leq 0.01$, *** $P \leq 0.001$, **** $P \leq 0.0001$.

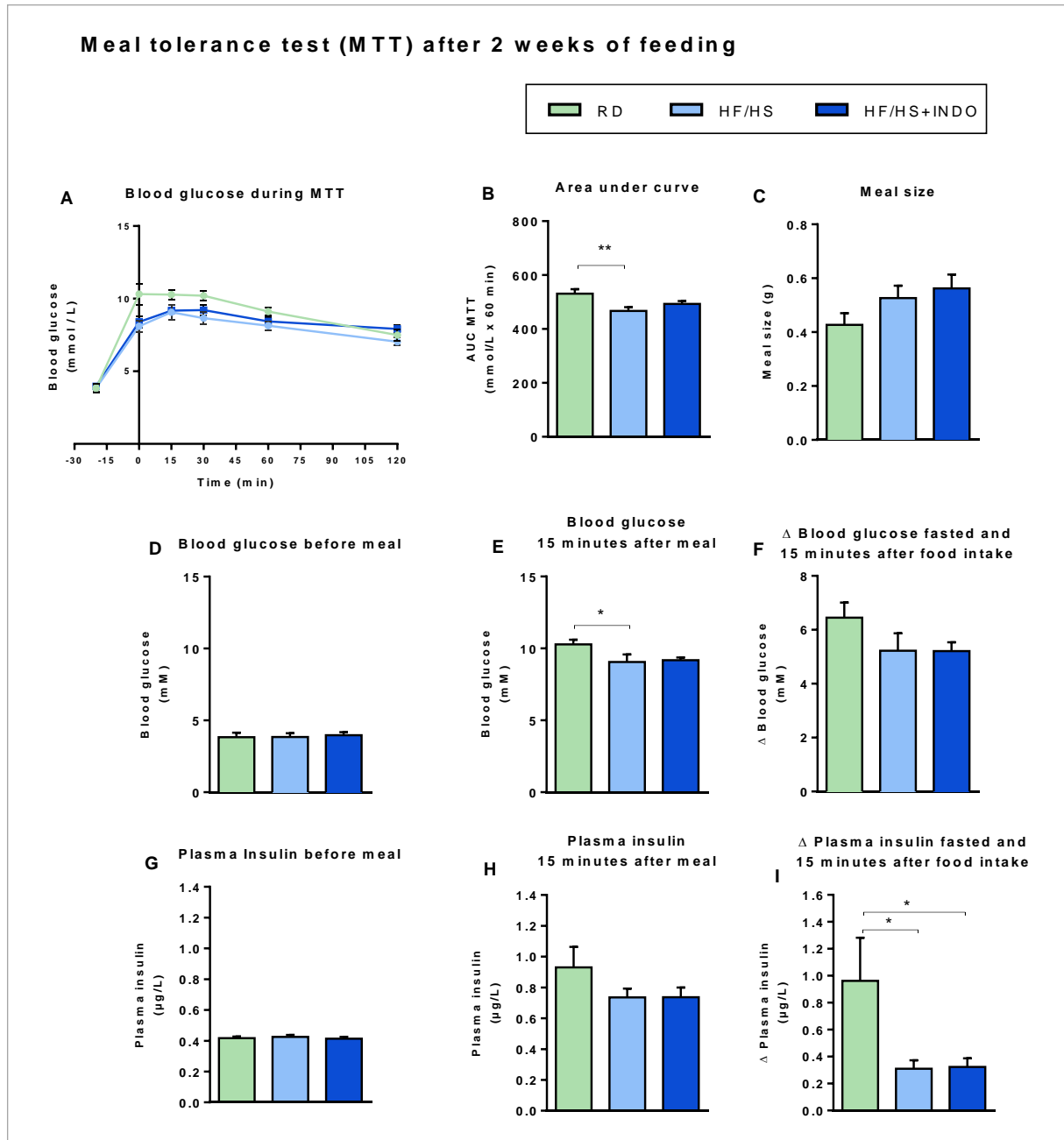


Figure 3.27: An MTT was performed on male C57BL/6J mice ($n=10$) after 2 weeks of feeding. The mice had fasted in 16 hours when the test started. The mice were given 1 gram feed of; RD, HF/HS or HF/HS+INDO in a 20 minute period **A:** Blood glucose levels during the MTT, the blood glucose levels were measured before the meal (-20 min) and when the feed was taken away (0 min), 15, 30, 60 and 120 minutes after. **B:** AUC. **C:** Meal size was calculated by the feed eaten subtracted from the feed given. **D:** Blood glucose after 16 hours of fasting. **E:** Blood glucose levels 15 minutes after the meal. **F:** Change in blood glucose levels from fasted to 15 minutes after the meal. **G:** Plasma insulin from 16 hours of fasting. **H:** Plasma insulin levels 15 minutes after the meal. **I:** Meal stimulated insulin secretion, the change in plasma insulin from fasted to 15 minutes after the meal. All results are presented as mean \pm SEM. Statistical differences are denoted with stars; * $P \leq 0.05$, ** $P \leq 0.01$.

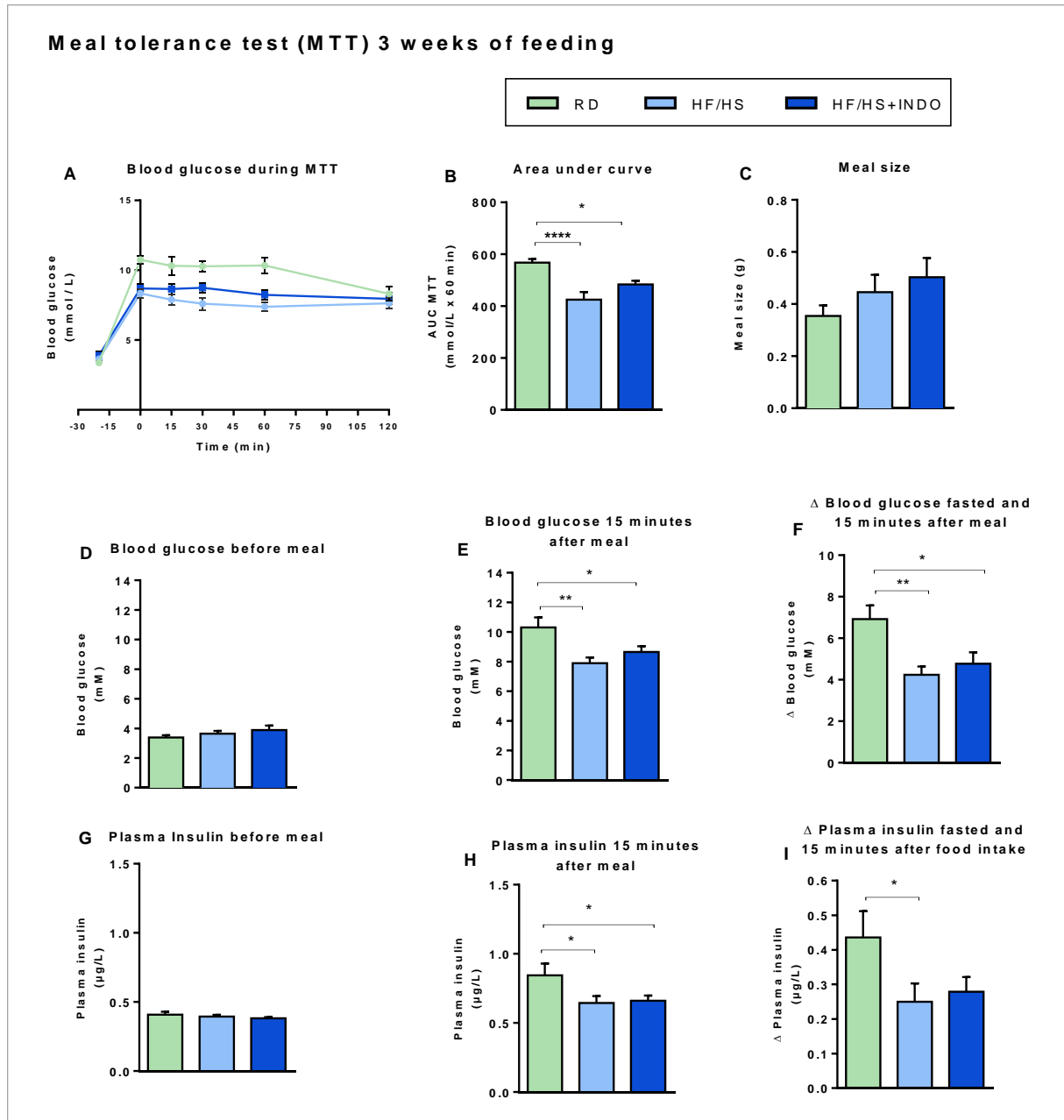


Figure 3.28: An MTT was performed on male C57BL/6J mice ($n=10$) after 3 weeks of feeding. The mice had fasted in 16 hours when the test started. The mice were given 1 gram feed of; RD, HF/HS or HF/HS+INDO in a 20 minute period **A:** Blood glucose levels during the MTT, the blood glucose levels were measured before the meal (-20 min) and when the feed was taken away (0 min), 15, 30, 60 and 120 minutes after. **B:** AUC. **C:** Meal size was calculated by the feed eaten subtracted from the feed given. **D:** Blood glucose after 16 hours of fasting. **E:** Blood glucose levels 15 minutes after the meal. **F:** Change in blood glucose levels from fasted to 15 minutes after the meal. **G:** Plasma insulin from 16 hours of fasting. **H:** Plasma insulin levels 15 minutes after the meal. **I:** Meal stimulated insulin secretion, the change in plasma insulin from fasted to 15 minutes after the meal. All results are presented as mean \pm SEM. Statistical differences are denoted with stars; * $P \leq 0.05$, ** $P \leq 0.01$, *** $P \leq 0.001$, **** $P \leq 0.0001$.

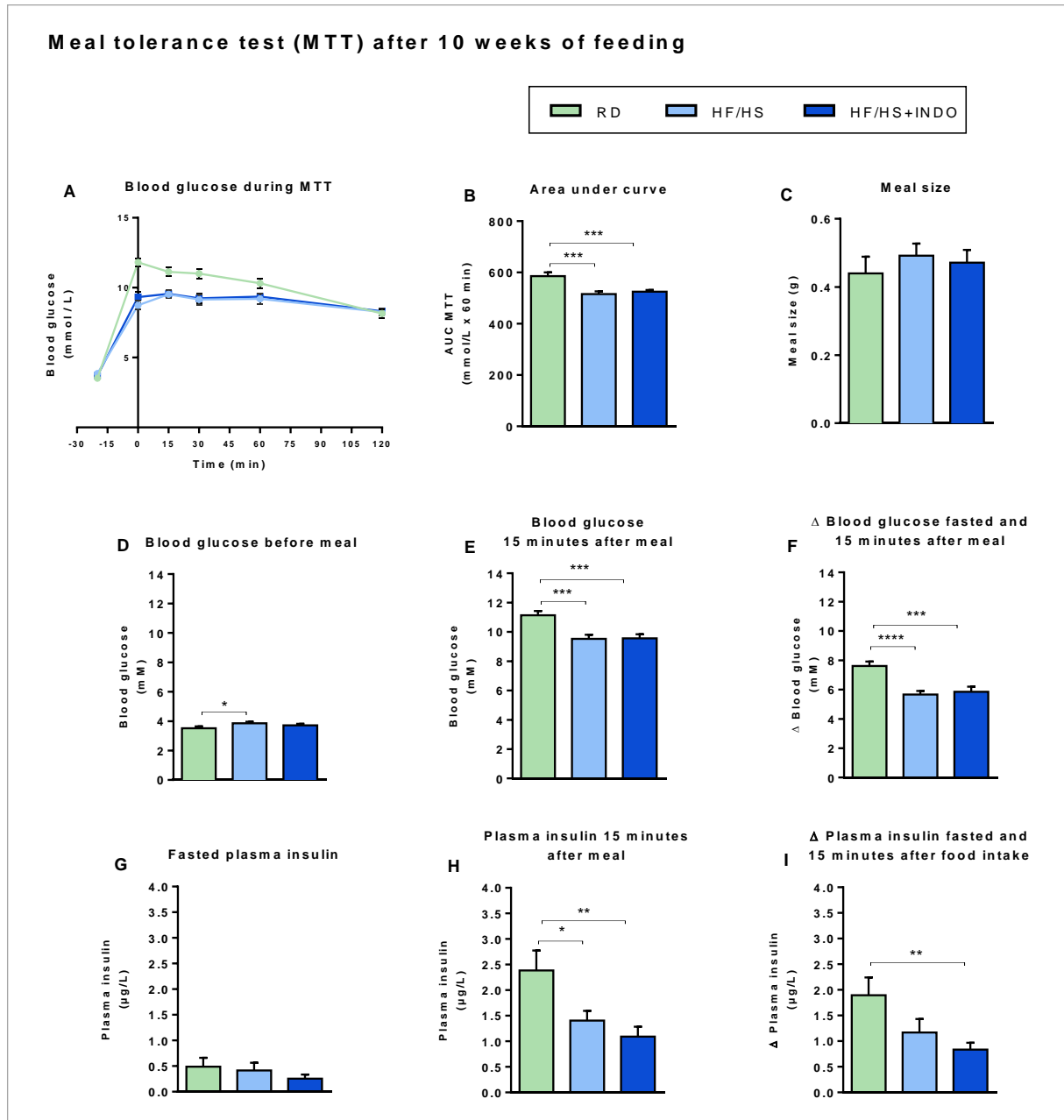


Figure 3.29: An MTT was performed on male C57BL/6J mice ($n=10$) after 10 weeks of feeding. The mice had fasted in 16 hours when the test started. The mice were given 1 gram feed of; RD, HF/HS or HF/HS+INDO in a 20 minute period **A:** Blood glucose levels during the MTT, the blood glucose levels were measured before the meal (-20 min) and when the feed was taken away (0 min), 15, 30, 60 and 120 minutes after. **B:** AUC. **C:** Meal size was calculated by the feed eaten subtracted from the feed given. **D:** Blood glucose after 16 hours of fasting. **E:** Blood glucose levels 15 minutes after the meal. **F:** Change in blood glucose levels from fasted to 15 minutes after the meal. **G:** Plasma insulin from 16 hours of fasting. **H:** Plasma insulin levels 15 minutes after the meal. **I:** Meal stimulated insulin secretion, the change in plasma insulin from fasted to 15 minutes after the meal. All results are presented as mean \pm SEM. Statistical differences are denoted with stars; * $P \leq 0.05$, ** $P \leq 0.01$, *** $P \leq 0.001$, **** $P \leq 0.0001$.

INDOMETHACIN DID NOT INHIBIT GSIS IN ORAL GLUCOSE TOLERANCE TEST

Since GSIS was attenuated in HF/HS+INDO-fed mice, whereas MSIS was unaffected, we speculated if this was related to the fact that glucose was injected *i.p* during the GTT. Therefore, after 8 weeks of feeding an OGTT was performed on mice fed RD, HF/HS and HF/HS+INDO. The blood glucose levels were lower when glucose was injected orally compared to the *i.p*-GTT performed after 9 weeks. This fact that it takes some time for the glucose to enter the blood in the OGTT, as it has to be transported through the lumen before it enters the blood. It appears that the RD-fed mice became as glucose intolerant as the HF/HS- and HF/HS+INDO-fed mice after 9 weeks of feeding (figure 3.16). This OGTT verifies that HF/HS+INDO-fed mice had lower fasting plasma insulin compared to HF/HS-fed mice. 15 minutes after the administration of glucose, the GSIS was not significantly attenuated in HF/HS+INDO-fed mice.

Oral glucose tolerance test (OGTT) after 8 week of feeding gavage injection with 2 mg/g body mass

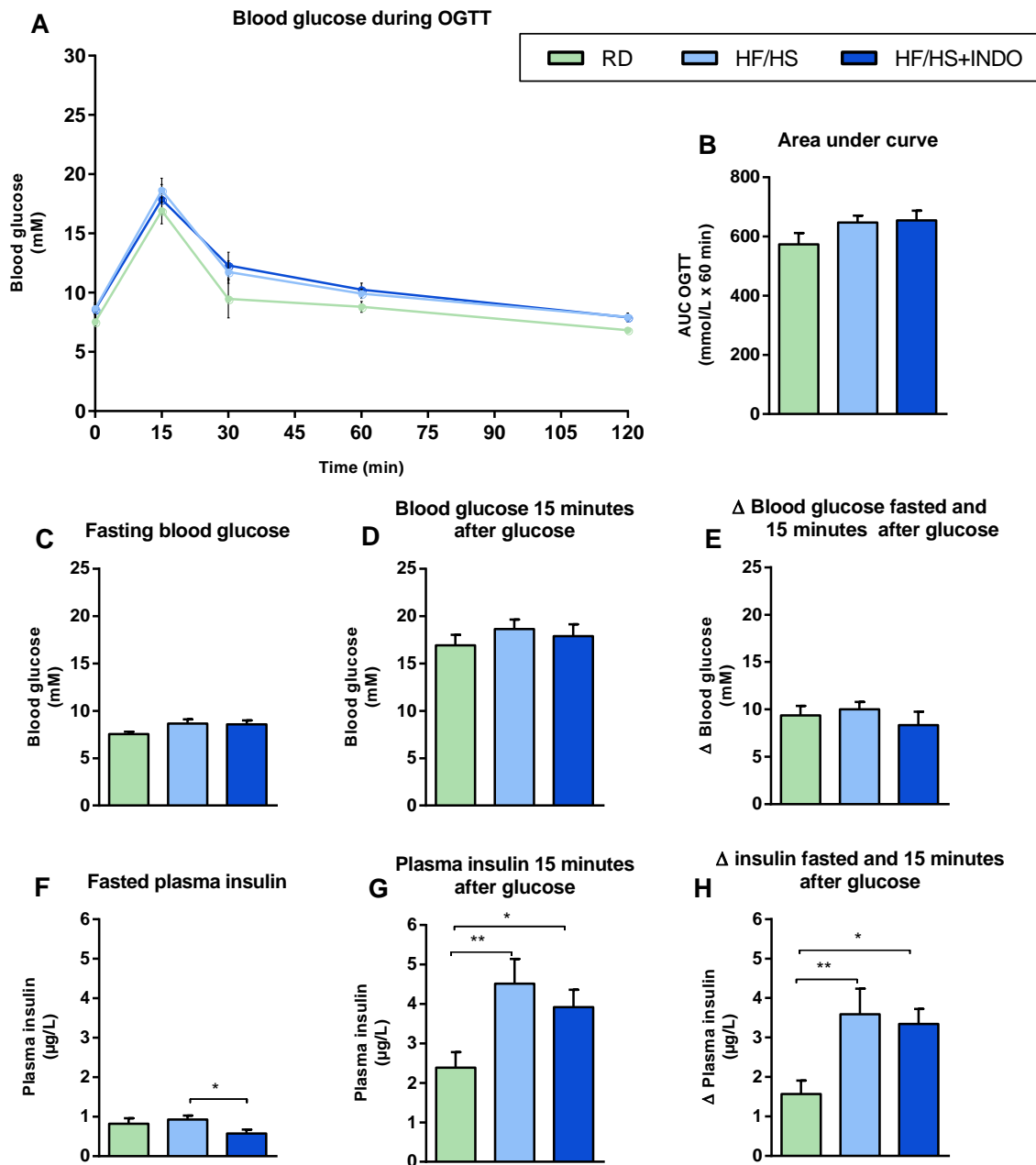


Figure 3.30: An OGTT was performed after 8 weeks on male C57BL/6J mice ($n=10$) fed RD, HF/HS and HF/HS+INDO. The mice had fasted for 6 hours when the test started. The glucose was injected orally (2 mg/g body mass) **A:** Blood glucose levels during the OGTT, the blood glucose levels were measured before- and 15, 30, 60 and 120 minutes after oral glucose injection. **B:** Area under curve **C:** Blood glucose levels after 6 hours of fasting. **D:** Blood glucose levels 15 minutes after the oral glucose injection. **E:** Change in blood glucose from fasted to 15 minutes after the oral glucose injection. **F:** Plasma insulin levels after 6 hours of fasting. **G:** Plasma insulin 15 minutes after the oral glucose injection **H:** Glucose stimulated insulin secretion, the change in plasma insulin from fasted to 15 minutes after the oral glucose injection. All results are presented as mean \pm SEM. Statistical differences are denoted with stars; * $P \leq 0.05$, ** $P \leq 0.01$.

4.0 DISCUSSION

The aim of this study was to investigate the mechanism(s) by which COX-inhibition with indomethacin attenuates DIO in mice fed an HF/HS-diet and investigate if indomethacin was able to reverse obesity in mice fed a HF/HS-diet. Furthermore, we aimed to explore the mechanism how glucose tolerance was impaired in lean and insulin sensitive HF/HS+INDO-fed mice. We examined if the effect of indomethacin on GSIS was an acute effect or if indomethacin specifically inhibits the compensatory insulin secretion induced by an HF/HS-diet. Finally, we explored the possibility if indomethacin could attenuate insulin secretion in response to a physiological condition, such as a meal.

4.1 INDOMETHACIN ATTENUATED HF/HS-INDUCED OBESITY, BUT DID NOT REVERSE IT

This study confirmed that indomethacin attenuated DIO in HF/HS fed mice. The difference between HF/HS+INDO and HF/HS-fed mice could not be explained by differences in energy intake. However, HF/HS+INDO fed mice had a clear reduction in feed efficiency compared to HF/HS-fed mice. Indomethacin has been reported to decrease bile acid secretion, which may reduce fat absorption (Dikopoulos, Schmid et al. 2007). However, a previous study performed in our group has calculated the fat digestibility by measuring the amount of consumed fat and total fat content in feces, showing that indomethacin treatment did not cause a decrease in fat absorption. Thus, neither reduced feed intake nor reduced digestibility could explain the attenuated DIO in HF/HS+INDO-fed mice. There is currently no obvious data that can be used to explain where the energy disappears. Thus, further investigations are required to understand the mechanism by which indomethacin attenuates DIO.

The finding that indomethacin was not able to reverse DIO in HF/HS-fed mice or reduce adipose tissue mass in RD-fed mice, might give a clue towards further investigations. However, one cannot exclude the possibility that the C57BL/6J strain is resistant towards weight loss. Still, an earlier study shows that obese C57BL/6J high HF-fed mice that were switched to a low-fat diet, reversed their obesity and diabetes completely (Parekh, Petro et al. 1998). Adiposity, fasting blood glucose and insulin values in the HF-fed mice were

equivalent to those mice of the same age that had spent 8-month on a low-fat diet (Parekh, Petro et al. 1998). Our findings suggest that indomethacin specifically attenuates an obesogenic signal from the HF/HS-diet.

4.2 HF/HS+INDO-FED MICE WERE LEAN, BUT AS GLUCOSE INTOLERANT AS HF/HS-FED MICE

Obesity is associated with impaired glucose tolerance and consequently a compensatory increased insulin secretion to do with a systematic insulin resistance in peripheral tissue, the increased adipose mass in the state of obesity is assumed to be the cause (Kahn and Flier 2000). Paradoxically, our study showed that indomethacin attenuated DIO in HF/HS-fed mice, but measurement of glucose tolerance using an *i.p.*-GTT showed that indomethacin did not attenuate HF/HS-induced glucose intolerance. Of note, concomitant with impaired glucose tolerance a compensatory increase in GSIS was observed in HF/HS-fed mice. Importantly, this compensatory increase in GSIS was not observed in the HF/HS+INDO-fed mice. In keeping with the earlier observation that plasma insulin levels in both fasted and fed state were lower in HF/HS+INDO-fed mice compared to HF/HS-fed mice (figure 1.5.H), it is reasonable to assume that indomethacin attenuates HF/HS-stimulated insulin secretion. This observation is in agreement with the earlier finding that inhibition of COX-activity has been demonstrated to impair GSIS in mice (Fujita, Kakei et al. 2007). Moreover, Indomethacin has been shown to decrease insulin secretion and increase blood glucose in T2DM patients (Pereira Arias, Romijn et al. 2000).

An important clue to understanding the mechanism by which indomethacin works was the observation that indomethacin did not inhibit GSIS when given to obese HF/HS-fed mice for several weeks. When indomethacin was given to the obese mice, there was neither no difference in fasting insulin levels between HF/HS+INDO- and HF/HS-fed mice. Furthermore, indomethacin did not reduce GSIS in RD-fed mice. In conclusion, indomethacin specifically attenuates HF/HS-induced GSIS, but was not able to reverse this effect. The reduced GSIS in HF/HS+INDO-fed mice, compared with HF/HS-fed mice, provides an explanation to their reduced glucose tolerance despite their lean phenotype.

In this study, the earlier notion that indomethacin attenuated HF/HS-induced insulin resistance (Figure 1.5.E) was not confirmed. In this study, insulin sensitivity measured by ITT was comparable in RD, HF/HS and HF/HS+INDO-fed mice. The lack of any measurable difference may however, be due to choice of method (see discussion page 79). Given that glucose tolerance was reduced and GSIS was induced in HF/HS-fed mice, it is reasonable to assume that the mice also had reduced insulin sensitivity, although not detected by the method chosen in this study. As the HF/HS-induced insulin resistance was attenuated by indomethacin in the earlier experiment (figure 1.5.E), we cannot exclude the possibility that the reduced GSIS in HF/HS+INDO-fed mice compared to HF/HS-fed mice is related to insulin sensitivity.

4.3 IS REDUCED GSIS RELATED TO THE REDUCED DIO IN HF/HS+INDO-FED MICE?

We have demonstrated that indomethacin inhibited GSIS in lean HF/HS-fed mice, but not in obese HF/HS-fed mice. Furthermore, we wanted to examine if the inhibiting effect of indomethacin on GSIS was an acute effect or if indomethacin specifically attenuated HF/HS-induced GSIS. An acute exposure of indomethacin would affect GSIS during an *i.p.*-GTT on both RD-fed mice and HF/HS-fed mice. Indomethacin had no acute inhibiting effect on GSIS either RD-fed mice or HF/HS-fed mice after 9 weeks. Thus, indomethacin seems to specifically attenuate HF/HS-induced GSIS. A new animal experiment was set-up to look into detail when the compensatory GSIS occurs in HF/HS-fed mice and additionally when indomethacin inhibits the GSIS in HF/HS-fed mice. A significantly increase in both insulin and blood glucose levels were observed after 3 weeks in HF/HS-fed mice. Importantly, this compensatory HF/HS-induced GSIS was inhibited when mice were administered indomethacin after 3 weeks. After 9 weeks this inhibited HF/HS-induced GSIS was significantly reduced. It appeared that HF/HS+INDO-fed mice became glucose intolerant before the HF/HS-fed mice, however, after 3 weeks there were no difference in blood glucose between the HF/HS and HF/HS+INDO-fed mice.

Insulin signaling in adipocytes is critical for development of obesity and glucose intolerance. It has been shown that FIRKO mice lacking insulin receptors in adipose tissue were protected against age-related obesity and obesity related glucose intolerance (Bluher, Michael et al.

2002) and new evidence pointing towards the importance of insulin signaling for obesity development is emerging. A study performed by (Mehran, Templeman et al. 2012) has limited insulin secretion from pancreatic β -cells in mice to study the role of hyperinsulemia in obesity and insulin resistance. In mice, insulin is expressed not only in pancreatic β -cells, but also in the brain. Insulin expression in the brain, especially applies during development, where it could possibly act locally and regulate neuronal development and energy homeostasis. Mice have two genes coding for insulin genes: *Ins1* and *Ins2*, whereas humans only have one. *Ins2* is expressed in the CNS and *Ins1* in pancreatic β -cells. Mehran, Templeman et.al generated a mouse model lacking both alleles of the *Ins2* gene and one allele of the *ins1* gene. The *ins1+/-:Ins2-/-*-mice consequently expressed insulin only in β -cells, with a 50 % reduces mRNA expression of insulin compared to control mice. The *ins1+/-:Ins 2-/-*-mice and a control group of mice were placed on a HF-diet. Whereas the controls on HF-diet gained significantly more weight than animals on chow diet, the *ins1+/-:Ins 2-/-*-mice did not. After 10 months of HF-feeding, the *ins1+/-:Ins 2-/-*-mice were as lean as the mice fed control-diet and *Ins1+/-:Ins 2-/-*-mice were protected against hyperinsulemia (Mehran, Templeman et al. 2012). Both FIRKO mice lacking insulin receptors in adipose tissue and *ins1+/-:Ins 2-/-*-mice that secreting small amounts of insulin, illustrates how important insulin is in obesity development. Thus, the ability of indomethacin to attenuate HF/HS-stimulated GSIS might be related to the ability to attenuate obesity. Indomethacin attenuated DIO and prevented a HF/HS-diet induced GSIS in HF/HS-fed mice. In obese HF/HS-fed mice, GSIS and presumably insulin signaling were already induced. Indomethacin was not able to reverse the HF/HS-induced GSIS. Given the importance of insulin in obesity development, the lack of effect on insulin secretion might be related to the lack of ability to reverse obesity. It is reasonable to assume that the obese HF/HS-fed mice had developed a compensatory GSIS due to insulin resistance. As it appears that indomethacin is not able to directly inhibit insulin secretion, but only specifically prevent the HF/HS-diet to induce GSIS, no effect on indomethacin in obese mice was seen. Thus, we believe that compared to RD-fed mice, HF/HS-fed mice become obese and the reduced insulin sensitivity and reduced glucose tolerance leads to a compensatory increase in GSIS. The increased insulin secretion in HF/HS-fed mice is thus an attempt to compensate for the impaired glucose tolerance. Indomethacin seems to specifically attenuate this compensatory effect.

On the other hand, if one assumes that the ability of indomethacin to attenuate HF/HS-induced GSIS is related to the ability of indomethacin to attenuate obesity, one would assume indomethacin to also affect MSIS. This was, however, not the case. Neither did indomethacin affect GSIS when glucose was administered orally. The lack of any effect of inhibition of MSIS and GSIS may however, be due to choice of protocol (see discussion page 79). However, further investigations are needed to elucidate this.

4.4 INDOMETHACIN DID NOT AFFECT MEAL STIMULATED INSULIN SECRETION IN HF/HS-FED MICE

A MTT test was performed to investigate the effects of the RD, HF/HS and HF/HS+INDO-diets on blood glucose levels and MSIS during and after a meal. Based on the inhibited GSIS in HF/HS+INDO-fed mice, we expected that the MSIS would be reduced in HF/HS+INDO-fed mice during the MTT, but surprisingly, this did not happen. There were no differences in blood glucose levels or MSIS between HF/HS and HF/HS+INDO-fed mice in the 4 first weeks of feeding or after 10 weeks. However, the RD-fed mice had significantly increased blood glucose after the meal and increased levels of MSIS. Most likely this increased levels of blood glucose and MSIS reflected the high amount of carbohydrates in the RD-feed. The lack of any measurable difference in MSIS between HF/HS and HF/HS+INDO may however, be due to choice of method (see discussion page 78).

An OGTT was performed after 8 weeks of feeding. The MTT and OGTT are similar in the way that the glucose passes the gastrointestinal tract and stimulates incretin, gastrointestinal hormones that cause increased insulin release from the β -cells (Drucker 2006). The glucose is, thus taken up more slowly during MTT and OGTT, than during an *i.p.*-GTT where glucose is injected. Surprisingly, during the OGTT, GSIS was similar in HF/HS and HF/HS+INDO-fed mice.

4.5 METHODOLOGICAL DISCUSSION

***i.p.*-GTT based on glucose dose given on body mass vs. lean mass**

In the first feeding experiment, an evaluation of *i.p.*-GTT on glucose load based on body mass and lean mass was performed. The reason for this evaluation is to due that obese mice with high body masses are injected with a larger dose of glucose during the *i.p.*-GTT. As most glucose is take up by muscle, and a high body mass often is due to increased adipose tissue mass that, the larger dose of glucose injected in obese mice may cause these mice to appear more glucose intolerant then mice with a smaller body mass. The dose of glucose based on lean mass makes the injection dose more similar between the mice, because there is less difference in lean mass then body mass between the feeding groups of mice.

Only small differences were seen between the *i.p.*-GTTs performed when the glucose load was given based on body mass and on lean mass. In the cohort of mice where *i.p.*-GTT was performed with glucose injection based on body mass, HF/HS-fed mice had significantly higher GSIS then RD-fed mice. This difference was not significant when the glucose load was based on lean mass. This may be due to the fact that fasting plasma insulin levels between RD- and HF/HS-fed mice were significantly different in fasted state in the cohort of mice where the *i.p.*-GTT was performed with glucose load based on body mass. Fasting insulin levels were not significantly different in the cohort of mice that were injected with glucose based on lean mass. Another difference between the cohorts was that blood glucose levels were not significantly different between HF/HS+INDO- and RD-fed mice 15 minutes after the injection with glucose based on body mass. This may due to that there were either no difference between fasting blood glucose between HF/HS+INDO- and RD-fed mice. When injection dose was based on lean mass, there was a significantly difference between RD- and HF/HS+INDO-fed mice in both fasted blood glucose and blood glucose 15 minutes after injection. Thus, our data suggest that the small differences between the two subsets of *i.p.*-GTTs and the differences could be explained by the variation between the two mice cohorts.

Insulin tolerance test

In this study, insulin sensitivity measured by ITT was comparable in RD-, HF/HS- and HF/HS+INDO-fed mice. The lack of any measurable difference may, however, be due to choice of protocol. To achieve base line blood glucose levels, all mice were allowed to eat for one hour, followed by one hour of fasting before the ITT was performed. We choose this protocol since too long fasting may cause hypoglycaemia in mice after the insulin injection. It appeared, however, that one hour of fasting was not sufficient to decrease the blood glucose that most likely was increased in repose to the one hour of feeding, as blood glucose levels were still high when insulin was injected. Thus, the injected dose with insulin was not sufficient to decrease the blood glucose levels and the results from the ITT simply illustrate the blood glucose levels before the injection. After 30 minutes, the blood glucose started to increase in all diet groups of mice, probably due to the compensatory mechanism to increase the blood glucose after the injection with insulin. Our data suggest that mice should not be re-fed before an ITT.

Meal tolerance test

We expected that MSIS would be decreased in HF/HS+INDO-fed mice compared to HF/HS-fed mice. However, this did not happen. Before the MTT the mice had fasted for 16 hours to ensure that the mice would eat the given amount of feed during 20 minutes. The half-life of indomethacin is 2.5-11.5 hours (Norsk legemiddelhåndbok 2010). Thus, after 16 hours of fasting, HF/HS-fed mice had likely metabolized the most of the indomethacin. When the HF/HS+INDO-fed mice receives their meal during the MTT, it is reasonable to assume that the HF/HS+INDO-meal induces an acute response of indomethacin, and as we have illustrated earlier, indomethacin had no acute effect in reducing GSIS in HF/HS-fed mice. A new MTT should be performed with a shorter time of fasting.

***i.p.*-GTT vs. OGTT**

After 8 weeks of feeding we tested the mice with glucose-administrated gavage instead of injecting the glucose *i.p.* We wanted to see how indomethacin influenced GSIS when glucose was administrated in a more physiologically relevant manner. The blood glucose and plasma insulin levels during the *i.p.*-GTT after 9 weeks were higher then in the OGTT performed after 8 weeks. This results are compatible with the results from a evaluation of OGTT and *i.p.*-GTT

performed by (Andrikopoulos, Blair et al. 2008). They found that plasma glucose levels during OGTT were significantly lower compared with *i.p*-GTT. The plasma insulin levels during *i.p*-GTT increased sharply and peaked at 15 minutes, whereas during the OGTT plasma insulin increased at a slower rate and reaching peak level at 30-60 minutes (Andrikopoulos, Blair et al. 2008). When glucose is injected orally by gavage, it takes some time for the glucose to enter the blood, as it has to be transported through the lumen before it enters the blood. When glucose is given *i.p*, the rise in blood glucose is much faster, and thus also insulin secretion is stimulated more quickly. Moreover, during administration of glucose via *i.p*, there is no incretin response. Incretin is known to potentiate glucose-mediated insulin response (Drucker 2006). OGTT is thus a more physiological correct method to examine glucose tolerance because it's more similar to a meal.

Glucose-stimulated insulin secretion and meal –stimulated insulin secretion

A similar feature between MTT and OGTT is that glucose is taken up in the lumen, and thus, blood glucose increase slower than when glucose is injected during an *i.p*-GTT. The *i.p*-GTT causes a rapidly increase in blood glucose, and consequently a rapid stimulation of insulin secretion. During the *i.p* GTT, MTT and OGTT insulin levels were measured 15 minutes after administration of glucose. Due to the presumably delayed stimulation of insulin secretion when glucose was given orally, measurements of insulin after 15 minutes may be too early to detect a potential difference. Whereas during an *i.p*-GTT, insulin levels reach its peak after 15 minutes, insulin levels reach its peak after 30-60 minutes during a OGTT (Andrikopoulos, Blair et al. 2008). Thus, timing of measuring insulin levels provides an explanation to why we did not observe an effect of indomethacin on GSIS during MSIS and OGTT. Perhaps, if the MSIS and GSIS were measured at a later time than 15 minutes, an effect of indomethacin on GSIS and MSIS would have been detected. However, more experiments are required to answer this question.

4.6 THE ANIMAL MODELS RELEVANCE TO HUMANS

Mice have a remarkably genetic similarity to humans and consequently mice and humans share many physiological and metabolic characteristics (Mural, Adams et al. 2002). Mice are found to require the same nutrients as humans, and are thereby a commonly used animal model in nutrition research. Inbred strains of mice have less genetic variety than humans. Thus, when using mice as a model in research it is important to be cautious not to misinterpret a specific effect to be general, as it might be a unique feature for the actual strain used (Gallaher 1992). The mice model used in this study, C57BL/6J is highly disposed to DIO, hyperinsulemia, hyperglycemia and insulin resistance when fed an HF/HS-diet. The C57BL/6J mice is thereby a suitable model to study the pathophysiology in obesity state quite similar to human obesity (Surwit, Feinglos et al. 1995).

The increasing consumption of both NSAIDs and consumption of a western diet, high in fat and sucrose, causes concern. The HF/HS+INDO-fed mice had attenuated GSIS and consequently developed increased blood glucose although they were lean. This potential ability of COX-inhibition to induce increased blood glucose levels, not associated with obesity is noteworthy. A deeper knowledge of the effect on how COX-inhibition with indomethacin inhibits GSIS and consequently increases blood glucose should be evaluated in details.

4.7 FUTURE PERSPECTIVES

The mechanisms by which COX-inhibition with indomethacin inhibits GSIS should be evaluated. *In vitro* studies using cell lines and isolated islets could be used in order to study indomethacin mechanism on inhibiting GSIS. Moreover, β -cells from HF/HS+INDO-fed mice could be analyzed with histology and immunohistochemistry. The HF/HS+INDO-fed mice had reduced feed efficiency and indomethacin attenuated HF/HS-induced obesity. The energy consumption of HF/HS+INDO and HF/HS-fed mice should be measured in metabolic cages to investigate energy expenditure in the different diet groups of mice. This should be performed during the development of obesity and when the mice already are obese.

In this study insulin resistance was measured with HOMA-IR-index and ITT. The HOMA-IR index illustrated improved insulin sensitivity compared to HF/HS-fed mice, but the ITT did not show any improved insulin sensitivity, as mentioned, this most likely was due with the choice of protocol. Earlier studies have shown improved insulin sensitivity measured with ITT in HF/HS-fed mice. To further investigate this improved insulin sensitivity in HF/HS+INDO-fed mice; a hyperinsulinemic euglycemic clamp should be performed. This method is the gold standard for investigating and quantifying insulin resistance. Hyperinsulinemic euglycemic clamp experiments measure the amount of glucose necessary to compensate for an increased insulin level without causing hypoglycemia (Muniyappa, Lee et al. 2008). Furthermore, by using labeled glucose, it is possible to identify the tissues that take up the glucose.

5.0 CONCLUSION

COX-inhibition with indomethacin attenuated HF/HS-induced obesity in male C57BL/6J mice. However, indomethacin was not able to reverse obesity in HF/HS-fed mice. Moreover, HF/HS+INDO-fed mice were lean, but paradoxically they developed impaired glucose tolerance. We establish that indomethacin inhibited the HF/HS-induced GSIS, but was not able to reverse the already increased GSIS in obese HF/HS-fed mice or to reduce GSIS in RD-fed mice. Given the importance of insulin in obesity development, it is reasonable to assume that the inability of indomethacin to reverse obesity in already obese mice is related to its inability to influence GSIS in the obese mice. Moreover, indomethacin had no acute inhibiting effect on GSIS in neither RD- nor HF/HS-fed mice. Thus, indomethacin seems to specifically attenuate HF/HS-induced GSIS. We were unable to detect any effect of COX-inhibition with indomethacin on insulin secretion when mice are fed a meal or the glucose load is administered orally, this needs further investigation. Thus, indomethacin selectively attenuates HF/HS-mediated stimulation of GSIS.

REFERENCES

- Andrikopoulos, S., A. R. Blair, et al. (2008). "Evaluating the glucose tolerance test in mice." Am J Physiol Endocrinol Metab **295**(6): E1323-1332.
- Bailes, B. K. (2002). "Diabetes mellitus and its chronic complications." AORN J **76**(2): 266-276, 278-282; quiz 283-266.
- Bluher, M. (2009). "Adipose tissue dysfunction in obesity." Exp Clin Endocrinol Diabetes **117**(6): 241-250.
- Bluher, M., M. D. Michael, et al. (2002). "Adipose tissue selective insulin receptor knockout protects against obesity and obesity-related glucose intolerance." Dev Cell **3**(1): 25-38.
- Bonora, E., G. Formentini, et al. (2002). "HOMA-estimated insulin resistance is an independent predictor of cardiovascular disease in type 2 diabetic subjects: prospective data from the Verona Diabetes Complications Study." Diabetes Care **25**(7): 1135-1141.
- Botting, R. M. (2006). "Inhibitors of cyclooxygenases: mechanisms, selectivity and uses." J Physiol Pharmacol **57 Suppl 5**: 113-124.
- Bruning, J. C., J. Winnay, et al. (1997). "Development of a novel polygenic model of NIDDM in mice heterozygous for IR and IRS-1 null alleles." Cell **88**(4): 561-572.
- Caumo, A. and L. Luzi (2004). "First-phase insulin secretion: does it exist in real life? Considerations on shape and function." Am J Physiol Endocrinol Metab **287**(3): E371-385.
- Chang-Chen, K. J., R. Mullur, et al. (2008). "Beta-cell failure as a complication of diabetes." Rev Endocr Metab Disord **9**(4): 329-343.
- Coate, K. C. and K. W. Huggins (2010). "Consumption of a high glycemic index diet increases abdominal adiposity but does not influence adipose tissue pro-oxidant and antioxidant gene expression in C57BL/6 mice." Nutr Res **30**(2): 141-150.
- Cypess, A. M., S. Lehman, et al. (2009). "Identification and importance of brown adipose tissue in adult humans." N Engl J Med **360**(15): 1509-1517.
- Cypess, A. M., A. P. White, et al. (2013). "Anatomical localization, gene expression profiling and functional characterization of adult human neck brown fat." Nat Med.
- de Luca, C. and J. M. Olefsky (2008). "Inflammation and insulin resistance." FEBS Lett **582**(1): 97-105.

- Dikopoulos, N., R. M. Schmid, et al. (2007). "Bile synthesis in rat models of inflammatory bowel diseases." Eur J Clin Invest **37**(3): 222-230.
- Donath, M. Y. and S. E. Shoelson (2011). "Type 2 diabetes as an inflammatory disease." Nature Reviews Immunology **11**(2): 98-107.
- Drucker, D. J. (2006). "The biology of incretin hormones." Cell metabolism **3**(3): 153-165.
- Enos, R. T., J. M. Davis, et al. (2012). "Negative Interaction between Indomethacin and Exercise in Mice." Int J Sports Med.
- Epstein, F. H., P. R. Shepherd, et al. (1999). "Glucose transporters and insulin action—implications for insulin resistance and diabetes mellitus." New England Journal of Medicine **341**(4): 248-257.
- Frühbeck, G. (2008). Overview of adipose tissue and its role in obesity and metabolic disorders. Adipose Tissue Protocols, Springer: 1-22.
- Fujita, H., M. Kakei, et al. (2007). "Effect of selective cyclooxygenase-2 (COX-2) inhibitor treatment on glucose-stimulated insulin secretion in C57BL/6 mice." Biochemical and biophysical research communications **363**(1): 37-43.
- Gallaher, D. D. (1992). "Animal models in human nutrition research." Nutrition in Clinical Practice **7**(1): 37-39.
- Giacca, A., C. Xiao, et al. (2011). "Lipid-induced pancreatic beta-cell dysfunction: focus on in vivo studies." Am J Physiol Endocrinol Metab **300**(2): E255-262.
- Goh, T. T., T. M. Mason, et al. (2007). "Lipid-induced β -cell dysfunction in vivo in models of progressive β -cell failure." American Journal of Physiology-Endocrinology And Metabolism **292**(2): E549-E560.
- Gonzalez-Angulo, A. M., J. Fuloria, et al. (2002). "Cyclooxygenase 2 inhibitors and colon cancer." Ochsner J **4**(3): 176-179.
- Guerra, C., R. A. Koza, et al. (1998). "Emergence of brown adipocytes in white fat in mice is under genetic control. Effects on body weight and adiposity." J Clin Invest **102**(2): 412-420.
- Harizi, H., J. B. Corcuff, et al. (2008). "Arachidonic-acid-derived eicosanoids: roles in biology and immunopathology." Trends Mol Med **14**(10): 461-469.

- Henquin, J., M. Ravier, et al. (2003). "Hierarchy of the β -cell signals controlling insulin secretion." European journal of clinical investigation **33**(9): 742-750.
- Henquin, J. C. (2009). "Regulation of insulin secretion: a matter of phase control and amplitude modulation." Diabetologia **52**(5): 739-751.
- Jacob, S., J. Machann, et al. (1999). "Association of increased intramyocellular lipid content with insulin resistance in lean nondiabetic offspring of type 2 diabetic subjects." Diabetes **48**(5): 1113-1119.
- Kahn, B. B. and J. S. Flier (2000). "Obesity and insulin resistance." Journal of Clinical Investigation **106**(4): 473-481.
- Kahn, S. E., R. L. Hull, et al. (2006). "Mechanisms linking obesity to insulin resistance and type 2 diabetes." Nature **444**(7121): 840-846.
- Kaul, K., J. M. Tarr, et al. (2012). "Introduction to diabetes mellitus." Adv Exp Med Biol **771**: 1-11.
- Kelly, T., W. Yang, et al. (2008). "Global burden of obesity in 2005 and projections to 2030." Int J Obes (Lond) **32**(9): 1431-1437.
- Kharroubi, I., L. Ladrière, et al. (2004). "Free fatty acids and cytokines induce pancreatic β -cell apoptosis by different mechanisms: role of nuclear factor- κ B and endoplasmic reticulum stress." Endocrinology **145**(11): 5087-5096.
- Kloting, N., M. Fasshauer, et al. (2010). "Insulin-sensitive obesity." Am J Physiol Endocrinol Metab **299**(3): E506-515.
- Klover, P. J. and R. A. Mooney (2004). "Hepatocytes: critical for glucose homeostasis." Int J Biochem Cell Biol **36**(5): 753-758.
- Koza, R. A., L. Nikonova, et al. (2006). "Changes in gene expression foreshadow diet-induced obesity in genetically identical mice." PLoS Genet **2**(5): e81.
- Lin, Y. and Z. Sun (2010). "Current views on type 2 diabetes." J Endocrinol **204**(1): 1-11.
- Madsen, L., B. Liaset, et al. (2008). "Macronutrients and obesity: views, news and reviews."
- Madsen, L., L. M. Pedersen, et al. (2010). "UCP1 induction during recruitment of brown adipocytes in white adipose tissue is dependent on cyclooxygenase activity." PLoS One **5**(6): e11391.

- Maraschin Jde, F. (2012). "Classification of diabetes." Adv Exp Med Biol **771**: 12-19.
- Mehran, A. E., N. M. Templeman, et al. (2012). "Hyperinsulinemia drives diet-induced obesity independently of brain insulin production." Cell Metab **16**(6): 723-737.
- Mitchell, J. A., P. Akarasereenont, et al. (1993). "Selectivity of nonsteroidal antiinflammatory drugs as inhibitors of constitutive and inducible cyclooxygenase." Proc Natl Acad Sci U S A **90**(24): 11693-11697.
- Montgomery, M. K., N. L. Hallahan, et al. (2013). "Mouse strain-dependent variation in obesity and glucose homeostasis in response to high-fat feeding." Diabetologia **56**(5): 1129-1139.
- Muniyappa, R., S. Lee, et al. (2008). "Current approaches for assessing insulin sensitivity and resistance in vivo: advantages, limitations, and appropriate usage." Am J Physiol Endocrinol Metab **294**(1): E15-26.
- Mural, R. J., M. D. Adams, et al. (2002). "A comparison of whole-genome shotgun-derived mouse chromosome 16 and the human genome." Science **296**(5573): 1661-1671.
- Nakagami, H. (2013). "The mechanism of white and brown adipocyte differentiation." Diabetes Metab J **37**(2): 85-90.
- NIFES (2005) 279-RT REAKSJON. MET.MOL-55. Nasjonalt institutt for ernærings - og sjømatforskning, Bergen.
- NIFES (2005). "280-Real Time PCR. MET.MOL-56. Nasjonalt institutt for ernærings - og sjømatforskning, Bergen."
- NIFES (2005) 281-RNA Rensing og RNA kvantitet. MET.MOL-66. Nasjonalt institutt for ernærings - og sjømatforskning, Bergen.
- Norsk legemiddelhåndbok (2010, 20.06.2010). "Indometacin." Retrieved 08.05.2013, from <http://legemiddelhandboka.no/Legemidler/75260#75261>.
- Parekh, P. I., A. E. Petro, et al. (1998). "Reversal of diet-induced obesity and diabetes in C57BL/6J mice." Metabolism **47**(9): 1089-1096.
- Pereira Arias, A. M., J. A. Romijn, et al. (2000). "Indomethacin decreases insulin secretion in patients with type 2 diabetes mellitus." Metabolism **49**(7): 839-844.
- Petersen, K. F. and G. I. Shulman (2002). "Pathogenesis of skeletal muscle insulin resistance in type 2 diabetes mellitus." The American journal of cardiology **90**(5A): 11G.

- Samuel, V. T., Z.-X. Liu, et al. (2004). "Mechanism of hepatic insulin resistance in non-alcoholic fatty liver disease." Journal of Biological Chemistry **279**(31): 32345-32353.
- Samuel, V. T. and G. I. Shulman (2012). "Mechanisms for insulin resistance: common threads and missing links." Cell **148**(5): 852-871.
- Sell, H. and J. Eckel (2010). "Adipose tissue inflammation: novel insight into the role of macrophages and lymphocytes." Curr Opin Clin Nutr Metab Care **13**(4): 366-370.
- Simmons, D. L., R. M. Botting, et al. (2004). "Cyclooxygenase isozymes: the biology of prostaglandin synthesis and inhibition." Pharmacological Reviews **56**(3): 387-437.
- Sinha, R., S. Dufour, et al. (2002). "Assessment of skeletal muscle triglyceride content by (1)H nuclear magnetic resonance spectroscopy in lean and obese adolescents: relationships to insulin sensitivity, total body fat, and central adiposity." Diabetes **51**(4): 1022-1027.
- Smith, W. L., D. L. DeWitt, et al. (2000). "Cyclooxygenases: structural, cellular, and molecular biology." Annual review of biochemistry **69**(1): 145-182.
- Sun, K., C. M. Kusminski, et al. (2011). "Adipose tissue remodeling and obesity." J Clin Invest **121**(6): 2094-2101.
- Surwit, R., M. Feinglos, et al. (1995). "Differential effects of fat and sucrose on the development of obesity and diabetes in C57BL/6J and AJ mice." Metabolism **44**(5): 645-651.
- The Jackson Laboratory (2007). "Physiological data summary C57BL/6J." Retrieved 08.05, 2013, from <http://jaxmice.jax.org/support/phenotyping/B6data000664.pdf>.
- The Jackson Laboratory (2013). Retrieved 08.05, 2013, from <http://jaxmice.jax.org/strain/000664.html>.
- Trayhurn, P. (2013). "Hypoxia and adipose tissue function and dysfunction in obesity." Physiol Rev **93**(1): 1-21.
- Uchizono, Y., C. Alarcon, et al. (2007). "The balance between proinsulin biosynthesis and insulin secretion: where can imbalance lead?" Diabetes, Obesity and Metabolism **9**(s2): 56-66.
- Valasek, M. A. and J. J. Repa (2005). "The power of real-time PCR." Advances in physiology education **29**(3): 151-159.

- van Marken Lichtenbelt, W. D., J. W. Vanhommerig, et al. (2009). "Cold-activated brown adipose tissue in healthy men." N Engl J Med **360**(15): 1500-1508.
- Vane, J. R., Y. S. Bakhle, et al. (1998). "Cyclooxygenases 1 and 2." Annu Rev Pharmacol Toxicol **38**: 97-120.
- Virtanen, K. A., M. E. Lidell, et al. (2009). "Functional brown adipose tissue in healthy adults." N Engl J Med **360**(15): 1518-1525.
- Vitali, A., I. Murano, et al. (2012). "The adipose organ of obesity-prone C57BL/6J mice is composed of mixed white and brown adipocytes." J Lipid Res **53**(4): 619-629.
- WHO (2012). "Obesity and overweight." from <http://who.int/mediacentre/factsheets/fs311/en/>.
- Wronska, A. and Z. Kmiec (2012). "Structural and biochemical characteristics of various white adipose tissue depots." Acta Physiol (Oxf) **205**(2): 194-208.
- Zimmet, P. Z. and K. G. Alberti (2006). "Introduction: Globalization and the non-communicable disease epidemic." Obesity (Silver Spring) **14**(1): 1-3.
- Zingaretti, M. C., F. Crosta, et al. (2009). "The presence of UCP1 demonstrates that metabolically active adipose tissue in the neck of adult humans truly represents brown adipose tissue." FASEB J **23**(9): 3113-3120.

APPENDIX

Appendix I: Mouse ELISA kit

Table A.1: Reagents in Insulin Mouse ELISA kit

Product	Vender
Insulin Mouse ELISA kit	DRG Instruments, GmbH, Germany
Coated plate	
Calibrator 0	
Calibrators 1,2,3,4,5	
Enzyme Conjugate 11X	
Enzyme Conjugate Buffer	
Wash Buffer 21X	
Substrate TMB	
Stop solution	

Appendix II: Histological methods

Table A.2: Chemicals and reagents used in fixation, dehydration, embedding, sectioning and staining.

Product	Vender
4 % formaldehyd	Merck, Germany
NaH ₂ PO ₄ x H ₂ O	Merck, Germany
Na ₂ HPO ₄ x H ₂ O	Merck, Germany
Ethanol	Arcus, Norway
Rectified Alcohol	Arcus, Norway
Xylene	Prolabo
Parafin	Histovax, OneMed
Hematoxylin	EMS
Eosin Y	Sigma, USA
Entellan	Merck, Germany

Appendix III – Reagents used in RealTime qPCR

Table A.3: Reagents used in RNA extraction.

Product	Vender
QIAzol reagent	QIAgen, Germany
Chloroform	Merch, Germany
Isopropanol	Arcus kjemi, Norway
Ethanol	Arcus kjemi, Norway
DEPC	Sigma, USA
RNase free ddH ₂ O	MiliQ Millipore, USA

Table A.4: Reagents in RT-reaction mix.

Product	Vender
RNase free ddH ₂ O	MiliQ Millipore, USA
TagMan RT buffer 10x	Applied Biosystems
25 mM magnesium chlorid	Applied Biosystems
10 mM DeoxyNTPs	Applied Biosystems
50 µM Oligo d(T) 16 primer	Applied Biosystems
RNase Inhibitor (20 U/µl)	Applied Biosystems
Multiscribe Reverse Transcriptase	Applied Biosystems

Table A.5: Reagents used in Real-Time qPCR

Product	Vender
RNase free ddH ₂ O	MiliQ Millipore, USA
SYBR GREEN Master	Roche, Norway
Primer (see table A.6)	Invitrogen, UK

Table A.6: List of primers used in Real-Time qPCR (obtained from Invitrogen, UK).

Housekeeping gen	Sequence 5' → 3'
TBP	Forward ACC CTT CAC CAA TGA CTC CTA TG
	Reverse ATG ATG ACT GCA GCA AAT CGC
β-actin	Forward ATG GGT CAG AAG GAC TCC TAG G
	Reverse AGT GGT ACG ACC AGA GGC ATA C
Primer	Sequence 5' → 3'
PEPCK1	Forward CCACACCATTGCAATTATGC
	Reverse CATATTTCTTCAGCTTGCGG
PPAR alpha	Forward CGTTTGTGGCTGGTCAAGTT
	Reverse AGAGAGGACAGATGGGGCTC
PPAR gamma	Forward ACAGCAATCTCTGTTTTATGC
	Reverse TGCTGGAGAAATCAACTGTGG
PPAR delta	Reverse TGCTGGAGAAATCAACTGTGG
	Forward CAGAGGTGCCTGGCACTC
JNK1	Forward TCTCCAGCACCCATACATCAAC
	Reverse TTCCTCAAATCCATTACCTCC
MCP1	Reverse GTGTTGGCTCAGCCAGATGC
	Forward GCTTGGTGACAAAACTA
PDK2	Reverse CTTCTACCTCAGCCGCATCTC
	Forward AGGCGTCTTTCACCACATCAG
FOXO1	Reverse TTTCTAAGTGGCCTGCGAGTC
	Forward CCCATCTCCCAGGTCATCC
SREBP1	Reverse GGA GCC ATG GAT TGC ACA TT
	Forward GCT TCC AGA GAG GAG CCC AG
GP6	Reverse CTT CAA GTG GAT TCT GTT TGG
	Forward AGA TGA CGT TCA AAC ACC GG

Appendix IV: qPCR- Gene expression liver**Figure A1: Gene expression of liver with Real Time qPCR**